FORMATION OF (HALO)ACETAMIDES AND (HALO)ACETONITRILES FROM THE REACTION OF MONOCHLORAMINE AND (HALO)ACETALDEHYDES IN WATER

BY

SUSANA YOKO KIMURA HARA

DISSERTATION

Submitted in partial fulfillment of the requirements
for the degree of Doctor of Philosophy in Environmental Engineering in Civil Engineering
in the Graduate College of the
University of Illinois at Urbana-Champaign, 2013

Urbana, Illinois

Doctoral Committee:

Professor Benito Jose Mariñas, Chair
Professor Michael Jacob Plewa
Assistant Professor Thanh Huong Nguyen
Associate Professor Shinya Echigo, Kyoto University

ABSTRACT

Chloramination is increasingly being used in the United States as a secondary disinfectant as a result of tighter regulations on selected disinfection by-products (DBPs) that include four trihalomethanes and five haloacetic acids. However, recent research suggests that unregulated nitrogen-containing DBPs formed by combined chlorine, such as haloacetonitriles and haloacetamides, might be more toxic than regulated DBPs.

Monochloramine has been shown to react with aldehydes, common DBPs formed from ozone and free chlorine disinfection, to form carbinolamines that slowly dehydrate to imines which undergo fast decomposition to nitriles. It is also known that nitriles can hydrolyze to its corresponding amides. However, in this study the formation rate of amides was found to be significantly higher and independent of nitrile hydrolysis.

The formation pathways of acetonitrile and two haloacetonitriles (chloro- and bromo-) and three haloacetamides (*N*,2-dichloroacetamide, 2-bromo-*N*-chloroacetamide, and *N*-chloroacetamide) from the reaction of monochloramine with acetaldehyde and two haloacetaldehydes (chloro- and bromo-) were investigated. Chloroacetaldehyde and monochloramine were found to quickly react to form and reach equilibrium with the carbinolamine 2-chloro-1-(chloroamino)ethanol. 2-chloro-1-(chloroamino)ethanol then decomposed through two concurrent pathways 1) slow dehydration to 1-chloro-2-(chloroimino)ethane, which in turn decomposed quickly to chloroacetonitrile, and 2) oxidation by monochloramine to form the previously unreported DBP *N*,2-dichloroacetamide. Similar pathway was found to take place for the formation of bromoacetonitrile and 2-bromo-*N*-chloroacetamide from the reaction between bromoacetaldehyde and monochloramine, and

acetonitrile and *N*-chloroacetamide formation from the reaction of acetaldehyde and monochloramine. These parallel reactions are acid/base catalyzed, and therefore, the influence of pH on (halo)acetonitrile and (halo)acetamide formation was investigated. A kinetic model was proposed.

This thesis is dedicated to my mom, dad, Akemi, Anna, Satoshi, and Oscar for their love and support throughout these years.

ACKNOWLEDGEMENTS

I would like to acknowledge several people that have been able to make this dissertation possible. First, I want to thank my advisor Professor Benito Mariñas for his guidance and encouragement throughout these years that has motivated me tremendously in academic research and in life. I could not have accomplished my graduate studies without his support. Also, I want to thank Shaoying Qi for all his help in the laboratory, maintenance of analytical instruments used in this study, and helpful discussions at the 4th floor. I also want to thank Professor Vern Snoeyink for having his house and office door open to students and for letting me be part of CASE. I want to thank Professor Michael Plewa for inviting me to his pizza parties, for his advice, and for letting me work in his lab. I want to thank Professor Shinya Echigo and Helen Nguyen for their comments and support as part of my dissertation committee. I would like to thank Alex Ulanov and Lucas Li from the Metabolomics Center at UIUC for their help on instrumentation.

For the past few years I have spent most of my time at Newmark's 4th floor and developed wonderful friendships with many students that worked there too. I would like to acknowledge many of those students and Mariñas and Plewa's group members especially Yukako Komaki for her help on the cytotoxicity work and feedback on my presentations; Ana Martinez and Bernardo Vazquez for our late night talks inside and outside the office; Bridget Curren and Trang Vu for their insights and help in the lab; and Marty Page for helping me during my first years in the group. I also want to acknowledge Jinyong Li for his help and guidance on NMR and chloroacetaldehyde synthesis, and Kathryn Guy for her help and guidance on

cyanogen iodide synthesis. I would like to acknowledge Li Liu for her help and encouragement especially through the toughest semester of grad school.

I would like to acknowledge CONACYT (Consejo Nacional de Ciencia y Tecnología) and WaterCAMPWS (Center of Advanced Materials for the Purification of Water with Systems) for their funding.

TABLE OF CONTENTS

CHAPTER 1

INTRODUCTION

Chlorine disinfection was first introduced to the United States in 1908 in Jersey City, New Jersey [1]. Thereafter, chlorination of water supplies expanded rapidly, reducing waterborne diseases such as cholera and typhoid. By the 1940s, chlorination was a world standard for water treatment. Consequently, disinfection represented one of the most important human health developments of the time. However, several studies in the mid-1970s found that chlorine reacts with compounds found in natural waters to produce disinfection by-products (DBPs) that cause negative health effects [2, 3]. As a result, EPA established minimum contaminant level (MCL) limits for trihalomethanes (THMs) [4]. Subsequently, other DBPs of concern have been added to the regulatory list such as haloacetic acids (HAAs), bromate ion (BrO_3^-), and chlorite ion (ClO_2^-).

In 2006, EPA promulgated Stage 2 Disinfection/Disinfection By-Product (D/DBP) Rule that stipulates maximum concentration levels of THMs and HAAs that must not be exceeded in each location in the distribution system instead of the averages of all collected samples, making it harder for water utilities to comply. For this reason, drinking water utilities were switching to alternative disinfection methods such as ozonation/combined chlorine. However, switching to other disinfectants can promote the formation of other classes of DBPs that are not well known. In the last 30 years more than 600 DBPs have been identified in finished drinking waters treated with most common disinfectants [5]. Approximately, 70% of identified DBPs remain unknown and THMs and HAAs constitute only 13.6% and 11.8% respectively of the total organic halogen

(TOX). However, occurrence and toxicological studies provide information of emerging DBPs that allows for prioritizing health effects studies, as well as regulation efforts.

Occurrence studies suggest that combined chlorine promotes compounds that contain nitrogen in their molecule known as nitrogenous DBPs (N-DBPs). Haloacetonitriles (HAN) and haloacetamides (HAcAm) are some examples of N-DBPs. HAN have been detected in several occurrence studies dichloro-, bromochloro-, dibromo-, and trichloroacetonitrile being the most commonly studied [6-8]. Dichloroacetonitrile had the highest median concentration ranging from 1.3 to 1.9 µg/L. The total HAN median concentration ranged from 2.5 to 4.0 µg/L. For the information collection rule (ICR) study, individual sample concentrations ranged between 0.5 and 41 µg/L in finished waters and from less than 0.5 to 51.6 µg/L in the distribution system. Additionally, data suggested that HAN concentration increased in water utilities that used combined chlorine instead of chlorine as secondary disinfectant. Chloral hydrate (hydrated trichloroacetaldehyde) was also detected with median concentration of 1.7 µg/L in finished waters and 2.9 µg/L in the distribution system with individual sample concentrations ranging from less than 0.5 to 46 µg/L. However, these studies used ammonium chloride as a dechlorinating agent and pH 4.5-5.5 to preserve their samples, conditions that will result in the formation of chloramines. Therefore, the results reported in these studies might be slightly influenced by the presence of chloramines in their samples.

In another nationwide occurrence study, 12 water utilities with high total organic carbon and/or bromide in their source water and using alternative disinfection schemes (i.e. ozonation/chloramination) were selected to detect emerging DBPs [9, 10]. Haloacetaldehydes (HaAcAl) was the third largest class of DBPs by weight found in drinking water, after THMs and HAAs. HaAcAl, HAN and HAcAm detected in the study are shown in Table 1.1. HAcAm

were identified in this study for the first time (median of total haloacetamides of 1.4 µg/L). Dichloroacetamide was the most prevalent in its class; however, it was also the most tested (26 samples) compared to the others (8 samples). Bromodichloroacetonitrile was also tested in 30 samples but it was not detected. Ascorbic acid (31 mg/L) and sulfuric acid were used to quench the disinfectant and to lower the pH to 3.5 for each sample.

Given the fact that more than 600 DBPs could be present in finished drinking waters, a comparative baseline of DBPs toxicity is needed to prioritize regulation efforts and chemical formation studies. Thus, DBPs have been tested by *in vitro* assays with *Salmonella typhimurium* strain TA100 and Chinese Hamster Ovary (CHO) cells. These *in vitro* assays provide a baseline where the toxicity results among test agents can be compared and conclusions can be inferred from.

Salmonella and CHO cytotoxicity represent the reduction of cell density by exposure to the test agent [11]. However, a different assay is used to test for CHO genotoxicity. Single cell gel electrophoresis (SCGE) assay in treated CHO cells detects DNA damage in the entire genome [12], unlike *Salmonella* mutagenicity that targets point mutations. CHO cells are exposed to different concentrations of a specific DBP for 4 hours and then DNA damage migrates electrophoretically in a gel by exposing the CHO nucleus to an electric current. The tail moment (response) is represented as the product of the DNA density that migrates times the distance traveled. Genetic potency is the midpoint of the slope in a concentration-response curve. Results are corrected for acute toxicity.

Toxicity studies [13, 14] have shown that N-DBPs are more cytotoxic and genotoxic than regulated THMs and HAAs. A cyto- and genotoxicity index for different chemical classes illustrated in Figure 1.1, show that HAN and HAcAm are significantly more toxic than THMs

and HAAs. Additionally, it was found that cyto- and genotoxicity increases with halogen substitution in the order of I > Br >> Cl. Iodoacetonitrile is slightly more genotoxic (3.71×10^{-5} M) than bromoacetonitrile (3.85×10^{-5} M), and over an order of magnitude more than chloroacetonitrile (6.1×10^{-4} M). A smaller concentration of iodoacetonitrile will produce the same DNA damage than higher concentrations of bromoacetonitrile and chloroacetonitrile. This tendency is consistent with the higher reactivity of iodinated and brominated compounds compared to their chlorinated homologs. Similarly, iodoacetamide is slightly more genotoxic (3.41×10^{-5} M) than bromoacetamide (3.68×10^{-5} M), and nearly two orders of magnitude more than chloroacetamide (1.38×10^{-3} M). Even though N-DBPs are found at low concentrations, they might pose a health risk due to their higher cyto- and genotoxicity compared to the toxicity of currently regulated DBPs (Figure 1.1).

HAN and HAcAm are toxic N-DBPs that are found in finished drinking waters. However, their chemical formation is not well understood. Occurrence studies suggest that HAN and HAcAm formation is more pronounced with chloramination compared to the use of free chlorine. Therefore, it is important to understand the formation mechanisms of HAN and HAcAm with combined chlorine. The purpose of this study is to characterize the formation pathway and kinetic rates of HAN and HAcAm from the reaction of monochloramine and (halo)acetaldehydes, compounds that are also frequently observed in finished drinking waters. This research aims to provide a better understanding of HAN and HAcAm formation potential in water which in turn would 1) assist in developing DBP control strategies, 2) explain why di-substituted HANs and HAcAm are more frequently observed in occurrence studies than their mono- and tri-substituted counterparts, and 3) aid in devising appropriate quenching and sample preservation methods for HAN and HAcAm detection.

Literature Cited

1. MWH, Water Treatment, Principles and Design. In 2nd ed.; John Wiley and Sons: 2005.

2. Bellar, T. A.; Lichtenberg, J. J., Determining Volatile Organics at Microgram-per-Litre Levels by Gas Chromatography. *J. AWWA* **1974,** *66*, (12), 739-744.

3. Rook, J. J., Formation of Haloforms During the Chlorination of Natural Water. *Water Treatment and Examination* **1974,** *23*, 234-243.

4. U.S.EPA, Control of Trihalomethanes in Drinking Water. Final Rule. *Federal Register* **1979,** *44*, 231.

5. Richardson, S. D., Drinking water disinfection by-products. In *Encyclopedia of Environmental Analysis and Remediation*, Meyers, R. A., Ed. John Wiley & Sons: 1998; Vol. 3, pp p. 1398-1421.

6. McGuire, M. J.; McLain, J. L.; Obolensky, A. *Information Collection Rute Data Analysis*; AwwaRF and AWWA: Denver, CO, 2002.

7. Krasner, S. W.; McGuire, M. J.; Jacangelo, J. G.; Patania, N. L.; Reagan, K. M.; Aieta, E. M., The occurrence of disinfection by-products in U.S. drinking water. *J. Am. Water Works Assoc.* **1989,** *81*, (8), 41-53.

8. Williams, D. T.; Lebel, G. L.; Benoit, F. M.; Centre, E. H.; Canada, H., Disinfection by-products in canadian drinking water. *Chemosphere* **1997,** *34*, 299-316.

9. Weinberg, H. S.; Krasner, S. W.; Richardson, S. D.; Thruston, A. D. J., 2002. *The Occurrence of Disinfection By-Products (DBPs) of Health Concern in Drinking Water : Results of a Nationwide DBP Occurrence Study*. Environmental Protection Agency, National Exposure Research Laboratory, Athens, GA. EPA/600/R-02/068.

10. Krasner, S. W.; Weinberg, H. S.; Richardson, S. D.; Pastor, S. J.; Chinn, R.; Sclimenti, M. J.; Onstad, G. D.; Thruston Jr, A. D., Occurrence of a New Generation of Disinfection Byproducts. *Environmental Science & Technology* **2006,** *40*, (23), 7175-7185.

11. Plewa, M. J.; Wagner, E. D.; Jazwierska, P.; Richardson, S. D.; Chen, P. H.; McKague, A. B., Halonitromethane Drinking Water Disinfection Byproducts: Chemical Characterization and Mammalian Cell Cytotoxicity and Genotoxicity. *Environmental Science & Technology* **2004,** *38*, (1), 62-68.

12. Plewa, M. J.; Kargalioglu, Y.; Vankerk, D.; Minear, R. A.; Wagner, E. D., Mammalian cell cytotoxicity and genotoxicity analysis of drinking water disinfection by-products. *Environmental and Molecular Mutagenesis* **2002,** *40*, (2), 134-142.

13. Muellner, M. G.; Wagner, E. D.; McCalla, K.; Richardson, S. D.; Woo, Y.-T.; Plewa, M. J., Haloacetonitriles vs regulated haloacetic acids are nitrogen-containing DBPs more toxic. *Environmental Science & Technology* **2007,** *41*, 645-51.

14. Plewa, M. J.; Muellner, M. G.; Richardson, S. D.; Fasano, F.; Buettner, K. M.; Yin-Tak, W.; McKague, A. B.; Wagner, E. D., Occurrence, Synthesis, and Mammalian Cell Cytotoxicity and Genotoxicity of Haloacetamides: An Emerging Class of Nitrogenous Drinking Water Disinfection Byproducts. *Environmental Science & Technology* **2008,** *42*, (3), 955-961.

Table and Figures

Table 1.1 Summary of HaAcAl, HAN, HAcAm detection in treated waters [9, 10]

DBP	Min (µg/L)	Median (µg/L)	75th Percentile (µg/L)	Max (µg/L)	No. Samples Detected	Total Samples Tested	% Sample Detection
Chloroacetaldehyde	0	0.2	0.4	2.4	17	25	68
Dichloroacetaldehyde	ND	2	3.28	14	72	79	91
Bromochloroacetaldehyde	ND	0.8	1.8	4	47	69	68
Chloral hydrate	ND	1	2.35	16	39	44	89
Tribromoacetaldehyde	ND	0.35	0.43	3	12	53	23
Chloroacetonitrile	ND	0.15	0.35	0.9	16	53	30
Bromoacetonitrile	ND	0.15	0.18	0.2	2	54	4
Dichloroacetonitrile	ND	1	2	12	47	53	89
Bromochloroacetonitrile	ND	0.8	1	3	42	54	78
Dibromoacetonitrile	ND	0.6	0.9	2	31	54	57
Trichloroacetonitrile	ND	0.1	0.18	0.4	6	53	11
Dibromochloroacetonitrile	ND	0.3	0.45	0.6	2	32	6
Chloroacetamide	0	0	0.1	0.5	2	8	25
Bromoacetamide	0	0	0.2	1.1	2	8	25
Dichloroacetamide	0	1.3	1.95	5.6	19	26	73
Dibromoacetamide	0	0.55	1.65	2.8	6	8	75
Trichloroacetamide	0	0.3	0.48	1.1	6	8	75

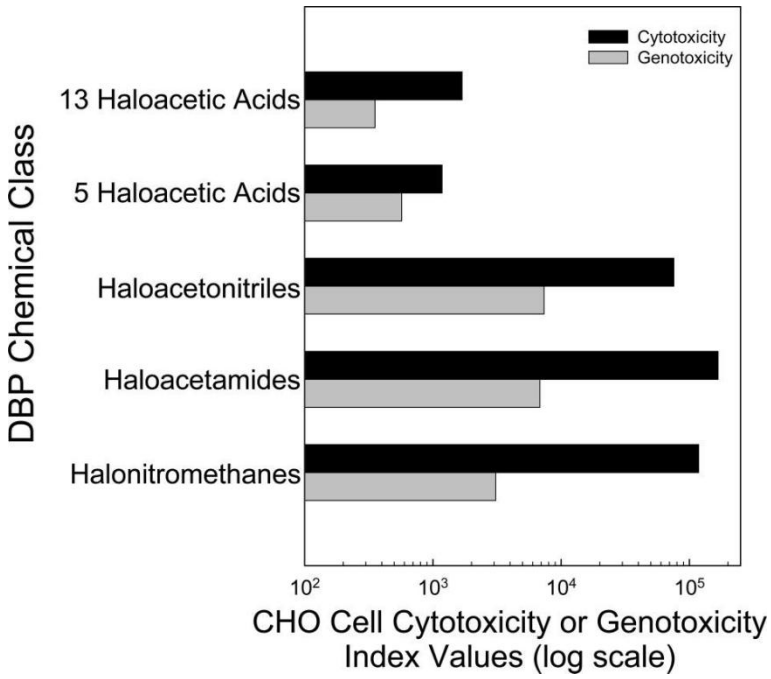

Figure 1.1 Combined CHO cell cytotoxicity and genotoxicity index values for different DBP classes [14]

CHAPTER 2

CHLOROACETONITRILE AND *N*,2-DICHLOROACETAMIDE FORMATION FROM THE REACTION OF CHLOROACETALDEHYDE AND MONOCHLORAMINE

Abstract

Combined chlorine has been used as an alternative disinfectant to free chlorine with the goal of reducing the formation of trihalomethanes (THMs) and haloacetic acids (HAAs) in drinking water. However, combined chlorine can promote the formation of others disinfection by-products (DBPs) such as haloacetonitriles and haloacetamides that are found to be more cyto-and genotoxic than regulated DBPs. Monochloramine quickly reacts with chloroacetaldehyde forming and reaching equilibrium with the carbinolamine 2-chloro-1-(chloroamino)ethanol. The equilibrium constant for this reaction was calculated to be K_1=1468 M^{-1}. 2-chloro-1-(chloroamino)ethanol undergoes slow dehydration to form 1-chloro-2-(chloroimino)ethane that immediately decomposes to chloroacetonitrile. 2-chloro-1-(chloroamino)ethanol is also oxidized by monochloramine to produce a previously unidentified DBP *N*,2-dichloroacetamide. The carbinolamine dehydration step was found to be acid/base catalyzed (k_2^0 = 2.98 x 10^{-6} s^{-1}, k_2^H = 2.65 and k_2^{OH} = 3.25 $M^{-1}s^{-1}$). In contrast, *N*,2-dichloroacetamide formation was observed to be only base catalyzed (k_3^{OH} = 3.13 x 10^4 $M^{-2}s^{-1}$). *N*,2-dichloroacetamide cytotoxicity (%C½ = 2.56 x 10^{-4} M) was found to be slightly less potent compared to chloroacetamide but higher than di- and trichloroacetamide.

2.1. Introduction

Chloramination is commonly used as a secondary disinfection process that provides a stable residual in the distribution system and produces lower levels of regulated disinfection by-products (DBPs). For these reasons, combined chlorine is used as an alternative disinfectant to comply with regulations. However, toxicity studies have suggested that unregulated nitrogen based DBPs (N-DBPs) formed by combined chlorine might be more toxic than regulated carbon-based DBPs. Haloacetonitriles (HAN) and haloacetamides (HAcAm) are two classes of N-DBPs that have been shown to be one to two orders of magnitud more cyto- and genotoxic than regulated haloacetic acids [1, 2]. Occurrence studies have associated an increased formation of HAN and HAcAm with chloramination [1, 2]. For example, chloroacetonitrile and chloroacetamide have been detected in finished waters with concentrations of 0.1-0.9 and 0.4-0.5 μg/L, respectively. Though they are detected at lower concentrations than regulated DBPs they pose a health risk due to their higher toxicity.

Several formation pathways have been reported for the formation of HAN and HAcAm [3]. The nitrogen in HAN and HAcAm can come from chloramines or aliphatic amino acids. Recent efforts to determine the precursors of HAN and HAcAm have suggested that monochloramine incorporation plays an important role in the formation of HAN and HAcAm. Chloramination of several NOM models using label $^{15}NH_2Cl$ showed >70% monochloramine-nitrogen incorporation to dichloroacetonitrile and dichloroacetamide [4, 5]. Additionally, during chloramination dichloroacetamide is produced at higher levels than dichloroacetonitrile.

Previous studies have shown that nitrile formation can occur from the reaction of monochloramine and aldehydes, the later reported as common DBPs resulting from ozonation

and chlorination [6, 7]. Formaldehyde, acetaldehyde, and chloroacetaldehyde are among some of the identified aldehydes in treated waters [1, 2, 8-10]. Monochloramine reacts with formaldehyde by nucleophilic addition to form the carbinolamine *N*-chloromethanolamine. *N*-chloromethanolamine then forms *N*-chloromethanimine via a general acid/base catalyzed dehydration, and the imine subsequently decomposes irreversibly to hydrogen cyanide (HCN) at a much faster rate compared to its formation at pH> 5 [6]. Similarly, although without characterizing the kinetics, monochloramine has shown to react with acetaldehyde to produce the carbinolamine 1-(chloroamino)ethanol that dehydrates to (chloroimino)ethane which in turns decomposes to acetonitrile [7].

Chlorinated aldehydes also react with primary amines and ammonia to form imines as intermediates [11]. Crampton et al. studied the reaction between chlorinated aldehydes (mono-, di- and tri-) and primary amines and ammonia. It was observed that chloroacetaldehyde and primary amines had >90% conversion to its corresponding imine in acetonitrile solutions. Further decomposition products were not identified. However, it has been shown that imines decompose to nitriles [12] and therefore it is possible that, chloroacetonitrile may form from the reaction of chloroacetaldehyde and monochloramine.

Furthermore, it is known that acetonitriles undergo hydrolysis to form acetamides [12, 13]. Glezer et al. studied the hydrolysis of mono-, di- and trihaloacetonitriles in water at different pH conditions [13]. The hydrolysis rate is dependent on the number of substitutions and type of halogen attached to the α-carbon. Trihaloacetonitriles were the least stable in basic (pH 8.7) and neutral (pH 7.2) conditions followed by dihaloacetonitriles with intermediate stability and monohaloacetonitriles being the most stable. Chlorinated compounds were found to undergo

slower hydrolysis than the brominated homologs and so chloroacetonitrile was the most stable of all pH levels tested (5.4, 7.2 and 8.7).

Another possible reaction for amide bond formation is through the oxidation of carbinolamines [14, 15]. Larsen et al. oxidized imines to amides in O^{18} labeled water-acetonitrile mixtures in the presence of potassium permanganate. It was observed that the imine incorporated O^{18} labeled water to form carbinolamine as an intermediate, and the resulting carbinolamine was oxidized to form amides. Similarly, Tank et al. observed high yields of amide formation starting from aromatic aldehydes and cyclic amines in the presence of aqueous hydrogen peroxide. Thus, haloacetamide formation from the reaction of carbinolamine with other oxidizing agents such as monochloramine is possible but remains to be demonstrated.

The objectives of this study are to characterize the reaction pathways for the formation of chloroacetonitrile and haloacetamide from the reaction of chloroacetaldehyde and monochloramine in drinking water. Batch experiments were performed with the goal of identifying reaction intermediates and products by mass spectrometry and determining major pathway reactions and their kinetic constants as a function of solution pH and reactant concentrations by UV-Vis spectrophotometry. Additionally, the haloacetamide directly formed from this reaction, not previously reported as DBP in drinking water, was tested for cytotoxicity and compared to the cytotoxicity of the haloacetamide typically reported even though it forms during quenching of drinking water samples commonly practiced for DBP preservation. Gaining such knowledge will allow a better understanding of haloacetonitrile and haloacetamide formation and devise appropriate sample quenching methods and strategies to control DBP formation.

2.2. Experimental Methods

Reagents and Solutions. Chloroacetaldehyde was synthesized using a modified method described by Hodgson et al. [16]. Initial reactants, 4-chloro-1,3-dioxolan-2-one (> 90%) and triethylamine (≥ 99%), were purchased from Sigma-Aldrich (St. Louis, MO). One drop of triethylamine was added to 7.35 g of 4-chloro-1,3-dioxolan-2-one and heated in an oil bath to 180ºC. Distillation fraction between 83-86 ºC was recovered in dry acetonitrile to avoid polymerization of hydrated and unhydrated species. Chloroacetaldehyde was stored at 4ºC and was found to be stable for several months in acetonitrile at this temperature. Chloroacetaldehyde purity was analyzed by UV-Vis spectrometry and 1H NMR. The chloroacetaldehyde stock concentration was determined by a titration method described by NIOSH [17].

Chloroacetonitrile (≥99%), 2-chloroacetamide (HPLC Grade ≥98%), and acetonitrile (GC Grade ≥99.5%) used to produce calibration curves for GC/MS analysis were purchased from Sigma-Aldrich (St. Louis, MO). Chloroacetonitrile and 2-chloroacetamide stock solutions were prepared daily by dissolving them in acetonitrile and water respectively. Stock solutions were then diluted to varying concentrations in buffered solutions similar to experimental samples.

Monochloramine was prepared daily by slowly adding sodium hypochlorite solution to a rapidly stirred ammonium chloride solution. Both solutions were previously buffered and adjusted to ionic strength of 0.1 M and pH 8.5 to minimize dichloramine formation. Sodium hypochlorite stock solution (5.65-6% Laboratory Grade) and ammonium chloride salt (ACS reagent) were purchased from Fisher Scientific (Pittsburgh, PA). Sodium hypochlorite stock solution was standardized spectrophotometrically (λ_{max} = 292 nm, 350 $M^{-1}cm^{-1}$). Resulting

monochloramine concentrations were also verified spectrophotometrically (λ_{max} = 243 nm, 461 $M^{-1}cm^{-1}$) and found to be stable for several hours [18].

N,2-dichloroacetamide was synthesized by reacting stoichiometric amounts of 2-chloroacetamide and sodium hypochlorite in buffered solutions at pH 7.5. The reaction was monitored by the disappearance of sodium hypochlorite by UV-Vis until completion. *N*,2-dichloroacetamide was observed to be stable at tested conditions (pH 3 to11) in the absence of a reducing agent such as those commonly used in drinking water sampling for DBP assessment.

Buffer stock solutions were prepared daily by dissolving ACS reagent grade KH_2PO_4 (Sigma Aldrich, St. Louis, MO) and $NaHCO_3$ (Fisher Scientific, Pittsburgh, PA) in nanopure water. Sodium perchlorate was used to adjust ionic strength for all solutions. Fluka 70% puriss perchloric acid and ACS reagent sodium hydroxide (Sigma Aldrich, St. Louis, MO) were used to adjust solution pH. Nanopure water was used to prepare all solutions.

Instrumentation and Methods. Equilibrium and reaction rate constants were determined from absorption measurements taken as a function of reaction time with a UV-Vis Spectrophotometer model 2550 (Shimadzu Scientific Instruments, Columbia, MD). Absorption spectras were scanned from 200 to 400 nm using 10 mm quartz cuvettes. Kinetic measurements were monitored at 210 and 243 nm. All reactions were maintained at 18ºC with a water bath recirculator model 9501 (PolyScience, Niles, IL).

Reaction pathway intermediates and products were identified and chloroacetonitrile and *N*,2-dichloroacetamide quantified by gas chromatography/mass spectrometry with a GC/MS model 6850/5975C (Agilent Technologies, Santa Clara, CA). Procedures used for reaction intermediate identification involved extracting unquenched samples with methyl tert-butyl

acetate (MTBE). In contrast, for product quantification, aliquots of 10 ml were first quenched with 1.5 mM sodium thiosulfate and adjusted to neutral pH (6.5-7.5) to minimize decomposition of products. Subsequently, all samples were vigorously mixed with 1 mL ethyl acetate, 6 mg/L 1,2 dichloropropane as internal standard, and 2.85 g sodium sulfate for 2 minutes. After 3 minutes of allowing phase separation, extracts were transferred to 200 μL vial inserts with no headspace for immediate analysis. Extracts were injected to the GC inlet port with temperature set at 230ºC and operated in splitless mode. The injected samples were carried by Helium gas at 1.0 mL/min and passed through a DB-624 column (Agilent J&W, Santa Clara, CA). The temperature of the GC oven was initially maintained at 35 ºC for 3 minutes, ramped at 10 ºC/min to 90 ºC, held at 90 ºC for 1 min and ramped again at 10 ºC/min to 190 ºC. Extracts were ionized by electron impact. Reaction products chloroacetonitrile and 2-chloroacetamide, and internal standard ions were detected by specific selective ion monitoring, and reaction intermediates were identified by scanning from 35 to 300 amu.

The pH and temperature of all solutions were measured with a Thermo Electron Orion ROSS Ultra pH electrode (Thermo Fisher Scientific, Waltham, MA) and temperature electrode (Fisher Scientific, Pittsburgh, PA) connected to an Accumet AB15 Plus pH meter (Fisher Scientific, Pittsburgh, PA). Activity coefficients were calculated with the extended DeBye Huckel equation and the Guntelberg approximation and used to calculate the actual hydrogen ion concentrations from the corresponding activities in all experiments.

Equilibrium and kinetic rate constants were obtained by fitting experimental data to the kinetic model with the simplex method available in Micromath Scientist 3.0 (St. Louis, MO). Kinetic model simulations were also obtained with Micromath Scientist 3.0.

Experimental Matrix. Experimental sets to determine equilibrium and reaction rate constants are shown in Table 2.1.

Cytotoxicity Tests. *N*,2-dichloroacetamide was tested with a chronic cytotoxicity assay using chinese hamster ovary (CHO) cells (line AS52, clone 11-4-8) [19]. Concentration-response curves are obtained from exposing CHO cells to increasing concentrations of *N*,2-dichloroacetamide for a period of 72 hours corresponding to three cell divisions under non-toxic conditions. Cell density for each concentration was measured with 8-16 replicates and compared as the mean percentage of the negative control. Detailed procedures are described elsewhere [20, 21]. Statistical and non-linear regression analyses were performed with Sigmaplot 12.0 (Systat Software Inc., San Jose, CA).

2.3. Results and Discussion

2.3.1. Monochloramine and chloroacetaldehyde reaction products and intermediates.

Monochloramine and chloroacetaldehyde react in a fast and reversible reaction to form the carbinolamine 2-chloro-1-(chloroamino)ethanol as shown in Figure 2.1. 2-chloro-1-(chloroamino)ethanol dehydrates slowly to imine 1-chloro-2-(chloroimino)ethane, the rate limiting step, which in turn decomposes quickly to chloroacetonitrile. GCMS results detected 1-chloro-2-(chloroimino)ethane and chloroacetonitrile (Figure 2.2 and 2.3). 1-chloro-2-(chloroamino)ethane was analyzed based on the m/z mass fragments. Evidence suggests that chloroacetonitrile is formed from the proposed reaction pathway. 2-chloro-1-(chloroamino)ethanol was not detected possibly because dehydration can occur in the GCMS injection port and/or extraction process.

Additionally, chloroacetamide was also identified with GC/MS suggesting it is a product from the reaction of monochloramine and chloroacetaldehyde. Experiments monitored with UV-Vis (Figure 2.4) showed a fast decreasing absorbance at 243 nm with a simultaneous increase in the <220 nm region with an isobestic point at 225 nm. Monochloramine and carbinolamine, compounds that strongly absorb at 243 nm, decompose to form an unknown species that strongly absorbs in the <220 nm region. Chloroacetonitrile does not absorb at the concentrations tested in this study. Initially it was hypothesized that chloroacetamide was the unknown species. However, mass balances performed on experiment set UV-2 did not support this idea.

While chloroacetonitrile can hydrolyze to chloroacetamide, reaction rates determined from UV-Vis data were much faster than the controls tested for chloroacetonitrile hydrolysis. Another possibility for amide formation is that monochloramine can oxidize carbinolamine 2-chloro-1-(chloroamino)ethanol to form *N*,2-dichloroacetamide as shown in Figure 2.1. *N*,2-dichloroacetamide was synthesized to obtain its molar absorptivity and compare them to the UV-2 results. Reaction mass balances were consistent with *N*,2-dichloroacetamide being the unknown species observed in Figure 2.4. Furthermore, *N*,2-dichloroacetamide can lose a chlorine atom from its N-Cl bond either by reacting with a quenching agent or when analyzed by GC/MS to form chloroacetamide. Even though the main product is not directly observable in the GC/MS, the decomposition product, chloroacetamide, is detected in the GC/MS chromatogram confirming the formation of *N*,2-dichloroacetamide.

2.3.2. Monochloramine and chloroacetaldehyde equilibrium constant determination

Chloroacetaldehyde mixed in water exists predominantly as two species, unhydrated and hydrated that are in equilibrium with each other. Total chloroacetaldehyde ($C_{T,\mathrm{ClCH2CHO}}$) is defined as the sum of both species, where each species can be expressed as a fraction of $C_{T,\mathrm{ClCH2CHO}}$

$$\frac{[\mathrm{ClCH_2CHO}]}{C_{T,\mathrm{ClCH2CHO}}} = \frac{K_{h1}}{1+K_{h1}} = \beta_0 \quad (1)$$

$$\frac{[\mathrm{ClCH_2CH(OH)_2}]}{C_{T,\mathrm{ClCH2CHO}}} = \frac{1}{1+K_{h1}} = \beta_1 \quad (2)$$

where, β_0 and β_1 are equal to 0.026 and 0.974 with chloroacetaldehyde hydration constant [22] is equal to

$$K_{h1} = \frac{[\mathrm{ClCH_2CHO}]}{[\mathrm{ClCH_2CH(OH)_2}]} = 0.027 \quad (3)$$

Monochloramine reacts in a fast and reversible reaction with chloroacetaldehyde to form 2-chloro-1-(chloroamino)ethanol by nucleophilic attack of the nitrogen lone pair to the carbonyl group. Equilibrium constant K_1 expressed as

$$K_1 = \frac{[\mathrm{ClCH_2CH(OH)NHCl}]_e}{[\mathrm{NH_2Cl}]_e[\mathrm{ClCH_2CHO}]_e} \quad (4)$$

where,

$[\mathrm{NH_2Cl}]_e$ = Monochloramine concentration at equilibrium

$[\mathrm{ClCH_2CH(OH)NHCl}]_e$= 2-chloro-1-(chloroamino)ethanol concentration at equilibrium

$[\mathrm{ClCH_2CHO}]_e$ = Unhydrated chloroacetaldehyde concentration at equilibrium

Experimental set UV-1 (Table 2.1) was used to determine K_1, conditions at which 2-chloro-1-(chloroamino)ethanol conversion to other products are minimized. Equilibrium was immediately established and samples were taken between 1-3 minutes (Figure 2.5). Experiments were conducted in excess chloroacetaldehyde to monochloramine so $[\mathrm{ClCH_2CHO}]_e \approx [\mathrm{ClCH_2CHO}]_0$ where, initial chloroacetaldehyde concentration and that at the time of equilibrium were not to differ significantly. Therefore, the chloroacetaldehyde spectrum was subtracted from reaction spectra resulting in absorbance values pertaining to monochloramine and 2-chloro-1-(chloroamino)ethanol species, or

$$A_{\lambda,e} = \varepsilon_{\mathrm{NH_2Cl}_\lambda}[\mathrm{NH_2Cl}]_e + \varepsilon_{\mathrm{ClCH_2CH(OH)NHCl}_\lambda}[\mathrm{ClCH_2CH(OH)NHCl}]_e \quad (5)$$

where, $\varepsilon_{\mathrm{NH_2Cl}_\lambda}$ and $\varepsilon_{\mathrm{ClCH_2CH(OH)NHCl}_\lambda}$ are the molar absorptivities at wavelength λ respectively.

At initial equilibrium, monochloramine concentration will equal to the initial monochloramine concentration minus the reacted to 2-chloro-1-(chloroamino)ethanol.

$$[\mathrm{NH_2Cl}]_e = [\mathrm{NH_2Cl}]_0 - [\mathrm{ClCH_2CH(OH)NHCl}]_e \quad (6)$$

Substituting equation 6 into equation 4 and 5 and with some algebraic manipulation we obtain

$$[\mathrm{ClCH_2CH(OH)NHCl}]_e = \frac{[\mathrm{NH_2Cl}]_0[\mathrm{ClCH_2CHO}]_0}{1/K_1 + [\mathrm{ClCH_2CHO}]_0} \quad (7)$$

$$A_{\lambda,e} = \varepsilon_{\mathrm{NH_2Cl}_\lambda}[\mathrm{NH_2Cl}]_0 + (\varepsilon_{\mathrm{ClCH_2CH(OH)NHCl}_\lambda} - \varepsilon_{\mathrm{NH_2Cl}_\lambda})[\mathrm{ClCH_2CH(OH)NHCl}]_e \quad (8)$$

that are combined to

$$A_{\lambda,e} = \varepsilon_{\mathrm{NH_2Cl}_\lambda}[\mathrm{NH_2Cl}]_o + (\varepsilon_{\mathrm{ClCH_2CH(OH)NHCl}_\lambda} - \varepsilon_{\mathrm{NH_2Cl}_\lambda})\frac{[\mathrm{NH_2Cl}]_0[\mathrm{ClCH_2CHO}]_0}{(1/K_1 + [\mathrm{ClCH_2CHO}]_0)} \quad (9)$$

where, the absorbance is expressed in terms of the two unknown coefficients: K_1 and $\varepsilon_{ClCH_2CH(OH)NHCl_\lambda}$. Experimental data was fitted to equation 9 for wavelengths between 235-245 nm to obtain an average K_1 value of 1468 ± 82 M^{-1}. A second round fitting of data was done with K_1=1468 M^{-1} to obtain $\varepsilon_{ClCH_2CH(OH)NHCl_\lambda}$ values for wavelengths 210-260 nm (Figure 2.6). Absorbance values at equilibrium were then calculated with equation 5 where monochloramine and 2-chloro-1-(chloroamino)ethanol concentrations are calculated with equation 6 and 7. Modeled results provided a good representation of experimental data (Figure 2.7).

Aldehydes are susceptible to nucleophilic attack to their carbonyl carbon [12]. Substituents attached to the α-position have a strong effect on the reactivity of the aldehyde. For example, chloroacetaldehyde is relatively more stable than formaldehyde because it contains a chlorinated methyl group that distributes the electron density. As a result, chloroacetaldehyde forms lower hydrated species than formaldehyde consistent with the higher hydration constant of 0.027 (Eq 3) for the former compared to that of 0.0005 for the later compound [23]. Similarly, chloroacetaldehyde is less susceptible to nucleophilic attack by amines to form carbinolamines consistent with its lower equilibrium constant of 1468 M^{-1} (Eq 4) compared to 660000 M^{-1} [6] for formaldehyde.

2.3.3. Chloroacetonitrile and *N*,2-dichloroacetamide Formation

Kinetic Model. Monochloramine attacks chloroacetaldehyde in a fast reaction reaching equilibrium with carbinolamine 2-chloro-1-(chloroamino)ethanol. The carbinolamine can either 1) slowly dehydrate to the imine 1-chloro-2-(chloroimino)ethane and immediately decompose to chloroacetonitrile or 2) be oxidized by monochloramine to *N*,2-dichloroacetamide (Figure 2.1). The overall rate expression is

$$\frac{dC_{T,NCl}}{dt} = -k_2[\mathrm{ClCH_2CH(OH)NHCl}] - k_3[\mathrm{ClCH_2CH(OH)NHCl}][\mathrm{NH_2Cl}] \quad (10)$$

where,

$$C_{T,NCl} = [\mathrm{NH_2Cl}] + [\mathrm{ClCH_2CH(OH)NHCl}] \quad (11)$$

The concentration of each species is expressed as the fraction of $C_{T,NCl}$ by substituting the equilibrium rate expression equation 4 into 11 to obtain

$$\frac{[\mathrm{NH_2Cl}]}{C_{T,NCl}} = \frac{1}{1+K_1[\mathrm{ClCH_2CHO}]} = \alpha_0 \quad (12)$$

$$\frac{[\mathrm{ClCH_2CH(OH)NHCl}]}{C_{T,NCl}} = \frac{K_1[\mathrm{ClCH_2CHO}]}{1+K_1[\mathrm{ClCH_2CHO}]} = \alpha_1 \quad (13)$$

where, α_0 and α_1 for 10 mM total chloroacetaldehyde concentration are 0.724 and 0.276 respectively.

Substituting equation 12 and 13 into 10, the rate expressions for $C_{T,NCl}$ decomposition and chloroacetonitrile and *N*,2-dichloroacetamide formation are

$$\frac{dC_{T,NCl}}{dt} = -k_2\alpha_1[C_{T,NCl}] - 2k_3\alpha_0\alpha_1[C_{T,NCl}]^2 \quad (14)$$

$$\frac{d\mathrm{ClCH_2CN}}{dt} = k_2\alpha_1[C_{T,NCl}] \quad (15)$$

$$\frac{d\mathrm{ClCH_2C(O)NHCl}}{dt} = k_3\alpha_0\alpha_1[C_{T,NCl}]^2 \quad (16)$$

where, $\frac{dC_{T,NCl}}{dt}$ is a mixed order reaction composed by a first and second order term. To conserve mass balance the second order term is multiplied by two. Monochloramine decomposition,

independent from its reaction with chloroacetaldehyde and products, is relevant for experimental conditions GC-1, GC-3, and UV-3 (Table 2.1), and was incorporated into the kinetic model [24].

pH > 9. Chloroacetonitrile and *N*,2-dichloroacetamide formation rates at pH > 9 were characterized to investigate the effect of base catalysis. Species concentrations were determined by following the chloroacetaldehyde and monochloramine reaction with UV-Vis at 210 and 243 nm (UV-2). *N*,2-dichloroacetamide, monochloramine, and carbinolamine absorb at these wavelengths and the absorbance is equal to

$$A_{\lambda,t} = \varepsilon_{\mathrm{NH_2Cl}_\lambda}[\mathrm{NH_2Cl}]_t + \varepsilon_{\mathrm{ClCH_2CH(OH)NHCl}_{\lambda,\mathrm{t}}}[\mathrm{ClCH_2CH(OH)NHCl}]_t + \varepsilon_{\mathrm{ClCH_2C(O)NHCl}_{\lambda,\mathrm{t}}}[\mathrm{ClCH_2C(O)NHCl}]_t \quad (17)$$

Substituting equilibrium equation 4, equation 17 is simplified to

$$A_{\lambda,t} = (\varepsilon_{\mathrm{NH_2Cl}_\lambda} + \varepsilon_{\mathrm{ClCH_2CH(OH)NHCl}_{\lambda,\mathrm{t}}} K_1[\mathrm{ClCH_2CHO}])[\mathrm{NH_2Cl}]_t + \varepsilon_{\mathrm{ClCH_2C(O)NHCl}_{\lambda,\mathrm{t}}}[\mathrm{ClCH_2C(O)NHCl}]_t \quad (18)$$

where, $[\mathrm{NH_2Cl}]$ and $[\mathrm{ClCH_2C(O)NHCl}]$ concentrations at time *t* are calculated from absorbance values at 210 and 243 nm. $[\mathrm{ClCH_2C(O)NHCl}]$ and $C_{T,NCl}$ were then calculated with equations 4 and 11. Experiments were replicated and analyzed with GC/MS (GC-2) to confirm species concentrations obtained from UV-2 as shown in Figures 2.8 and 2.9. Initial decay results were then fitted to the kinetic model to obtain k_2 and k_3 (Figure 2.10) assuming monochloramine decomposition is negligible for experimental conditions of UV-2 and GC-2. Results display a

strong base catalysis effect for the formation of *N*,2-dichloroacetamide and chloroacetonitrile. Experimental data and kinetic model predictions for *N*,2-dichloroacetamide are shown in Figure 2.11. Model predictions for chloroacetonitrile are shown in Figure 2.12.

pH = 7.5. At neutral pH, chloroacetonitrile and *N*,2-dichloroacetamide formation rates are considerably slower, and side reactions with trace impurities from the synthesized chloroacetaldehyde becomes relevant, making it difficult to obtain kinetic constants for the reactions under study. Therefore, a higher concentration of monochloramine of 2 mM and a lower concentration of chloroacetaldehyde of 5 mM was used to obtain kinetic constants at neutral pH (GC-1). Chloroacetonitrile and *N*,2-dichloroacetamide formation were quantified by GC/MS for 24 hrs. Initial formation results were then fitted to the kinetic model as shown in Figure 2.13 to obtain rate constants k_2 and k_3 (Figure 2.10).

Additionally, experiments at high and neutral pH display a higher *N*,2-dichloroacetamide formation rate compared to that of chloroacetonitrile. This phenomenon is consistent with a previous study where four different NOM models were chloraminated and observed a higher formation rate of HAcAm compared to that of HAN [4].

3.64 < pH < 6. The acid catalysis effect on k_2 and k_3 was investigated in the pH range between 3.64 and 6 with UV-3 and GC-3 experiments (Table 2.1). Chloroacetonitrile and *N*,2-dichloroacetamide were quantified with data from experimental set GC-3. However, *N*,2-dichloroacetamide was so low that it could not be accurately determined within the detection limits of the instrument. For this reason, *N*,2-dichloroacetamide was assumed negligible in this pH range and only initial chloroacetonitrile formation from each experiment was fitted to the kinetic model as shown in Figure 2.14 to determine k_2 (Figure 2.10).

Monochloramine, carbinolamine, and dichloramine concentrations were calculated from UV-3 over time assuming that *N*,2-dichloroacetamide was also negligible at these conditions. Similar analysis for UV-2 was used to obtain species concentrations at wavelengths 210 and 243 nm except that the absorbance is expressed as

$$A_{\lambda,t} = (\varepsilon_{\mathrm{NH_2Cl}_\lambda} + \varepsilon_{\mathrm{ClCH_2CH(OH)NHCl}_{\lambda,t}} K_1[\mathrm{ClCH_2CHO}])[\mathrm{NH_2Cl}]_t + \varepsilon_{\mathrm{NHCl_2}_{\lambda,t}}[\mathrm{NHCl_2}]_t \qquad (19)$$

where, $[\mathrm{NH_2Cl}]$ and $[\mathrm{NHCl_2}]$ at time *t* were calculated. $C_{T,NCl}$ and $[\mathrm{NHCl_2}]$ were fitted to the kinetic model to determine k_2. Results are in agreement with an acid catalysis that was observed with GC-3.

Rate Constants. Chloroacetonitrile was found to be acid and base catalyzed according to

$$k_2 = k_2^0 + k_2^H[H^+] + k_2^{OH}[OH^-] \qquad (20)$$

Acid and base rate constants were fitted simultaneously with reaction rates shown in Figure 2.10. Data sets GC-3, UV-3, UV-2, and GC-1 were fitted to equation 20. The acid and base rate constants were calculated to be 2.65 and 3.25 $M^{-1}s^{-1}$, respectively. k_2^0 was estimated to be 2.98 x 10^6 s^{-1}.

N,2-dichloroacetamide was found to be base catalyzed according to the following

$$k_3 = k_3^{OH}[OH^-] \qquad (21)$$

where, equation 21 was fitted with data set UV-2. Results are shown in Figure 2.10. The base rate constant was calculated to be 3.13 x 10^4 $M^{-2}s^{-1}$.

2.3.4. *N*,2-dichloroacetamide Cytotoxicity

Experimental results were analyzed with a one-way analysis of variance (ANOVA) test which determined that there was a statistically significant difference between groups ($F_{11,164}$ = 95.477 , $P \leq 0.001$). The lowest cytotoxic concentration (150 μM) was identified by performing a Holm-Sidak pairwise comparison with the control group ($1\text{-}\beta \geq 0.8$, $\alpha=0.05$). Additionally, non-linear regression analysis was performed to a 4-parameter sigmoidal equation ($R^2=0.99$) to estimate the lethal concentration that reduces the cell density by 50% (%C½) compared to the negative control group. Experimental results and analysis are shown in Figure 2.15.

Several studies [21, 25-30] have tested numerous DBPs with chronic CHO cell cytotoxicity biological assay that allows a direct comparison between the toxicity of single DBP compounds. Haloacetamides have shown to be 142 times more cytotoxic than the 5 regulated haloacetic acids and twice more cytotoxic than haloacetonitriles[28]. *N*,2-dichloroacetamide falls in the same chemical class and so the importance of characterizing its cytotoxicity. Cytotoxicity of *N*,2-dichloroacetamide (%C½ = 2.56×10^{-4} M) was found to be slightly less potent compared to chloroacetamide (%C½ = 1.48×10^{-4} M) but more toxic than dichloro- and trichloroacetamide (%C½ of 1.92 and 2.05×10^{-3} M respectively).

2.3.5. Implications for Drinking Water

Oxidizing agents, such as chlorine, monochloramine, and ozone, react with organic matter to produce aldehydes including formaldehyde, acetaldehyde, halogenated acetaldehydes, and higher molecular weight aldehydes [1, 2, 8-10]. In particular, chloroacetaldehyde in the presence of monochloramine will quickly react and reach equilibrium with carbinolamine 2-

chloro-1-(chloroamino)ethanol. Therefore, this carbinolamine, a previously unreported DBP, will exist in the distribution system in the presence of chloroacetaldehyde.

Carbinolamine decomposition is acid and base catalyzed to form chloroacetonitrile and newly identified DBP *N*,2-dichloroacetamide. At high pH, carbinolamine dehydration and reaction are catalyzed to chloroacetonitrile and *N*,2-dichloroacetamide, respectively. Whereas at low pH, acid catalysis is observed only for chloroacetonitrile formation. Kinetic model simulations at drinking water conditions shown in Figure 2.16, predicts the formation of chloroacetonitrile, *N*,2-dichloroacetamide, and the carbinolamine at high and neutral pH conditions for a period of 5 days similar to the retention time in a distribution system. Chloroacetonitrile and *N*,2-dichloroacetamide formation is higher for pH 9.0 compared to neutral pH 7.8 and concentrations are observed in occurrence studies within similar order of magnitud [1, 2]. However, carbinolamine concentrations are relatively low and constant for the time simulated. Monochloramine and chloroacetaldehyde concentration effect at pH 9.0 are shown in Figures 2.17 and 2.18 where, higher reactant concentration produces a higher product formation.

However, DBPs speciation and identification in treated waters is highly influenced by water quality, and could also be an artifact of sample quenching and storage conditions and/or analytical method limitations. Common sampling methods include the addition of a quencher, such as ascorbic acid or sodium thiosulfate, followed by pH adjustment to 3.5 or 10 for further analysis. In the case of ascorbic acid, reaction with monochloramine is slow and will not fully be quenched [31, 32]. Storage conditions (pH 3.5 or 10) will then promote the formation of chloroacetonitrile and/or *N*,2-dichloroacetamide, resulting in artifacts of the sampling method. Alternatively, sodium thiosulfate was found to rapidly quench monochloramine followed by pH adjustment to 7-7.5 to minimize nitrile hydrolysis. Experiments under the same conditions but

analyzed with two different methods where 1) sodium thiosulfate was used as a quencher (GC-2) and 2) no quencher was applied (UV-2) both provided similar chloroacetonitrile and *N*,2-dichloroacetamide concentrations. Therefore, the sample quenching method did not produce an artifact in the results of this study.

Haloacetamides and haloacetonitrile formation is a growing concern due to their higher toxicity compared to regulated DBPs. Understanding the chemical formation of such compounds is necessary for controlling and monitoring DBPs that exist in drinking water. At high and/or low pH conditions, *N*,2-dichloroacetamide and chloroacetonitrile formation are enhanced and should be avoided. Instead, at neutral pH conditions the formation rate of both species is the slowest and their formation can be minimized. Such DBP control strategies can be applied to drinking water treatment and distribution systems to reduce their formation.

Literature Cited

1. Weinberg, H. S.; Krasner, S. W.; Richardson, S. D.; Thruston, A. D. J. *The Occurrence of Disinfection By-Products (DBPs) of Health Concern in Drinking Water: Results of a Nationwide DBP Occurrence Study*; EPA National Exposure Research Laboratory: Athens, GA, EPA/600/R-02/068, 2002.

2. Krasner, S. W.; Weinberg, H. S.; Richardson, S. D.; Pastor, S. J.; Chinn, R.; Sclimenti, M. J.; Onstad, G. D.; Thruston Jr, A. D., Occurrence of a New Generation of Disinfection Byproducts. *Environmental Science & Technology* **2006,** *40*, (23), 7175-7185.

3. Shah, A. D.; Mitch, W. A., Halonitroalkanes, Halonitriles, Haloamides, and N-Nitrosamines: A Critical Review of Nitrogenous Disinfection Byproduct Formation Pathways. *Environmental Science & Technology* **2012,** *46*, (1), 119-131.

4. Huang, H.; Wu, Q. Y.; Hu, H. Y.; Mitch, W. A., Dichloroacetonitrile and dichloroacetamide can form independently during chlorination and chloramination of drinking waters, model organic matters, and wastewater effluents. *Environmental Science & Technology* **2012,** *46*, (19), 10624-10631.

5. Yang, X.; Fan, C.; Shang, C.; Zhao, Q., Nitrogenous disinfection byproducts formation and nitrogen origin exploration during chloramination of nitrogenous organic compounds. *Water Research* **2010,** *44*, (9), 2691-2702.

6. Pedersen, E. J.; Urbansky, E. T.; Marinas, B. J., Formation of Cyanogen Chloride from the Reaction of Monochloramine with Formaldehyde. *Environmental Science & Technology* **1999,** *33*, 4239-4249.

7. Le Cloirec, C.; Martin, G., In *Water Chlorination*, Jolley, R. L., Ed. Lewis Publishers, Inc: Chelsea, MI, 1985; Vol. 5, pp 821-834.

8. Schechter, D. S.; Singer, P. C., Formation of aldehydes during ozonation. *Ozone: Sci. Eng.* **1995,** *17*, (1), 53-69.

9. Richardson, S. D.; Thruston, A. D., Jr.; Caughran, T. V.; Chen, P. H.; Collette, T. W.; Floyd, T. L.; Schenck, K. M.; Lykins, B. W., Jr.; Sun, G.-r.; Majetich, G., Identification of New Ozone Disinfection Byproducts in Drinking Water. *Environmental Science & Technology* **1999,** *33*, (19), 3368-3377.

10. Krasner, S. W.; McGuire, M. J.; Jacangelo, J. G.; Patania, N. L.; Reagan, K. M.; Aieta, E. M., The occurrence of disinfection by-products in U.S. drinking water. *J. Am. Water Works Assoc.* **1989,** *81*, (8), 41-53.

11. Crampton, M. R.; Lord, D. S.; Millar, R., Some reactions of ammonia and primary amines with propanal, 2-chloroethanal, 2,2-dichloroethanal and 2,2,2-trichloroethanal in acetonitrile. *Journal Chemical Society, Perkin Transactions 2* **1997**, 909-916.

12. Jones, M. J., *Organic Chemistry*. 3rd ed.; Norton&Co: New York, 2005.

13. Glezer, V.; Harris, B.; Tal, N.; Iosefzon, B.; Lev, O., Hydrolysis of haloacetonitriles: Linear free energy relationship. Kinetics and products. *Water Research* **1999,** *33*, (8), 1938-1948.

14. Larsen, J.; Jorgensen, K. A.; Christensen, D., Duality of the permanganate ion in the oxidation of imines. Oxidation of imines to amides. *Journal of the Chemical Society, Perkin Transactions 1* **1991**, (5), 1187-1190.

15. Tank, R.; Pathak, U.; Vimal, M.; Bhattacharyya, S.; Pandey, L. K., Hydrogen peroxide mediated efficient amidation and esterification of aldehydes: Scope and selectivity. *Green Chemistry* **2011,** *13*, (12), 3350-3354.

16. Hodgson, D. M.; Kloesges, J.; Evans, B., Terminal aziridines by addition of Grignard reagents or organoceriums to an (alfa-chloro)sulfinylimine. *Synthesis* **2009**, (11), 1923-1932.

17. NIOSH Manual of Analytical Methods. In *Method S11, DHEW (NIOSH) Publ. No. 79-141*, U.S. Department of Health and Human Services, C., NIOSH, Ed. Cincinnati, OH, 1979; Vol. 5.

18. Kumar, K.; Day, R. A.; Margerum, D. W., Atom-transfer redox kinetics general-acid-assisted oxidation of iodide by chloramines and hypochlorite. *Inorganic Chemistry* **1986,** *25*, 4344-4350.

19. Wagner, E. D.; Rayburn, A. L.; Anderson, D.; Plewa, M. J., Analysis of mutagens with single cell gel electrophoresis, flow cytometry, and forward mutation assays in an isolated clone of Chinese hamster ovary cells. *Environmental and Molecular Mutagenesis* **1998,** *32*, (4), 360-368.

20. Plewa, M. J.; Kargalioglu, Y.; Vankerk, D.; Minear, R. A.; Wagner, E. D., Mammalian cell cytotoxicity and genotoxicity analysis of drinking water disinfection by-products. *Environmental and Molecular Mutagenesis* **2002,** *40*, (2), 134-142.

21. Plewa, M. J.; Wagner, E. D. *Mammalian Cell Cytotoxicity and Genotoxicity of Disinfection By-Products*; Water Research Foundation: Denver, CO, 2009; p 134.

22. Greenzaid, P.; Luz, Z.; Samuel, D., A Nuclear Magnetic Resonance Study of the Reversible Hydration of Aliphatic Aldehydes and Ketones. I. Oxygen-17 and Proton Spectra and equilibrium constants. *Journal of the American Chemical Society* **1966,** *89*, 749-756.

23. Bell, R. P.; Evans, P. G., Kinetics of the Dehydration of Methylene Glycol in Aqueous Solution. *Proceedings of the Royal Society of London. Series A, Mathematical and Physical Sciences* **1966,** *291*, (1426), 297-323.

24. Valentine, R. L.; Jafvert, C. T., Reaction Scheme for the Chlorination of Ammoniacal Water. *Environmental Science & Technology* **1992,** *26*, 577-586.

25. Plewa, M. J.; Wagner, E. D.; Jazwierska, P.; Richardson, S. D.; Chen, P. H.; McKague, A. B., Halonitromethane Drinking Water Disinfection Byproducts: Chemical Characterization and Mammalian Cell Cytotoxicity and Genotoxicity. *Environmental Science & Technology* **2004,** *38*, (1), 62-68.

26. Richardson, S. D.; Crumley, F. G.; Ellington, J. J.; Evans, J. J.; Blount, B. C.; Silva, L. K.; Cardinali, F. L.; Plewa, M. J.; Wagner, E. D., Occurrence and toxicity of iodo-acid and iodo-THM DBPs in chloraminated drinking water. *Proceedings of Symposium on Safe Drinking Water: Where Science Meets Policy* **2006**.

27. Muellner, M. G.; Wagner, E. D.; McCalla, K.; Richardson, S. D.; Woo, Y. T.; Plewa, M. J., Haloacetonitriles vs. regulated haloacetic acids: Are nitrogen-containing DBFs more toxic? *Environmental Science & Technology* **2007,** *41*, (2), 645-651.

28. Plewa, M. J.; Muellner, M. G.; Richardson, S. D.; Fasano, F.; Buettner, K. M.; Yin-Tak, W.; McKague, A. B.; Wagner, E. D., Occurrence, Synthesis, and Mammalian Cell Cytotoxicity and Genotoxicity of Haloacetamides: An Emerging Class of Nitrogenous Drinking Water Disinfection Byproducts. *Environmental Science & Technology* **2008,** *42*, (3), 955-961.

29. Richardson, S. D.; Thruston Jr, A. D.; Rav-Acha, C.; Groisman, L.; Popilevsky, I.; Juraev, O.; Glezer, V.; McKague, A. B.; Plewa, M. J.; Wagner, E. D., Tribromopyrrole, brominated acids, and other disinfection byproducts produced by disinfection of drinking water rich in bromide. *Environmental Science & Technology* **2003,** *37*, (17), 3782-3793.

30. Plewa, M. J.; Wagner, E. D.; Richardson, S. D.; Thruston, A. D.; Woo, Y.-T.; McKague, A. B., Chemical and biological characterization of newly discovered iodoacid drinking water disinfection byproducts. *Environmental Science & Technology* **2004,** *38*, 4713-22.

31. Bedner, M.; MacCrehan, W. A.; Helz, G. R., Making chlorine greener: investigation of alternatives to sulfite for dechlorination. *Water Research* **2004,** *38,* (10), 2505-2514.

32. Basu, O. D.; De Souza, N. P., Comparison of dechlorination rates and water quality impacts for sodium bisulfite, sodium thiosulfate and ascorbic acid. *Journal of Water Supply: Research and Technology - AQUA* **2011,** *60,* (3).

Tables and Figures

Table 2.1 Summary of chloroacetaldehyde and monochloramine experimental conditions and instrumentation used to monitor the reaction

Exp Set	$p[H^+]$	$[NH_2Cl]_0$ (M)	$C_{T,ClCH2CHO}$ (M)	Buffer	$C_{T,\ Buffer}$ (M)	Instrument
UV-1	7.6	0.001	0.010 – 0.040	Phosphate	0.020	UV-Vis
UV-2	9.39 - 9.99	0.001	0.010	Carbonate	0.020	UV-Vis
UV-3	3.64 & 4.00	0.001	0.010	Phosphate	0.020	UV-Vis
GC-1	7.49 - 7.5	0.002	0.005	Phosphate	0.020	GC/MS
GC-2	9.39 & 9.87	0.001	0.010	Carbonate	0.020	GC/MS
GC-3	4.22 - 5.99	0.001	0.010	Phosphate	0.020	GC/MS

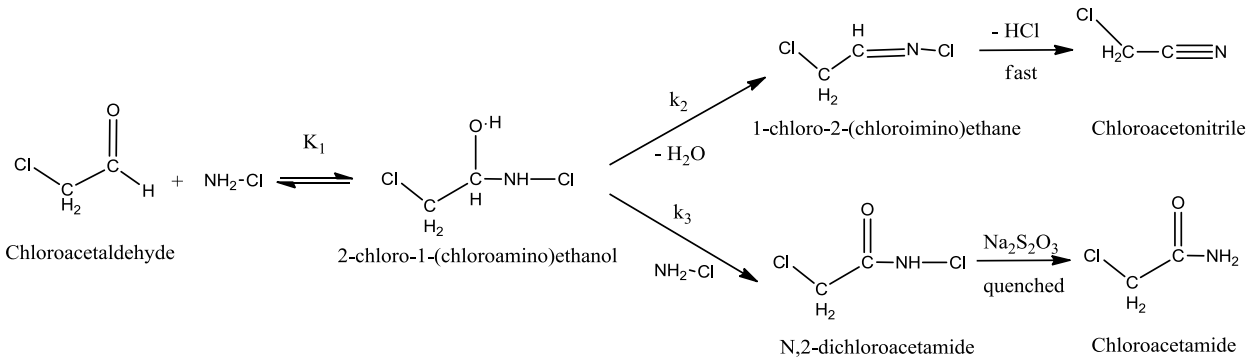

Figure 2.1 Proposed *N*,2-dichloroacetamide and chloroacetonitrile formation pathway from the reaction of chloroacetaldehyde and monochloramine

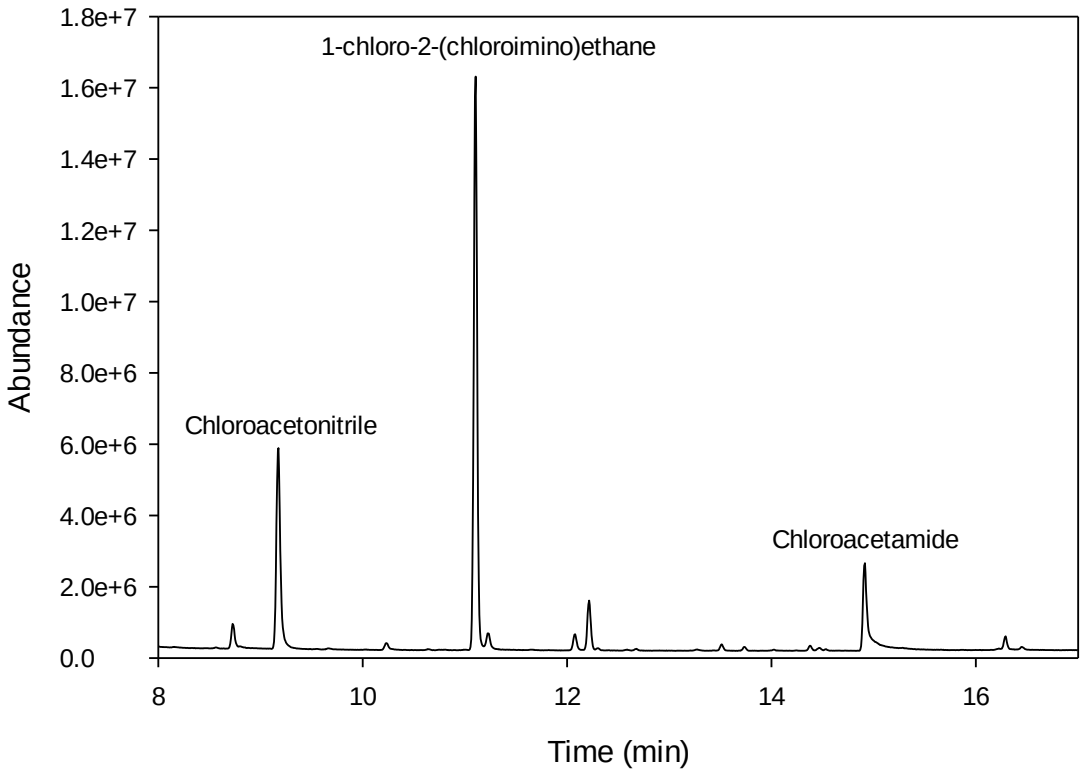

Figure 2.2 GC/MS Total Ion Chromatogram, 30 minutes reaction extract $[NH_2Cl]_0$ = 1 mM, $[ClCH_2CHO]_{T,0}$ = 10 mM, $[CO_3]_{T,0}$ = 0.02 M, pH 9.00 ± 0.1, μ = 0.1 M, 18 ± 0.1^{0}C.

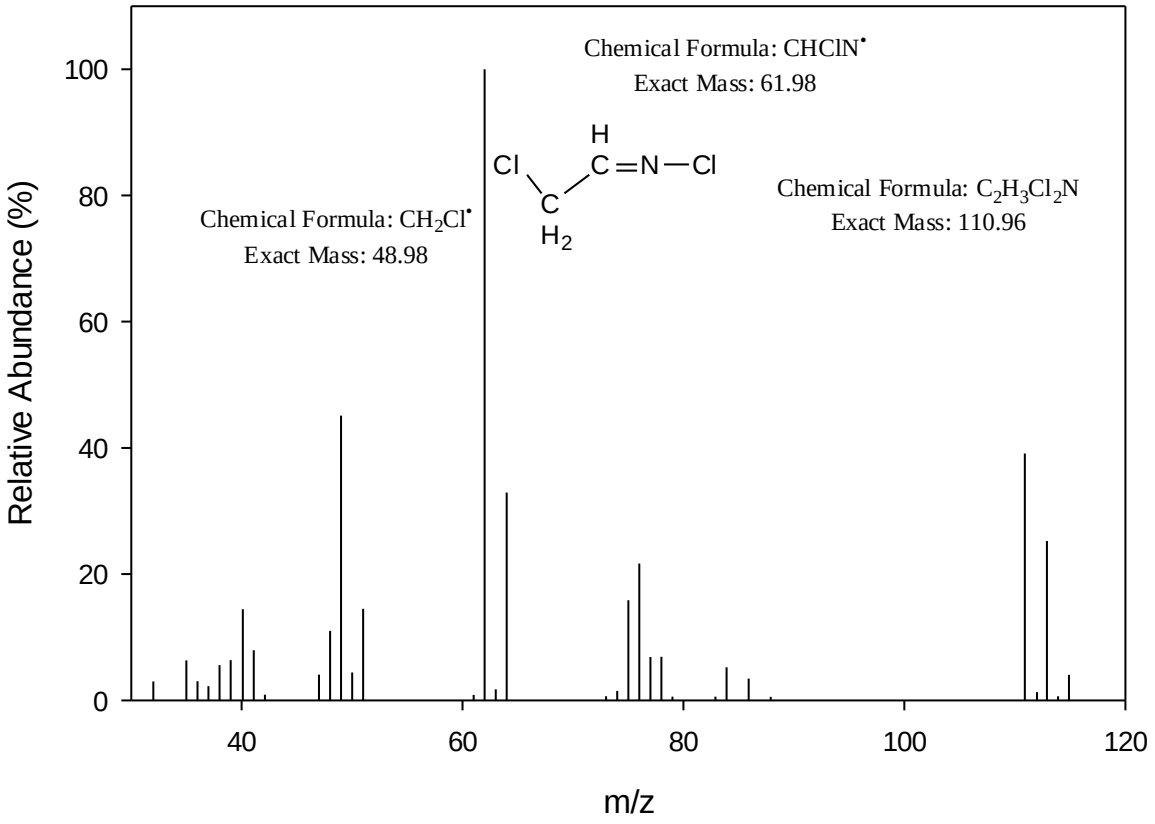

Figure 2.3 1-chloro-2-(chloroimino)ethane mass spectra m/z: 62(100%), 64(33%), 49 (45%), 51(14%), 111(39%), 113(25%)

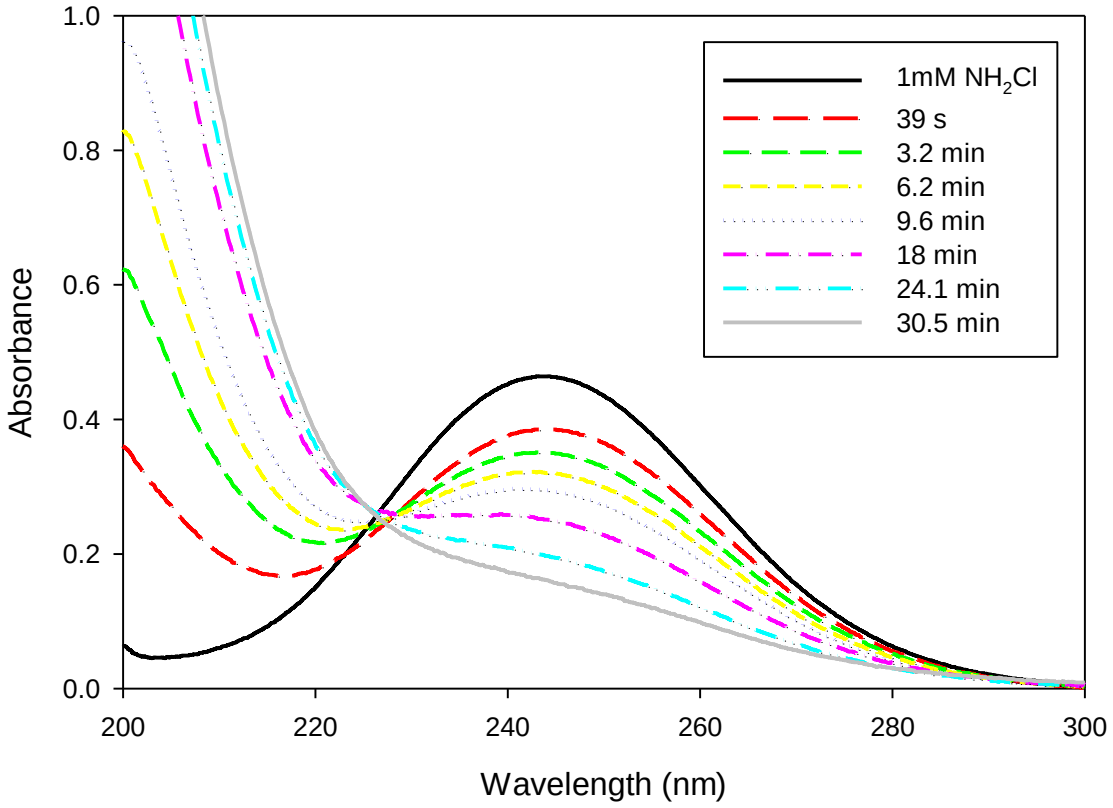

Figure 2.4 Chloroacetaldehyde and monochloramine reaction spectras over time, $[NH_2Cl]_0$ = 1 mM, $[ClCH_2CHO]_{T,0}$ = 10 mM, $[CO_3]_{T,0}$ = 0.02 M, pH 9.34 ± 0.1, μ = 0.1 M, 18 ± 0.1^oC

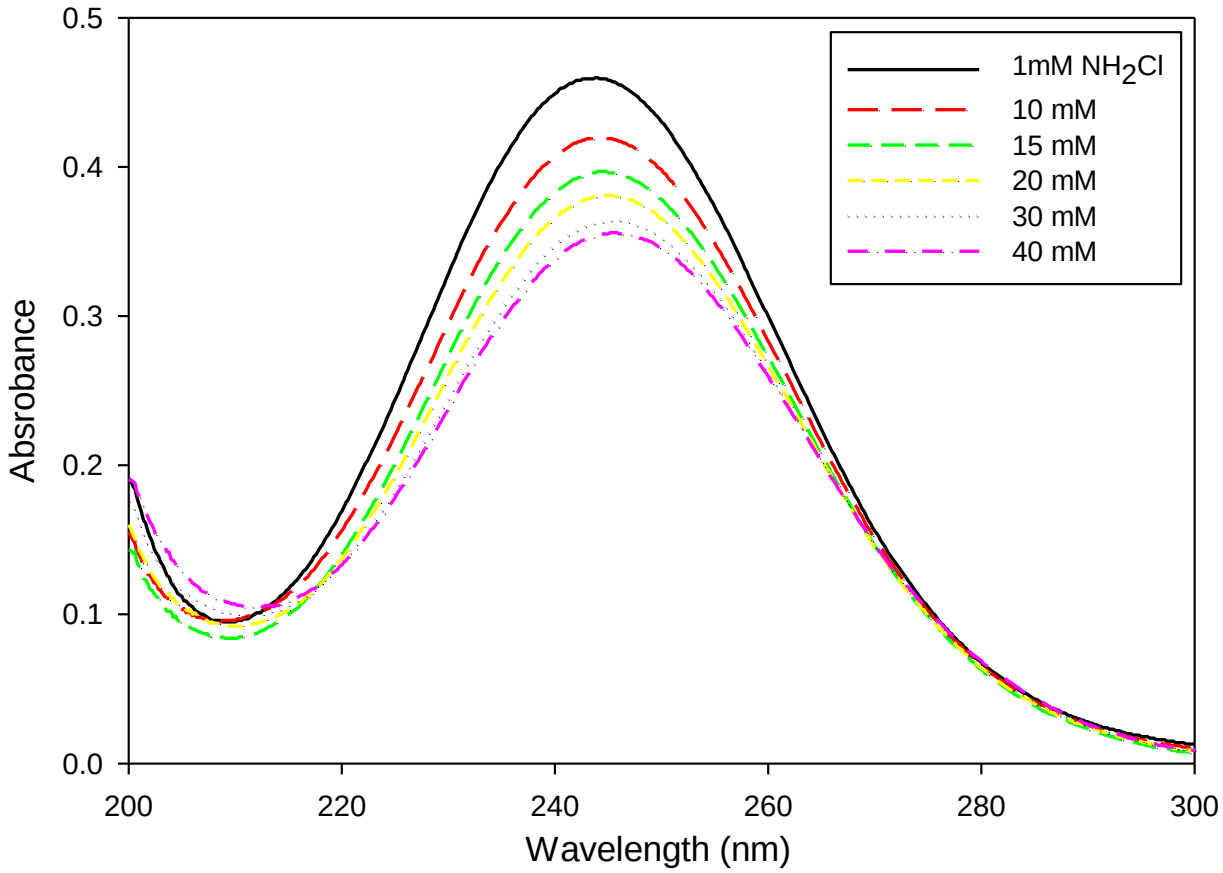

Figure 2.5 Chloroacetaldehyde and monochloramine reaction taken at 1 to 3 min (UV-1) with increasing chloroacetaldehyde concentration, $[NH_2Cl]_0$ = 1 mM, $[ClCH_2CHO]_{T,0}$ = 15 - 40 mM, $[PO_4]_{T,0}$ = 0.02 M, pH 7.8 ± 0.1, μ = 0.1 M, 18 ± 0.1^{0}C

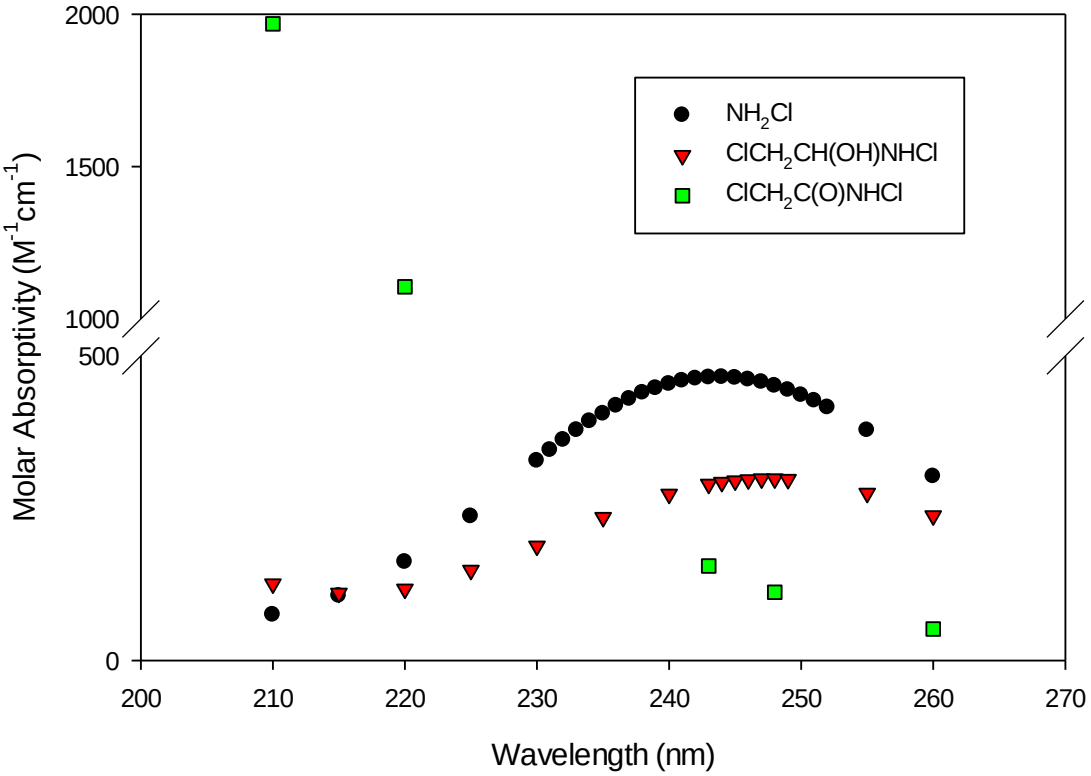

Figure 2.6 Monochloramine, 2-chloro-1-(chloroamino)ethanol and *N*,2-dichloroacetamide molar absorptivities determined in this study

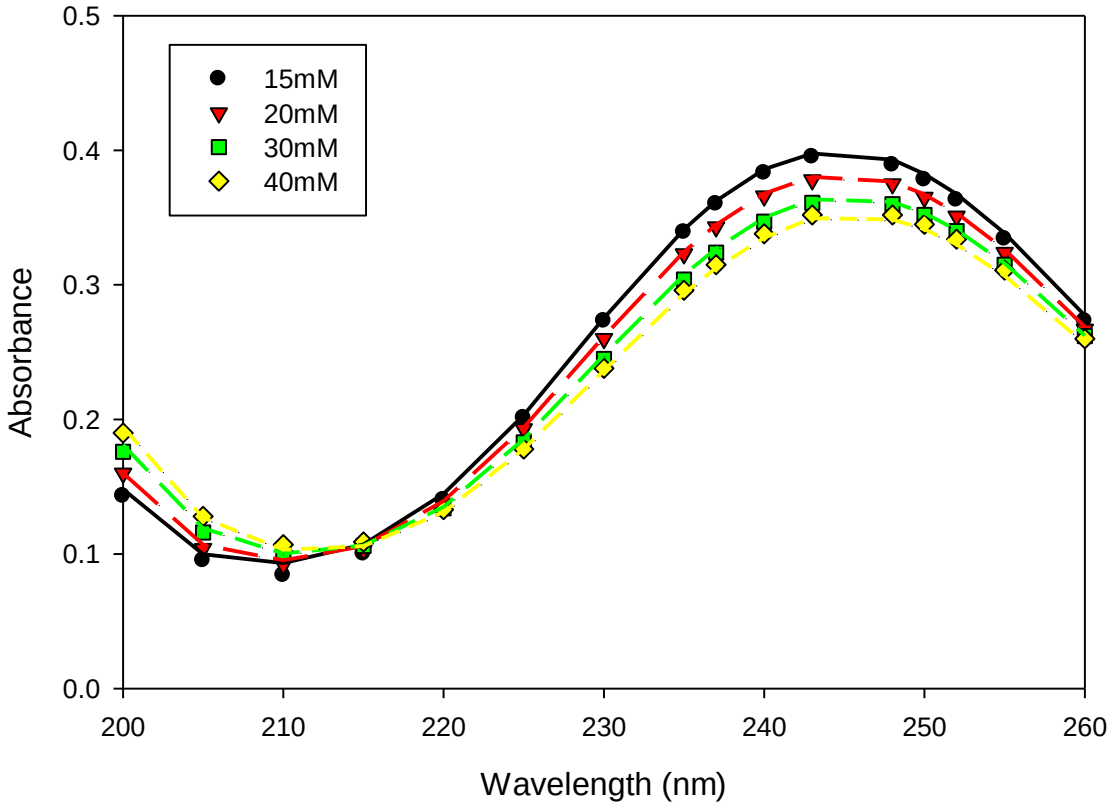

Figure 2.7 Chloroacetaldehyde and monochloramine 1-3 min equilibrium spectras (UV-1) and absorbance values calculated with K_1 and 2-chloro-1-(chloroamino)ethanol molar absorptivities

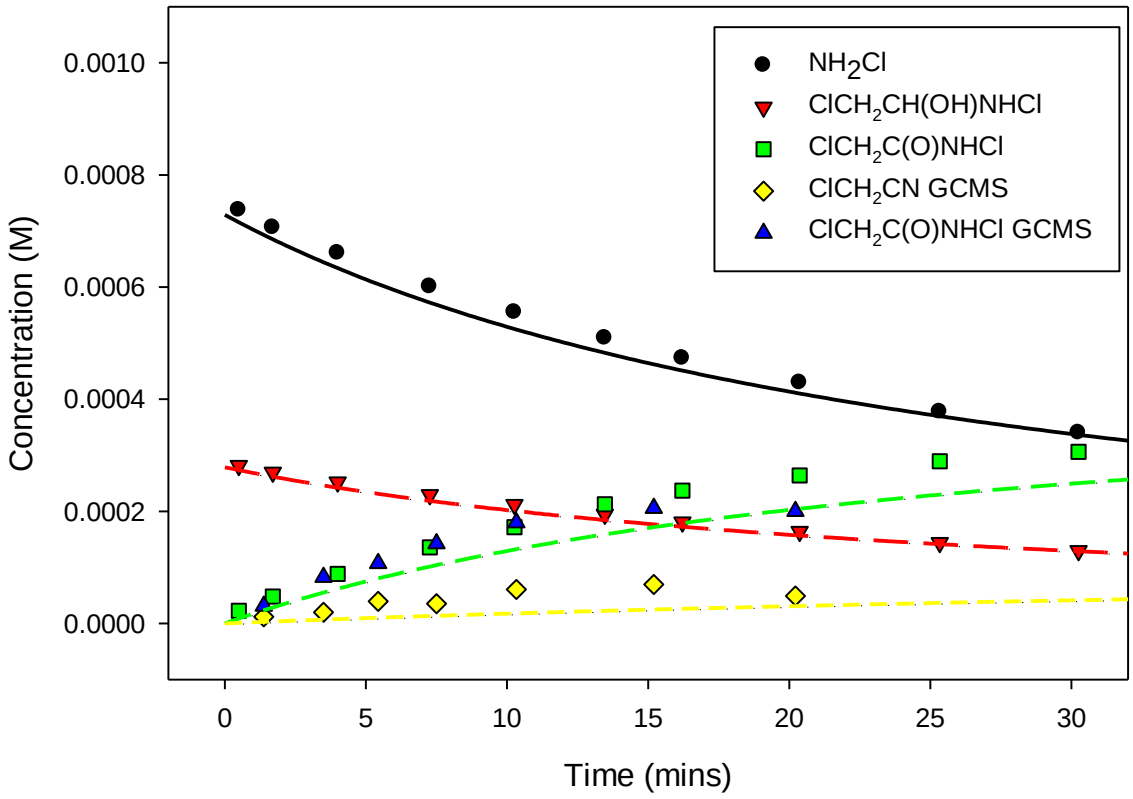

Figure 2.8 Monochloramine, 2-chloro-1-(chloroamino)ethanol, *N*,2-dichloroacetamide, and chloroacetonitrile concentrations over time (UV-2 and GC-2) $[NH_2Cl]_0$ = 1 mM, $[ClCH_2CHO]_{T,0}$ = 10 mM, $[CO_3]_{T,0}$ = 0.02 M, pH 9.34 ± 0.1, μ = 0.1 M, 18 ± 0.1^{0}C

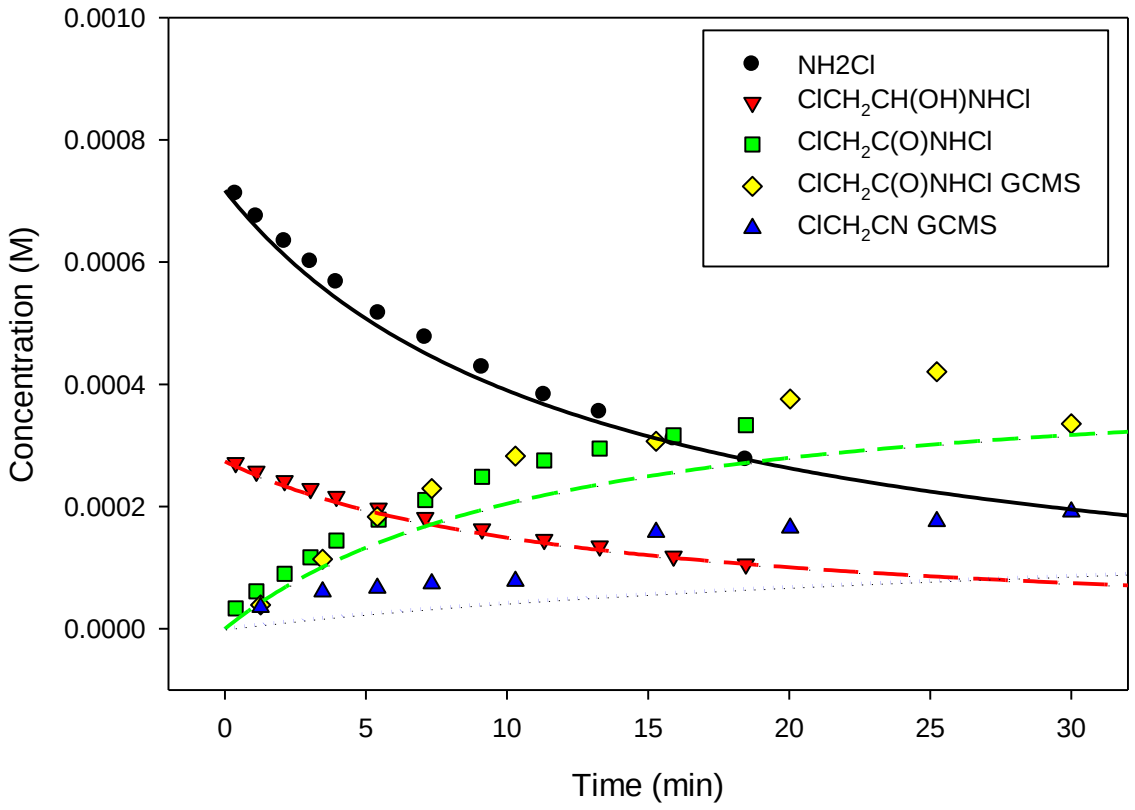

Figure 2.9 Monochloramine, 2-chloro-1-(chloroamino)ethanol, *N*,2-dichloroacetamide, and chloroacetonitrile concentrations over time (UV-2 and GC-2). $[NH_2Cl]_0$ = 1 mM, $[ClCH_2CHO]_{T,0}$ = 10 mM, $[CO_3]_{T,0}$ = 0.02 M, pH 9.83 ± 0.1, μ = 0.1 M, 18 ± 0.1^{0}C

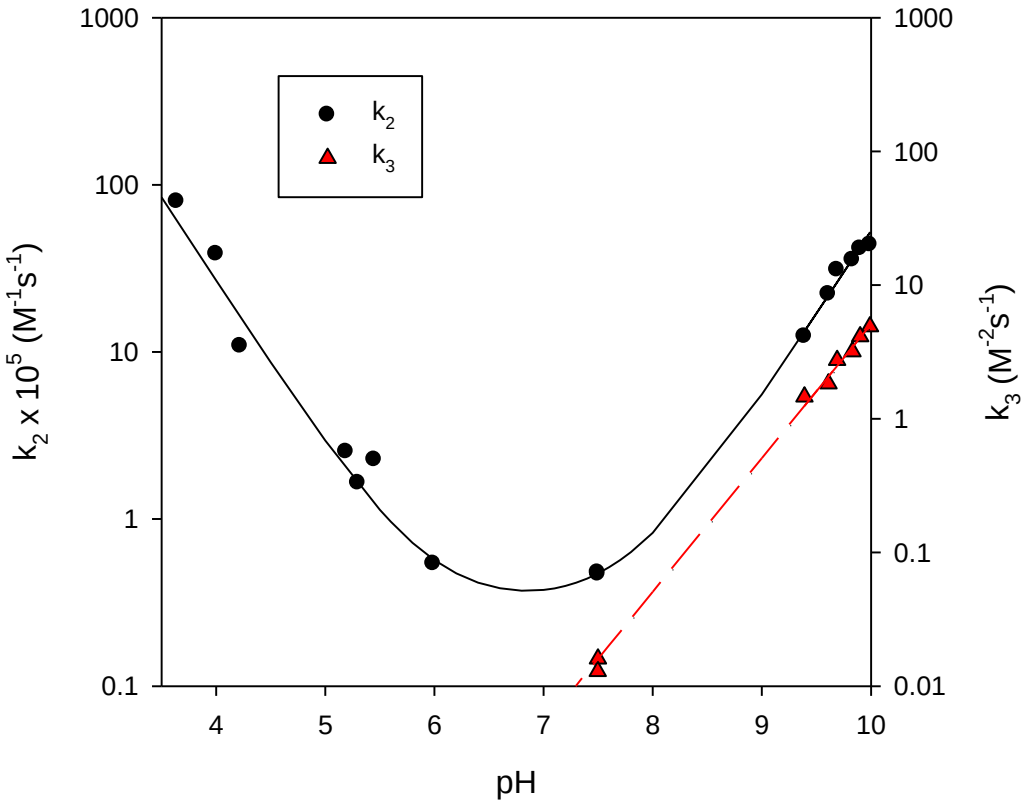

Figure 2.10 Chloroacetonitrile (k_2) and *N*,2-Dichloroacetamide (k_3) rate formation from the reaction of chloroacetaldehyde and monochloramine (UV-2, UV-3, GC-1, GC-2, GC-3)

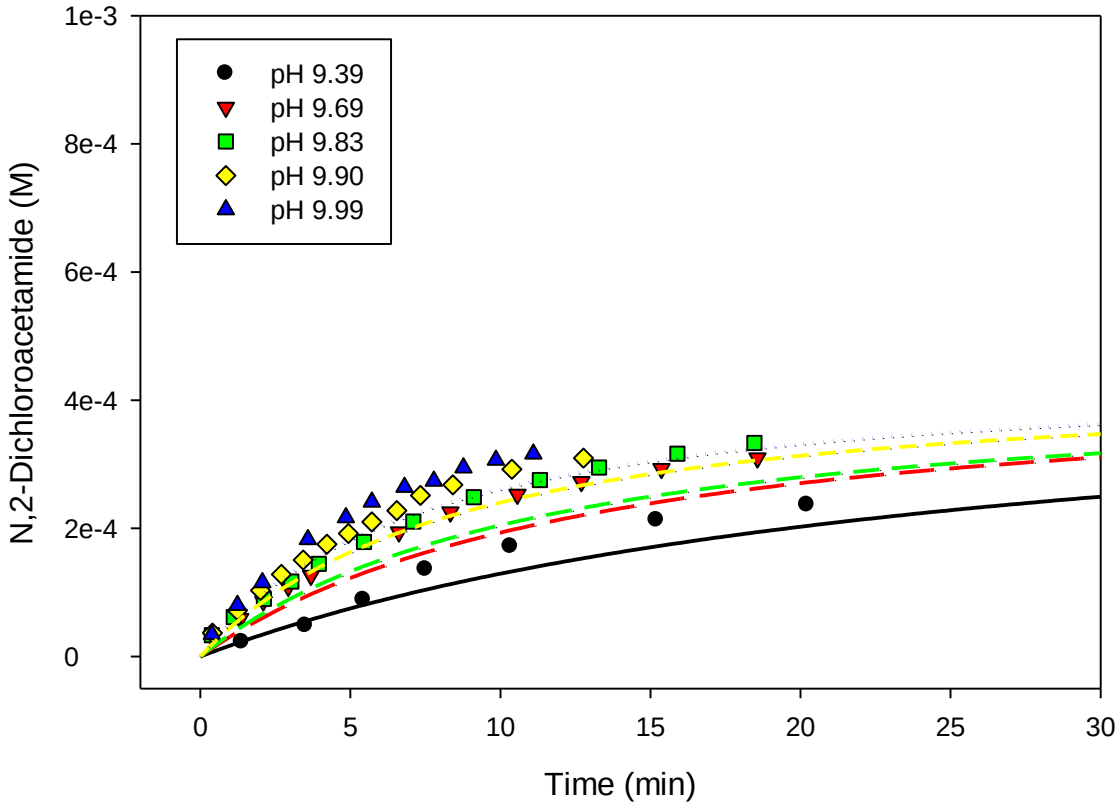

Figure 2.11 *N*,2-Dichloroacetamide UV-2 data and model prediction

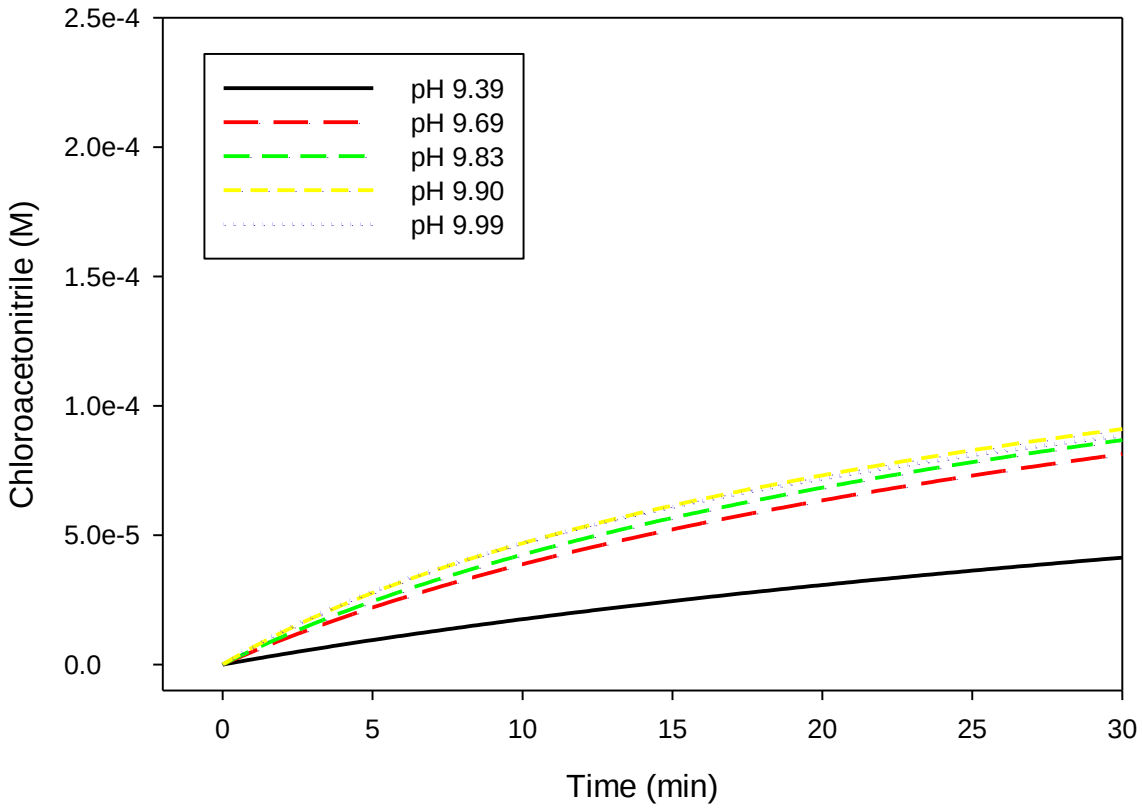

Figure 2.12 Chloroacetonitrile UV-2 model prediction

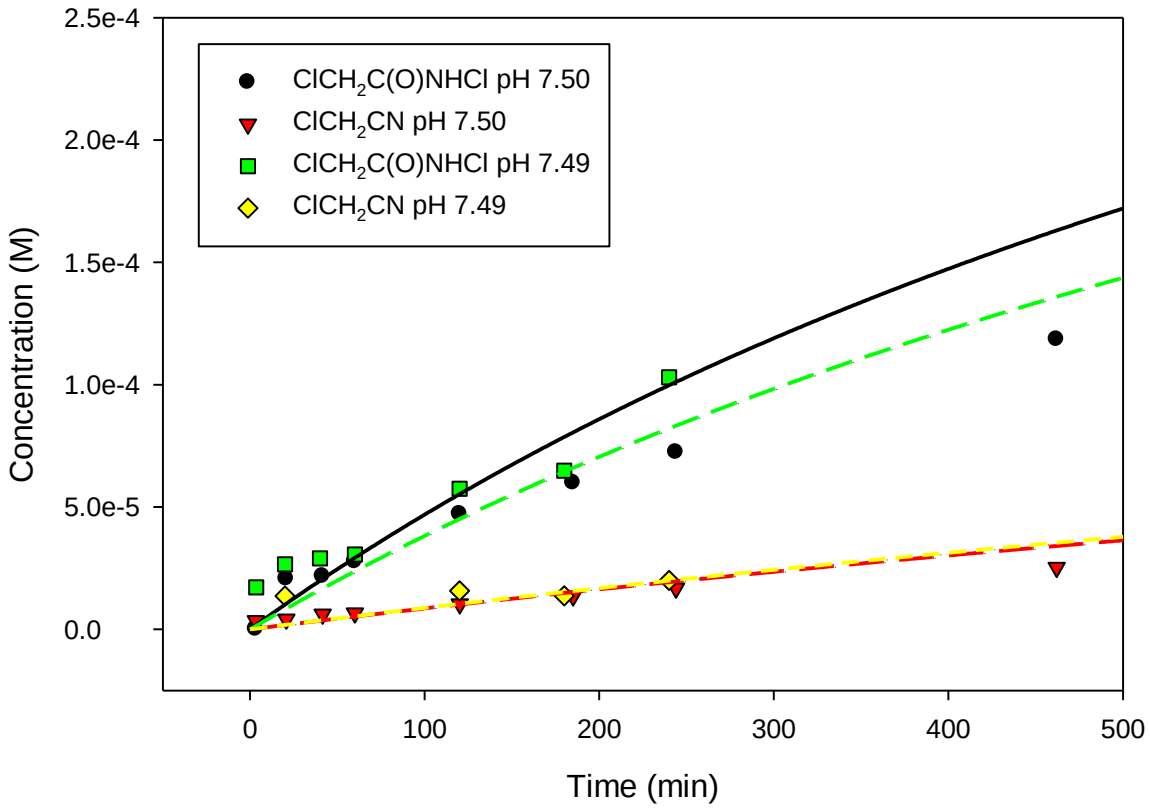

Figure 2.13 GC-1 data and model prediction

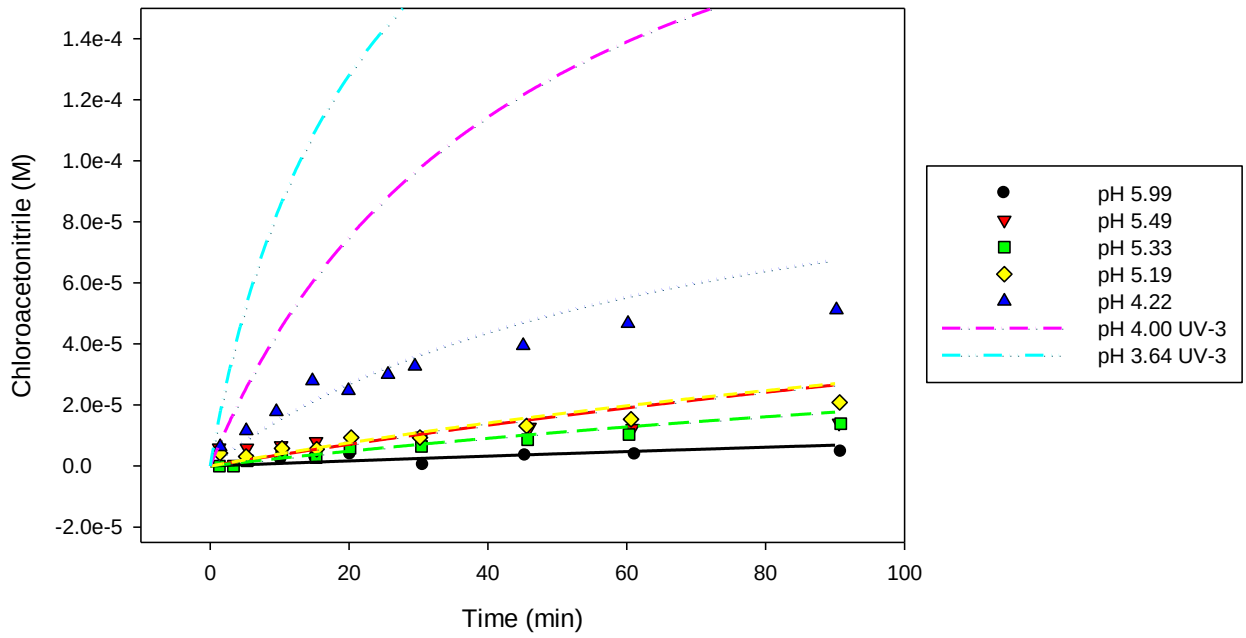

Figure 2.14 Chloroacetonitrile GC-3 data and model prediction and UV-3 model prediction

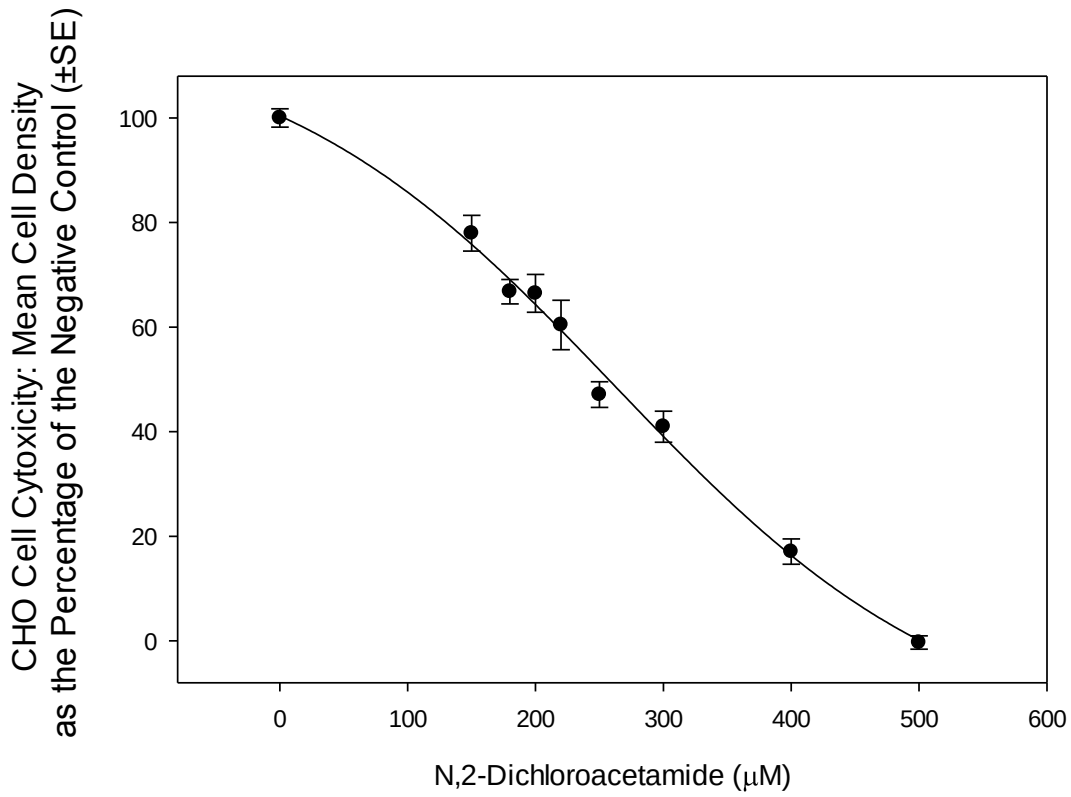

Figure 2.15 *N*,2-dichloroacetamide concentration-response curve and regression curve for chronic CHO cell cytotoxicity

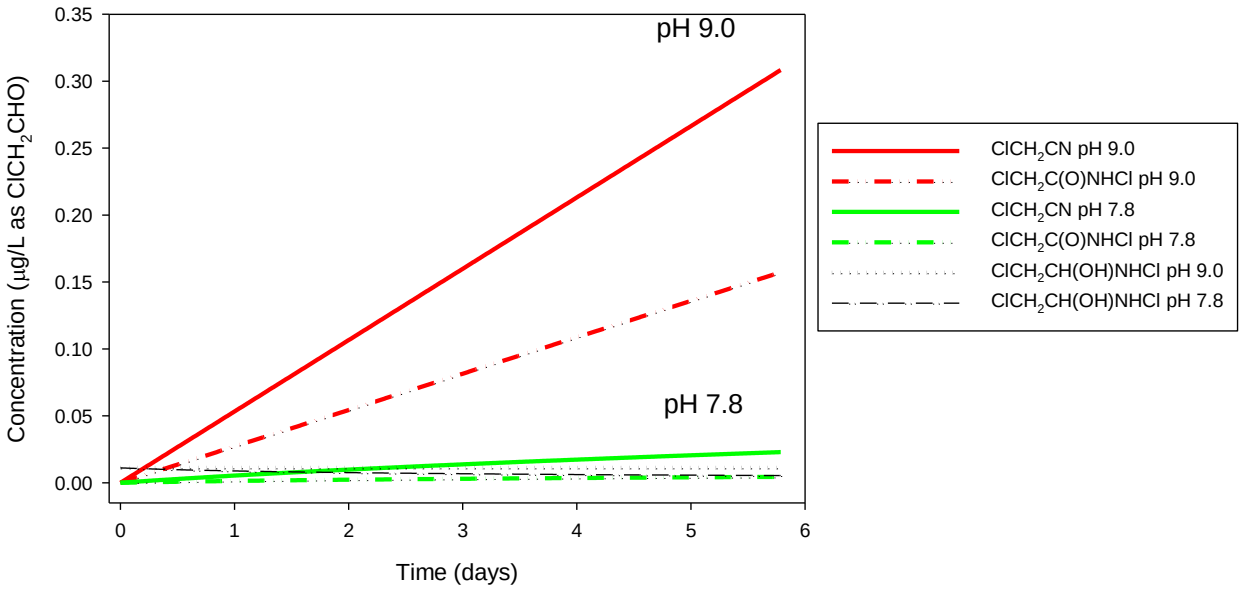

Figure 2.16 pH effect on chloroacetonitrile, *N*,2-dichloroacetamide, and 2-chloro-1-(chloroamino)ethanol formation over time at drinking water conditions. $[NH_2Cl]_0$ = 4 mg/L as Cl_2, $[ClCH_2CHO]_{T,0}$ = 5 µg/L, pH=9.0 & 7.8, 18°C

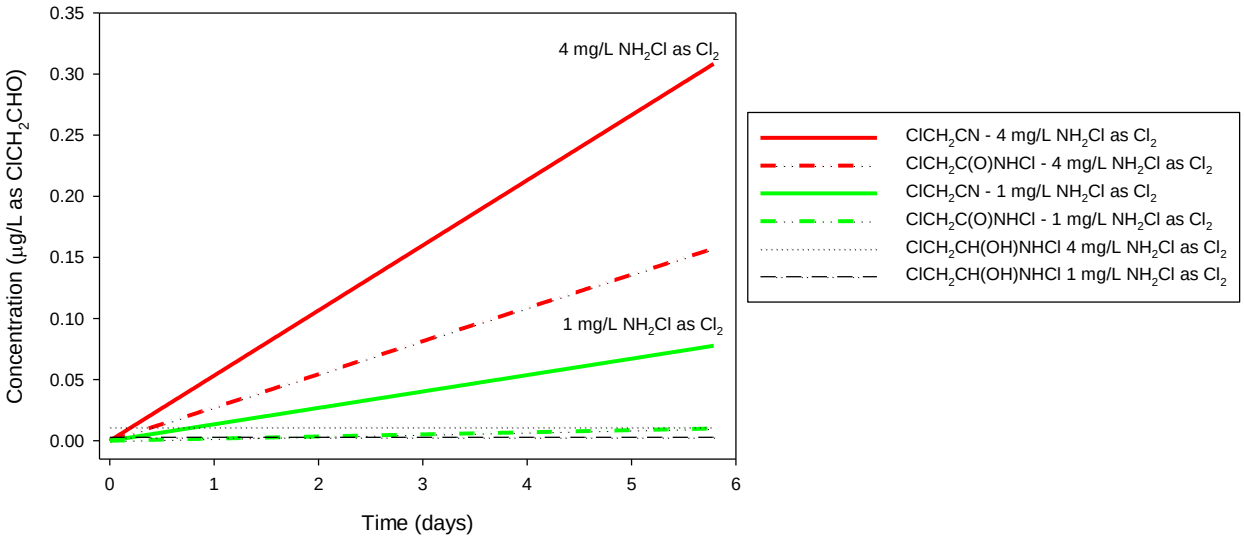

Figure 2.17 Monochloramine concentration effect on chloroacetonitrile, *N*,2-dichloroacetamide, and 2-chloro-1-(chloroamino)ethanol formation over time at drinking water conditions. $[NH_2Cl]_0$ = 1 & 4 mg/L as Cl_2, $[ClCH_2CHO]_{T,0}$ = 5 µg/L, pH=9.0, 18°C

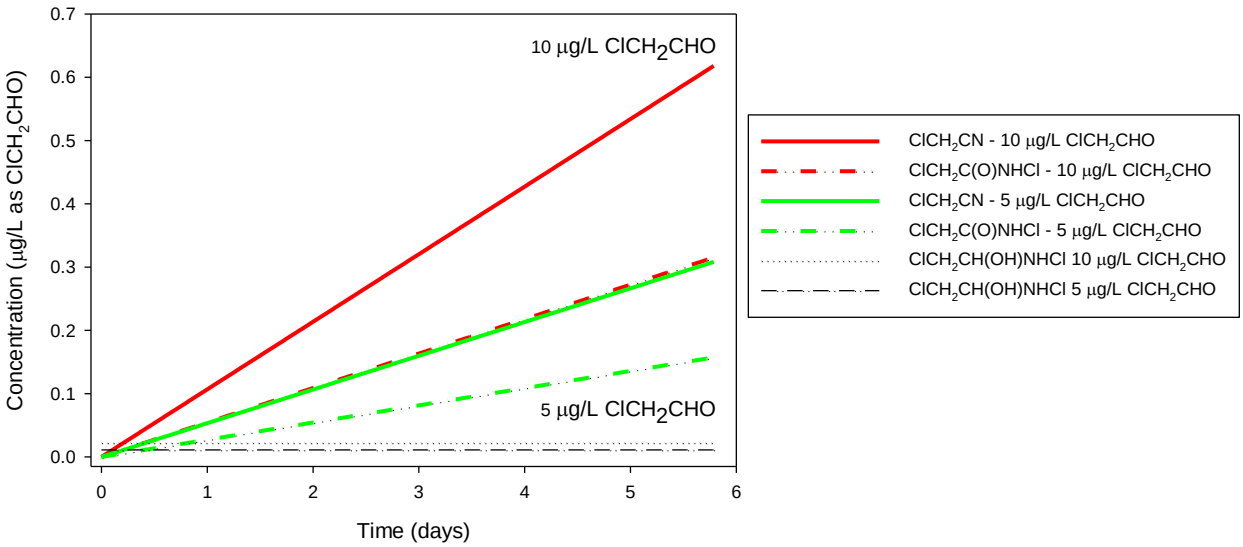

Figure 2.18 Chloroacetaldehyde concentration effect on chloroacetonitrile, *N*,2-dichloroacetamide, and 2-chloro-1-(chloroamino)ethanol formation over time at drinking water conditions. $[NH_2Cl]_0$ = 4 mg/L as Cl_2, $[ClCH_2CHO]_{T,0}$ = 5 & 10 µg/L, pH=9.0, 18°C

CHAPTER 3

ACETONITRILE AND *N*-CHLOROACETAMIDE FORMATION FROM THE REACTION OF ACETALDEHYDE AND MONOCHLORAMINE

Abstract

Nitriles and acetamides are two classes of nitrogenous disinfection by-products (N-DBPs) that are more toxic than regulated DBPs and their formation is increased with chloramination. Monochloramine reacts with acetaldehyde, a common ozone and free chlorine disinfection by-product, to form 1-(chloroamino)ethanol. Equilibrium constants between initial reactants and 1-(chloroamino)ethanol were calculated to be 147 ± 2.42 M^{-1} and 109 ± 2.59 M^{-1} for 18 and 25 ° C and enthalpy change (ΔH^{o}) equal to -30.84 kJ/mol. In parallel reactions, 1-(chloroamino)ethanol 1) slowly dehydrates to (chloroimino)ethane that further decompose to acetonitrile and 2) is oxidized by monochloramine to produce *N*-chloroacetamide. Both reactions were found to be acid and base catalyzed with dehydration rate constants equal to k_{ii}^{H} = 137 $M^{-1}s^{-1}$ and k_{ii}^{OH} = 1.92 $M^{-1}s^{-1}$ for 18 °C and k_{ii}^{H} = 251 $M^{-1}s^{-1}$ and k_{ii}^{OH} = 4.43 $M^{-1}s^{-1}$ for 25°C. Rate constants for the oxidation reaction are equal to $k_{iii}^{H} = 1.37 \times 10^{6}$ $M^{-2}s^{-1}$ and $k_{iii}^{OH} = 1.27 \times 10^{4}$ $M^{-2}s^{-1}$ for 18°C and $k_{iii}^{H} = 2.02 \times 10^{6}$ $M^{-2}s^{-1}$ and $k_{iii}^{OH} = 3.55 \times 10^{4}$ $M^{-2}s^{-1}$ for 25°C. Carbonate buffer did not affect the reaction rates.

3.1. Introduction

Acetonitriles and acetamides are nitrogenous disinfection by-products (N-DBPs) of growing concern because of their elevated toxicity compared to regulated trihalomethanes and haloacetic acids. N-DBPs have an enhanced formation as a result of chloramination [1-3]. However, some water utilities need to comply with stricter regulations and as a result use alternative disinfection schemes such as ozonation/chloramination as an alternative to free chlorination.

Nitrile formation in treated waters can be formed by different reaction pathways such as reactions involving organic nitrogen (e.g. free amino acids) found in source waters with disinfectants [4]. However, recent research has found that greater than 70% of the nitrogen contained in nitriles and acetamides are incorporated from labeled $^{15}NH_2Cl$ when reacted with different NOM models [3, 5]. Previous studies have suggested that nitriles are also formed from a reaction pathway initiated by monochloramine reacting with aldehydes (e.g. formaldehyde, acetaldehyde) [6, 7], by-products predominantly formed by ozonation [8-10] and free chlorine [11]. Monochloramine reacts with formaldehyde in a fast and reversible reaction to form the carbinolamine *N*-chloroaminomethanol [6]. *N*-chloroaminomethanol slowly, under acid/base catalyzed dehydration, form *N*-chloromethanimine, the rate-limited neutral pH conditions encountered in drinking water. *N*-chloromethanimine subsequently decomposes to hydrogen cyanide. Further reaction of cyanide with monochloramine produces cyanogen chloride.

A similar reaction pathway was proposed for acetonitrile formation by monochloramine reacting with acetaldehyde [7]. Monochloramine can attach to the slightly positive carbonyl carbon to produce 1-(chloroamino)ethanol followed by a dehydration to (chloroimino)ethane that

decomposes to acetonitrile. However, kinetic rates were not determined and consequently, the formation of acetonitrile under different conditions remains unknown. Due to the similarity to the formaldehyde and monochloramine reaction it is expected that dehydration of the intermediate 1-(chloroamino)ethanol would be rate limiting step and acid and base catalyzed.

In Chapter 2 it was shown that carbinolamine produced from the reaction of monochloramine and chloroacetaldehyde react with monochloramine to form *N*,2-dichloroacetamide. Therefore, it is hypothesized that 1-(chloroamino)ethanol is also oxidized by monochloramine to produce *N*-chloroacetamide. The objective of this study is to characterize the reaction pathways and rate constants for the reaction of monochloramine and acetaldehyde.

3.2. Experimental Section

Reagents. All chemical reagents of ACS or laboratory grade were purchased from Sigma-Aldrich (St. Louis, MO) and Fisher Scientific (Pittsburgh, PA). All solutions were prepared at specific pH, phosphate or carbonate buffer concentration of 0.02 M, and ionic strength of 0.1 M in nanopure water. Potassium phosphate monobasic and sodium bicarbonate were first added as corresponding phosphate or carbonate buffers followed by sodium perchlorate for ionic strength adjustment. Fluka 70% puriss perchloric acid (70%) and 10 M sodium hydroxide solutions were then used to adjust pH to a desired value.

Acetaldehyde stock solutions of 1 to 2 M were prepared by diluting acetaldehyde (>99 %) in oxygen-free nanopure water and let depolymerize for several hours before use. Acetaldehyde was then standardized spectrophotometrically (λ_{max}=277nm, 7.2 $M^{-1}cm^{-1}$ @ 25°C) [12].

Monochloramine was prepared daily by mixing equal volumes of sodium hypochlorite solution and ammonium chloride solution. Both solutions were previously adjusted to pH of 8.5 to minimize the formation of dichloramine. The mixing consisted of a slow addition of sodium hypochlorite solution to a rapidly stirred ammonium chloride solution. Final monochloramine had an N/Cl molar ratio of 1.1. Sodium hypochlorite stock solution was standardized spectrophotometrically (λ_{max}=292 nm, 362 $M^{-1}cm^{-1}$). After mixing, monochloramine solutions were adjusted to a desired pH value. Monochloramine concentrations were measured spectrophotometrically (λ_{max}=243nm, 461 $M^{-1}cm^{-1}$) [13].

Acetamide and sodium thiosulfate stock solutions were prepared by dissolving each solid compound in nanopure water. Acetamide standard solutions were prepared by diluting acetamide stock solution to buffered solutions similar to experimental conditions.

N-chloroacetamide was prepared by reacting equal concentrations of acetamide and sodium hypochlorite at pH 7.5. *N*-chloroacetamide concentrations were calculated from the difference between the initial and remaining sodium hypochlorite concentrations determined from λ_{max}=292 nm.

Instrumental Methods. A batch reactor at constant temperature was maintained at 18 or 25 ºC with a water recirculator model 9501 (PolyScience, Niles, IL). Samples were taken over time and placed in 10 mm quartz cuvettes and analyzed with a UV-Vis Spectrophotometer model 2550 (Shimadzu Scientific Instruments, Columbia, MD). Equilibrium constant was determined from absorption spectras taken between 200 and 400 nm. Reaction rates were obtained from absorption measurements at 243 or 250 nm.

Volatile reaction pathway intermediates and products were identified by extracting with solid phase microextraction (SPME, Sigma Aldrich, St. Louis, MO) and analyzed with gas chromatography mass spectrometry (GC/MS) model 6850/5975C (Agilent Technologies, Santa Clara, CA). A 10 ml sample was mixed with 2.85 g of sodium sulfate in a 15 ml vial. The headspace was extracted for 30 minutes at 25ºC with a 85 μm Carboxen/PDMS fiber (Sigma Aldrich, St. Louis, MO) and desorbed at 250ºC for 1 minute and carried the sample thru a DB-624 column (Agilent J&W, Santa Clara, CA) at 1 ml/min. Oven was maintained at 35 ºC for 2 minutes and ramped at 10 ºC/min to 230ºC. Sample was ionized with electron impact technique and scanned from 30 to 250 amu.

Non-volatile acetamide were identified with liquid-liquid extraction. 10 ml samples were first quenched by 1.5 mM sodium thiosulfate followed by a pH adjustment to 7.8 for immediate extraction (<30 minutes). Standard solutions and samples were mixed with 1 ml of ethyl acetate, 2.85 g of sodium sulfate, and 6 mg/L of 1,2-dichloropropane as internal standard for 2 minutes and followed by a 3 minute separation phase. Extracts were then injected into the inlet at 230 ºC in splitless mode. GC/MS method differed from above in that sample was monitored using both scan from 30 to 200 amu and select ion monitoring for internal standard (m/z 63, 41.1) and acetamide ions (m/z 59, 44.1).

pH and temperature measurements were taken with a Thermo Electron Orion ROSS Ultra pH electrode (Thermo Fisher Scientific, Waltham, MA) and Accumet temperature (Fisher Scientific, Pittsburgh, PA) electrode connected to an Accumet AB15 Plus pH meter (Fisher Scientific, Pittsburgh, PA). Electrode calibration was performed with commercial 4, 7, and 10 pH standards. Actual hydrogen ion concentrations were corrected with activity coefficients calculated with the extended DeBye Huckel/Guntelberg equations.

Micromath Scientist 3.0 (St. Louis, MO) was used to obtain rate constants by fitting experimental data to the kinetic model using the simplex method. Model simulations under different conditions were also obtained with this software. Dissociation constants (K_a) for acid and bases used in this study were obtained from literature that summarizes K_a values at ionic strength of 0.1 M [14].

Experimental Matrix. Reaction rates and equilibrium constants were determined at different conditions specified in Table 3.1 with UV-Vis spectrophotometry. Experimental sets UV-1 and UV-2 were used to determine equilibrium constants between the reaction of acetaldehyde and monochloramine with intermediate 1-(chloroamino)ethanol. Dehydration and decomposition of *N*-chloro(ethanolamine) to its final products was monitored at conditions specified in experimental set UV-3, UV-4, UV-5, and UV-6. The occurrence of carbonate catalysis was also tested (UV-7). Acetaldehyde absorption at the monitored wavelengths was subtracted from all experiments.

3.3. Results and Discussion

3.3.1. Reaction pathway. Previous research has shown that monochloramine can attack aldehydes by nucleophilic addition on the slightly positive carbonyl carbon to form carbinolamines [6, 7]. Carbinolamines can further dehydrate to imine which then decompose to nitriles. Similarly, monochloramine reacts with acetaldehyde fast and reversibly to form 1-(chloroamino)ethanol as shown in Figure 3.1. 1-(chloroamino)ethanol loses water to form (chloroimino)ethane followed by decomposition to acetonitrile.

Reaction pathway intermediate and products were confirmed by GC/MS. Acetonitrile is volatile and thus it was extracted prior to analysis with SPME. However, this approach was only applicable for reactant concentrations that were relatively low within the concentration range investigated. Total acetaldehyde concentration of 0.2 mM was added to a stirred reactor containing 71 uM monochloramine at pH 7.53. Samples were extracted over time with SPME followed by GC/MS analysis. Results confirm the presence of acetonitrile and (chloroimino)ethane formation as shown in Figure 3.2. The intermediate 1-(chloroamino)ethanol was not observed possibly due to dehydration at the inlet to (chloroimino)ethane. Because (chloroimino)ethane standard is not commercially available, the compound was identified by analyzing the m/z fragments from the mass spectra pertaining to the compound's chromatogram peak (Figure 3.3). Acetonitrile mass spectra was compared to prepared standards.

N-chloroacetamide was also found to be a product from the reaction of monochloramine and acetaldehyde. Acetaldehyde and monochloramine reaction over time has a decreasing absorbance at 243 nm, where monochloramine and carbinolamine absorbs the highest, with a simultaneous increasing absorbance at the < 220 nm region that is related to *N*-chloroacetamide (Figure 3.4 and 3.5). *N*-chloroacetamide decomposes when analyzed by GC/MS. Furthermore, when reaction samples were quenched *N*-chloroacetamide was transformed to acetamide. Acetamide formation was identified from the reaction of 10 mM acetaldehyde and 1 mM monochloramine at pH 9.5 (Figure 3.6). Acetamide peak increased over time suggesting that its formation is the result of 1-(chloroamino)ethanol oxidation since acetonitrile hydrolysis is a slow reaction confirmed by controls. GC/MS sensitivity for acetamide concentrations was low and for accurate quantification by this technique was not possible.

3.3.2. Acetaldehyde and monochloramine reaction

Acetaldehyde in aqueous solution exists as 1,1-ethanediol at equilibrium with acetaldehyde (Equation 1).

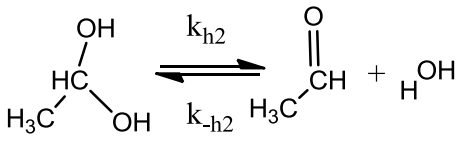

(1)

Equilibrium constant K_{h2} defined as

$$K_{h2}=\frac{CH_3CHO}{CH_3CH(OH)_2} \quad (2)$$

is equal to 0.671 at 25ºC and ionic strength of 0.2 M [15, 16]. The total acetaldehyde concentration is equal to the sum of both 1,1-ethanediol and acetaldehyde (Equation 3).

$$C_{T,CH3CHO} = [CH_3CHO] + [CH_3CH(OH)_2] \quad (3)$$

Combining equations 2 and 3, acetaldehyde species are expressed as a fraction of $C_{T,CH3CHO}$

$$[CH_3CHO] = C_{T,CH3CHO} * \frac{K_{h2}}{1+K_{h2}} = C_{T,CH3CHO}\,\gamma_0 \quad (4)$$

$$[CH_3CH(OH)_2] = C_{T,CH3CHO} * \frac{1}{1+K_{h2}} = C_{T,CH3CHO}\,\gamma_1 \quad (5)$$

where, γ_0 and γ_1 are 0.401 and 0.599 respectively. Acetaldehyde is ~40% of the total acetaldehyde in aqueous solution at 25ºC.

Unhydrated acetaldehyde reacts with monochloramine in a fast and reversible reaction to form 1-(chloroamino)ethanol. Absorbance spectras of the reaction were taken with increasing concentrations of acetaldehyde at neutral pH (UV-1 and UV-2) at which 1-(chloroamino)ethanol

decomposition is slow. Acetaldehyde concentrations were in excess of monochloramine therefore, acetaldehyde absorbance spectras did not vary significantly and were subtracted from each reaction spectra taken at equilibrium illustrated in Figure 3.7. The resulting absorbance spectra corresponds to the sum of monochloramine and 1-(chloroamino)ethanol concentrations times their respective molar absorptivities.

$$A_{\lambda,e} = \varepsilon_{\mathrm{NH_2Cl}_\lambda}[\mathrm{NH_2Cl}]_e + \varepsilon_{\mathrm{CH_3CH(OH)NHCl}_\lambda}[\mathrm{CH_3CH(OH)NHCl}]_e \quad (6)$$

Previous research on the formaldehyde and monochloramine reaction has shown isobestic points shifts with increasing formaldehyde concentrations because di-substituted species *N*-chlorodimethanolamine is formed from the reaction of intermediate *N*-chloromethanolamine and excess formaldehyde. However, in this study 1,1'-(chloroazanediyl)diethanol formation was not observed even at high concentrations of acetaldehyde (Equation 7). A possible explanation is that 1-(chloroamino)ethanol is sterically hindered compared to *N*-chloromethanolamine making the di-substituted species formation a less favorable reaction.

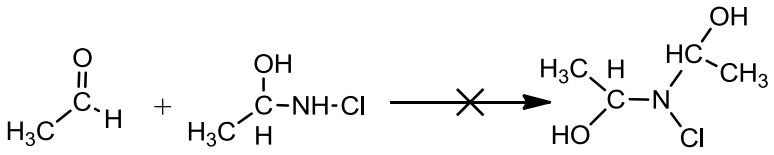

(7)

The equilibrium constant K_i is defined as

$$K_i = \frac{[\mathrm{CH_3CH(OH)NHCl}]_e}{[\mathrm{NH_2Cl}]_e[\mathrm{CH_3CHO}]_e} \quad (8)$$

where,

$[\mathrm{NH_2Cl}]_e$ = Monochloramine concentration at equilibrium

$[\mathrm{CH_3CH(OH)NHCl}]_e$=1-(chloroamino)ethanol concentration at equilibrium

$[\mathrm{CH_3CHO}]_e$ = Unhydrated acetaldehyde concentration at equilibrium

Performing a mass balance at equilibrium, monochloramine concentration at equilibrium equals the initial concentration minus the 1-(chloroamino)ethanol produced.

$$[NH_2Cl]_e = [NH_2Cl]_0 - [CH_3CH(OH)NHCl]_e \quad (9)$$

Substituting eq 9 into eq 8 and 6 and simplifying we obtain

$$A_{\lambda,e} = \varepsilon_{NH_2Cl_\lambda}[NH_2Cl]_0 + (\varepsilon_{CH_3CH(OH)NHCl_\lambda} - \varepsilon_{NH_2Cl_\lambda})\frac{[NH_2Cl]_0[CH_3CHO]_e}{(K_i+[CH_3CHO]_e)} \quad (10)$$

where, the absorbance spectra is expressed in terms of unknown K_i and $\varepsilon_{CH_3CH(OH)NHCl_\lambda}$. Equation 10 was fitted to experimental data from UV-1 and UV-2 experiments to calculate K_i and $\varepsilon_{CH_3CH(OH)NHCl_\lambda}$ at different wavelengths. An average value of K_i was fixed and $\varepsilon_{CH_3CH(OH)NHCl_\lambda}$ were determined for different wavelengths (Figure 3.5). Average values of the equilibrium constant K_i were 147 ± 2.42 M^{-1} for 18°C and 109 ± 2.59 M^{-1} for 25°C. Molar absorptivities at both temperatures were calculated to be the same.

According to Van't Hoff equation, the enthalpy of reaction (ΔH°) can be estimated assuming ΔH° does not vary with temperature with

$$ln\frac{K_1}{K_2} = \frac{\Delta H^\circ}{R}\left(\frac{1}{T_2} - \frac{1}{T_1}\right) \quad (11)$$

where, R is the universal gas constant (8.314 J/mol-K), and K_1 and K_2 are equilibrium constants at temperature T_1 and T_2 in Kelvin [17]. Substituting K_i values obtained at different temperatures (291.15 and 298.15 K) in equation 11, ΔH° is estimated as -30.84 kJ/mol. Equilibrium constant K_i at other temperatures can be estimated with equation 11 and ΔH°.

3.3.3. 1-(chloroamino)ethanol Dehydration to Acetonitrile and Oxidation to *N*-chloroacetamide

Kinetic Model. 1-(chloroamino)ethanol at equilibrium with monochloramine and acetaldehyde is followed by two concurrent reactions 1) dehydration to (chloroimino)ethane, the rate limiting reaction for acetonitrile formation, and 2) oxidation by monochloramine to form *N*-chloroacetamide. The concentrations of monochloramine and 1-(chloroamino)ethanol over time is represented as

$$\frac{dC_{T,NCl}}{dt} = -k_{ii}[\mathrm{CH_3CH(OH)NHCl}] - k_{iii}[\mathrm{CH_3CH(OH)NHCl}][\mathrm{NH_2Cl}] \quad (12)$$

where,

$$C_{T,NCl} = [\mathrm{NH_2Cl}] + [\mathrm{CH_3CH(OH)NHCl}] \quad (13)$$

Each species concentration is expressed as the fraction of $C_{T,NCl}$ by substituting equation 8 into 13 to obtain

$$[\mathrm{NH_2Cl}] = C_{T,NCl} * \frac{1}{1+K_i[\mathrm{CH_3CHO}]} = C_{T,NCl}\,\delta_0 \quad (14)$$

$$[\mathrm{CH_3CH(OH)NHCl}] = C_{T,NCl} * \frac{K_i[\mathrm{CH_3CHO}]}{1+K_i[\mathrm{CH_3CHO}]} = C_{T,NCl}\delta_1 \quad (15)$$

where, δ_0 and δ_1 are 0.629 and 0.371, respectively at $C_{T,\mathrm{CH3CHO}}$ = 0.010 M.

Substituting equation 14 and 15 into 12, the rate expression for $C_{T,NCl}$ is simplified and acetonitrile and *N*-chloroacetamide formation rates are expressed as

$$\frac{dC_{T,NCl}}{dt} = -k_{ii}\delta_1[C_{T,NCl}] - 2 * k_{iii}\delta_0\delta_1[C_{T,NCl}]^2 \quad (16)$$

$$\frac{d\mathrm{CH_3CN}}{dt} = k_{ii}\delta_1[C_{T,NCl}] \quad (17)$$

$$\frac{d\mathrm{CH_3C(O)NHCl}}{dt} = k_{iii}\delta_0\delta_1[C_{T,NCl}]^2 \quad (18)$$

where, $\frac{dC_{T,NCl}}{dt}$ is a mixed order reaction composed by a first and second order term. To conserve mass balance the second order term is multiplied by two.

This mixed order expression will approximate a first order reaction at lower initial concentrations of $C_{T,NCl}$ or a second order reaction at higher initial concentrations of $C_{T,NCl}$ [18]. For low concentrations of $C_{T,NCl}$= 0.001 M used in all experiments, the initial apparent rate constant or k_{obs} was first order as shown in Figures 3.8 and 3.9. Results for all experiments are shown in Figure 3.10. There is a strong acid-base catalysis and temperature effect for the disappearance of intermediate 1-(chloroamino)ethanol. Individual kinetic rates for the concurrent dehydration and oxidation reaction are evaluated in the following section.

Acid and base catalysis. The acetaldehyde and monochloramine reaction was studied under different pH conditions to assess the catalysis effect of acid and base. Similar analysis to the chloroacetaldehyde and monochloramine reaction was performed. Reactions were monitored by following UV-Vis absorbance over time at 210 and 243 nm, wavelengths where 1-(chloroamino)ethanol, monochloramine and *N*-chloroacetamide absorb the highest. Absorbance is defined as the total sum of the product of each species concentration times its corresponding molar absorptivity at a given time.

$$A_{\lambda,t} = \varepsilon_{\mathrm{NH_2Cl}_\lambda}[\mathrm{NH_2Cl}]_t + \varepsilon_{\mathrm{CH_3CH(OH)NHCl}_{\lambda,\mathrm{t}}}[\mathrm{CH_3CH(OH)NHCl}]_t + \varepsilon_{\mathrm{CH_3C(O)NHCl}_{\lambda,\mathrm{t}}}[\mathrm{CH_3C(O)NHCl}]_t \quad (19)$$

Monochloramine and 1-(chloroamino)ethanol are related by the equilibrium constant (equation 8) therefore, equation 19 is simplified to

$$A_{\lambda,t} = (\varepsilon_{\mathrm{NH_2Cl}_\lambda} + \varepsilon_{\mathrm{CH_3CH(OH)NHCl}_{\lambda,\mathrm{t}}} K_i[\mathrm{CH_3CHO}])[\mathrm{NH_2Cl}]_t + \varepsilon_{\mathrm{CH_3C(O)NHCl}_{\lambda,\mathrm{t}}}[\mathrm{CH_3C(O)NHCl}]_t \quad (20)$$

where, $[\mathrm{NH_2Cl}]_t$ and $[\mathrm{CH_3C(O)NHCl}]_t$ are the monochloramine and *N*-chloroacetamide concentrations at a given time. Both concentrations were obtained by solving equation 20 for experimental values at 210 and 243 nm. 1-(chloroamino)ethanol and $C_{T,NCl}$ were calculated with equation 8 and 13.

Reaction rates k_{ii} and k_{iii} were obtained by fitting $C_{T,NCl}$ and $[\mathrm{CH_3C(O)NHCl}]$ concentrations from the initial 10% of the reaction to the kinetic model with the simplex method. Data sets UV-3, UV-4, UV-5, and UV-6 were analyzed and rate constants are shown in Figures 3.11 and 3.12. k_{ii} was found to be influenced by the initial values of the simplex method therefore, k_{ii} that best fitted the data was reported. Additionally, at neutral and acidic conditions, monochloramine decomposition is relevant and was included in the kinetic model for UV-3 and UV-4 [19].

Reaction rates k_{ii} and k_{iii} were evaluated for acid (k^{H}) and base (k^{OH}) catalysis according to equation 21. Results are shown in Table 3.2. It was found that the 1-(chloroamino)ethanol

dehydration step was acid and base catalyzed analogous to the chloroacetaldehyde and formaldehyde reactions with monochloramine. Likewise, the carbinolamine oxidation reaction was found to be acid and base catalyzed. However, 1-(chloroamino)ethanol oxidation, produced from the chloroacetaldehyde reaction, differs from this study in that it was not acid catalyzed. It is possible that the 1-(chloroamino)ethanol oxidation reaction is acid catalyzed but still significantly slower than chloroacetonitrile formation that it was not quantifiable at the tested pH conditions.

$$k = k^{H}[H^{+}] + k^{OH}[OH^{-}] \quad (21)$$

Model predictions and experimental data at basic, neutral, and acidic pH conditions at 18°C are shown in Figures 3.13 – 3.15. There is a good agreement between model and experimental data.

Temperature and Carbonate Effect. Figures 3.11 and 3.12 also illustrate the temperature effect on both 1-(chloroamino)ethanol dehydration and oxidation reaction. Rates were slightly higher for 25°C than for 18°C.

Two buffers were used in all experiments, carbonate and phosphate. Previous research done on similar reaction pathway found that phosphate buffer did not have as significant effect [6]. However, carbonate was not tested. Figure 3.16 shows the apparent rate constant for 1-(chloroamino)ethanol decomposition to products. It was found that carbonate does not catalyzes the reaction either.

3.3.4. Implications for Water Treatment

Acetaldehyde formation is significant and has been identified in waters treated with ozone and free chlorine. Monochloramine can react with acetaldehyde to later form *N*-chloroacetamide and acetonitrile as end products. *N*-chloroacetamide and acetonitrile modeling results at drinking water conditions for a period of 5 days graphed in Figure 3.17, illustrate that the formation of both products is increased at high ph (>8.5), while at neutral pH (7-8) their formation is slower. Carbinolamine concentrations over time remain low and relatively constant compared to the end products. Increasing concentrations of acetaldehyde and monochloramine, as shown in Figures 3.18 and 3.19, also increases the formation of *N*-chloroacetamide and acetonitrile.

Sample quenching and preservation methods may affect the formation of haloacetamides and haloacetonitriles as described in Chapter 2. Similarly, *N*-chloroacetamide and acetonitrile formation would be accelerated if monochloramine would not be properly quenched followed by preserving samples at high or low pH conditions. Therefore, water samples quenched with sodium thiosulfate, reducer that quickly quenches monochloramine, followed by a pH adjustment to neutral pH is recommended prior to analysis.

Recent research efforts have been focused on halogenated acetamides and acetonitriles due to their higher toxicity than regulated DBPs. Newly identified *N*-chloroacetamide might also pose a health risk due to its similarity to haloacetamides. While at high and low pH conditions *N*-chloroacetamide and acetonitrile formation is enhanced, at neutral pH, the formation of both products is the slowest. Understanding the chemical formation of such compounds is necessary to develop DBP control strategies for water treatment and to devise appropriate sample and preservation methods to monitor such DBPs in water.

Literature Cited

1. Weinberg, H. S.; Krasner, S. W.; Richardson, S. D.; Thruston, A. D. J., 2002. *The Occurrence of Disinfection By-Products (DBPs) of Health Concern in Drinking Water : Results of a Nationwide DBP Occurrence Study*. Environmental Protection Agency, National Exposure Research Laboratory, Athens, GA. EPA/600/R-02/068.

2. Krasner, S. W.; Weinberg, H. S.; Richardson, S. D.; Pastor, S. J.; Chinn, R.; Sclimenti, M. J.; Onstad, G. D.; Thruston Jr, A. D., Occurrence of a New Generation of Disinfection Byproducts. *Environmental Science & Technology* **2006,** *40*, (23), 7175-7185.

3. Yang, X.; Fan, C.; Shang, C.; Zhao, Q., Nitrogenous disinfection byproducts formation and nitrogen origin exploration during chloramination of nitrogenous organic compounds. *Water Research* **2010,** *44*, (9), 2691-2702.

4. Shah, A. D.; Mitch, W. A., Halonitroalkanes, halonitriles, haloamides, and N-nitrosamines: A critical review of nitrogenous disinfection byproduct formation pathways. *Environmental Science & Technology* **2012,** *46*, (1), 119-131.

5. Huang, H.; Wu, Q. Y.; Hu, H. Y.; Mitch, W. A., Dichloroacetonitrile and dichloroacetamide can form independently during chlorination and chloramination of drinking waters, model organic matters, and wastewater effluents. *Environmental Science & Technology* **2012,** *46*, (19), 10624-10631.

6. Pedersen, E. J.; Urbansky, E. T.; Marinas, B. J., Formation of Cyanogen Chloride from the Reaction of Monochloramine with Formaldehyde. *Environmental Science & Technology* **1999,** *33*, 4239-4249.

7. Le Cloirec, C.; Martin, G., In *Water Chlorination*, Jolley, R. L., Ed. Lewis Publishers, Inc: Chelsea, MI, 1985; Vol. 5, pp 821-834.

8. Schechter, D. S.; Singer, P. C., Formation of aldehydes during ozonation. *Ozone: Sci. Eng.* **1995,** *17*, (1), 53-69.

9. Richardson, S. D.; Thruston, A. D., Jr.; Caughran, T. V.; Chen, P. H.; Collette, T. W.; Floyd, T. L.; Schenck, K. M.; Lykins, B. W., Jr.; Sun, G.-r.; Majetich, G., Identification of New Ozone Disinfection Byproducts in Drinking Water. *Environmental Science & Technology* **1999,** *33*, (19), 3368-3377.

10. Can, Z. S.; Gurol, M., Formaldehyde formation during ozonation of drinking water. *Ozone: Sci. Eng.* **2003,** *25*, (1), 41-51.

11. Krasner, S. W.; McGuire, M. J.; Jacangelo, J. G.; Patania, N. L.; Reagan, K. M.; Marco Aieta, E., Occurrence of disinfection by-products in US drinking water. *Journal / American Water Works Association* **1989,** *81*, (8), 41-53.

12. Xu, H.; Wentworth, P. J.; Howell, N. W.; Joens, J. A., Temperature dependent near-UV molar absorptivities of aliphatic aldehydes and ketones in aqueous solution. *Spectrochimica Acta Part A: Molecular Spectroscopy* **1993,** *49*, 1171-1178.

13. Kumar, K.; Day, R. A.; Margerum, D. W., Atom-transfer redox kinetics general-acid-assisted oxidation of iodide by chloramines and hypochlorite. *Inorganic Chemistry* **1986,** *25*, 4344-4350.

14. Smith, R. M.; Martell, A. E., *Critical Stability Constants*. Plenum Press: New York, 1976; Vol. 4.

15. Bell, R. P.; Evans, P. G., Kinetics of the Dehydration of Methylene Glycol in Aqueous Solution. *Proceedings of the Royal Society of London. Series A, Mathematical and Physical Sciences* **1966,** *291*, (1426), 297-323.

16. Lombardi, E.; Sogo, P. B., NMR Study of Acetaldehyde-Water Mixtures. *The Journal of Chemical Physics* **1960,** *32*, (2), 635-636.

17. Snoeyink, V. L.; Jenkins, D., *Water Chemistry*. John Wiley & Sons: 1980; p 71-74.

18. Espenson, J. H., Homogeneous Inorganic Reactions. In *Investigation of Rates and Mechanisms of Reactions*, 4th ed.; Bernasconi, C. F., Ed. John Wiley & Sons: USA, 1986; Vol. 1, pp 479-564.

19. Valentine, R. L.; Jafvert, C. T., Reaction Scheme for the Chlorination of Ammoniacal Water. *Environmental science and technology* **1992,** *26*, 577-586.

Table and Figures

Table 3.1 Summary of acetaldehyde and monochloramine experimental conditions

Exp Set	$p[H^+]$	$[NH_2Cl]_0$ (M)	$C_{T,CH3CHO}$ (M)	Buffer	$C_{T,\ Buffer}$ (M)	Temperature (°C)
UV-1	7.78 - 7.85	0.001	0.010-0.090	Phosphate	0.020	18
UV-2	7.53 - 7.59	0.001	0.010-0.070	Phosphate	0.020	25
UV-3	5.87 - 7.89	0.001	0.010	Phosphate	0.020	18
UV-4	6.19 – 7.51	0.001	0.010	Phosphate	0.020	25
UV-5	8.93 – 9.99	0.001	0.010	Carbonate	0.020	18
UV-6	8.93 - 9.94	0.001	0.010	Carbonate	0.020	25
UV-7	9.8	0.001	0.010	Carbonate	0.010-0.035	25

Table 3.2 Summary of constants characterized in this study

Reaction	Constant (18°C)	Constant (25°C)
$CH_3CHO + NH_2Cl \leftrightarrow CH_3CH(OH)NHCl$	$K_i = 147\ M^{-1}$	$K_i = 109\ M^{-1}$
$CH_3CH(OH)NHCl \rightarrow CH_3CHNCl$	$k_{ii}^{H} = 137\ M^{-1}s^{-1}$ $k_{ii}^{OH} = 1.92\ M^{-1}s^{-1}$	$k_{ii}^{H} = 251\ M^{-1}s^{-1}$ $k_{ii}^{OH} = 4.43\ M^{-1}s^{-1}$
$CH_3CH(OH)NHCl + NH_2Cl \rightarrow CH_3C(O)NHCl$	$k_{iii}^{H} = 1.37 \times 10^{6}\ M^{-2}s^{-1}$ $k_{iii}^{OH} = 1.27 \times 10^{4}\ M^{-2}s^{-1}$	$k_{iii}^{H} = 2.02 \times 10^{6}\ M^{-2}s^{-1}$ $k_{iii}^{OH} = 3.55 \times 10^{4}\ M^{-2}s^{-1}$

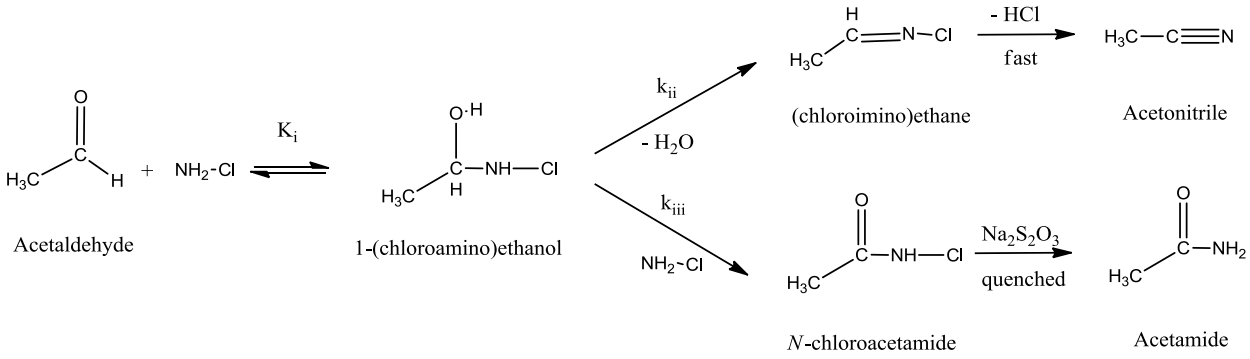

Figure 3.1 Acetonitrile and *N*-chloroacetamide reaction pathway formation from the reaction of acetaldehyde and monochloramine

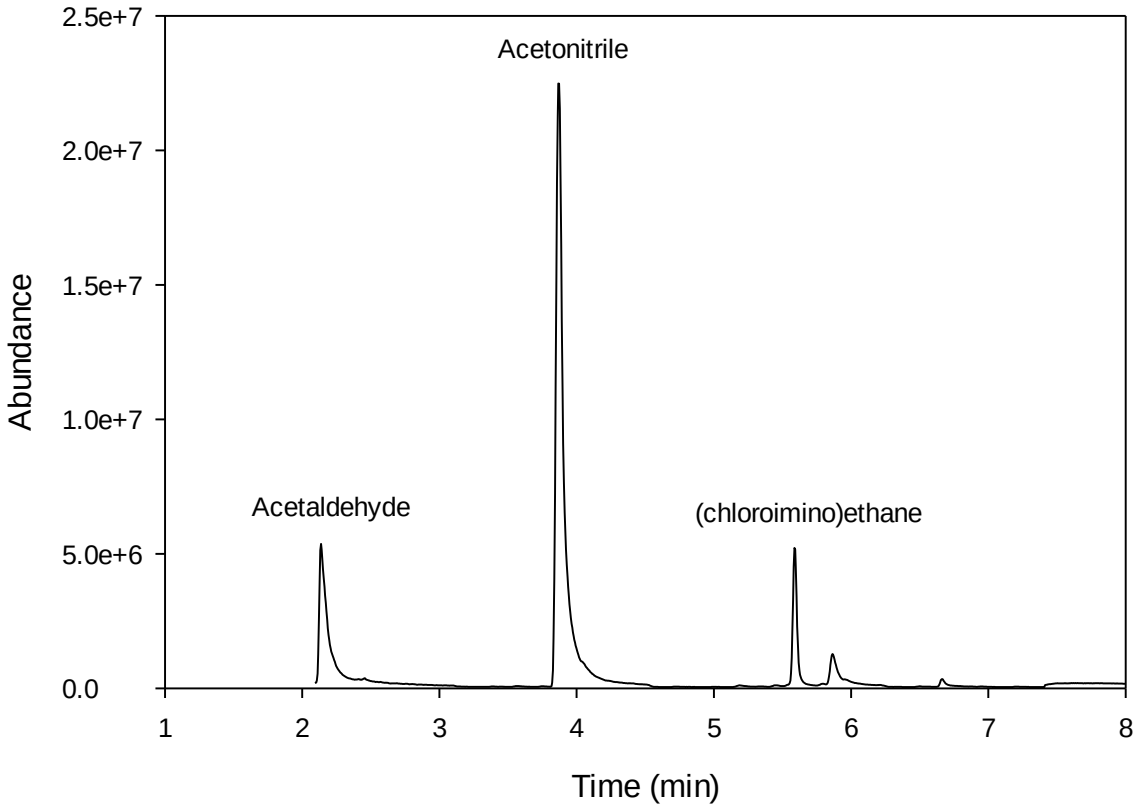

Figure 3.2 Total Ion Chromatogram. Sample extraction at 1 hr with SPME $[NH_2Cl]_0$ = 1mM, $[CH_3CHO]_{T,0}$ = 71 μM, $[PO_4]_{T,0}$ = 0.02 M, pH=7.53, μ = 0.1 M, 18 ± 0.1ºC

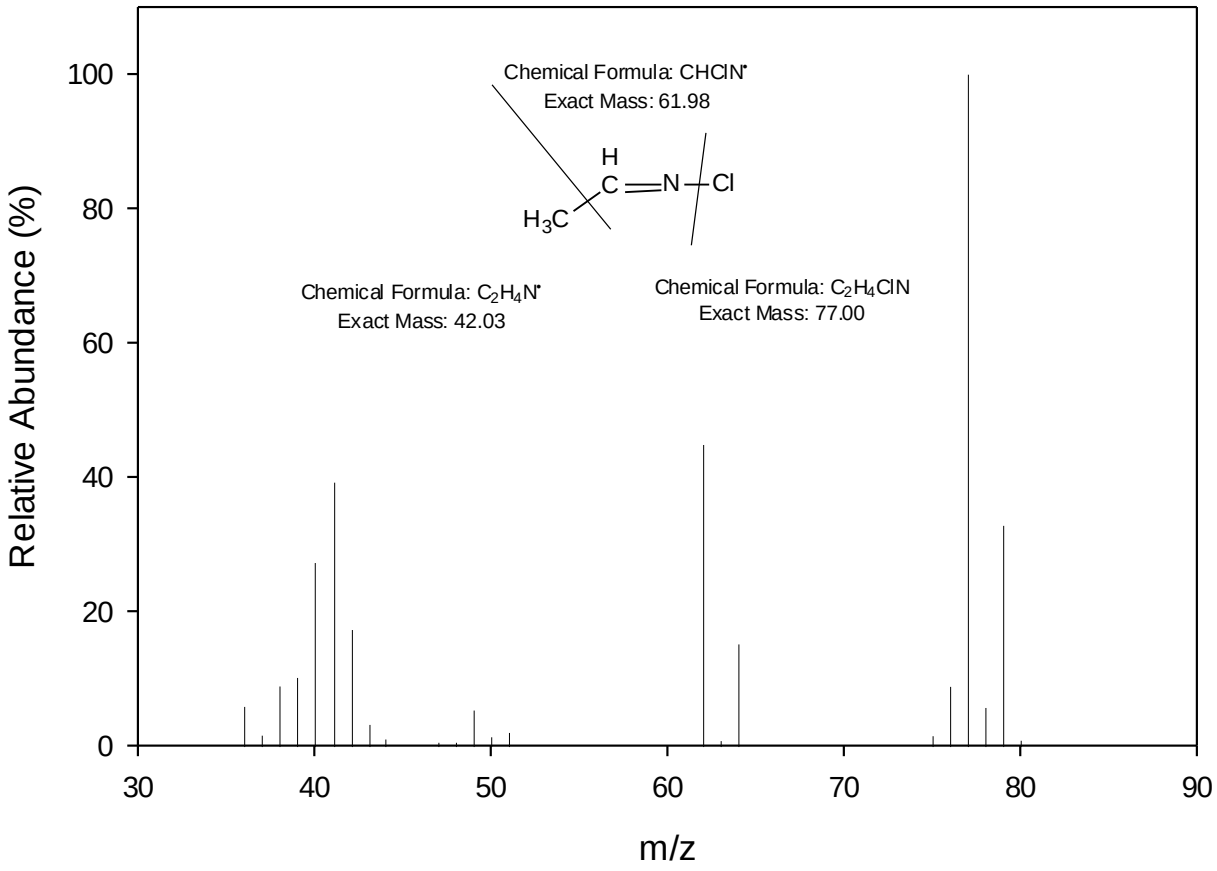

Figure 3.3 (chloroimino)ethane mass spectra m/z: 77(100%), 79 (33%), 62 (45%), 64 (15%)

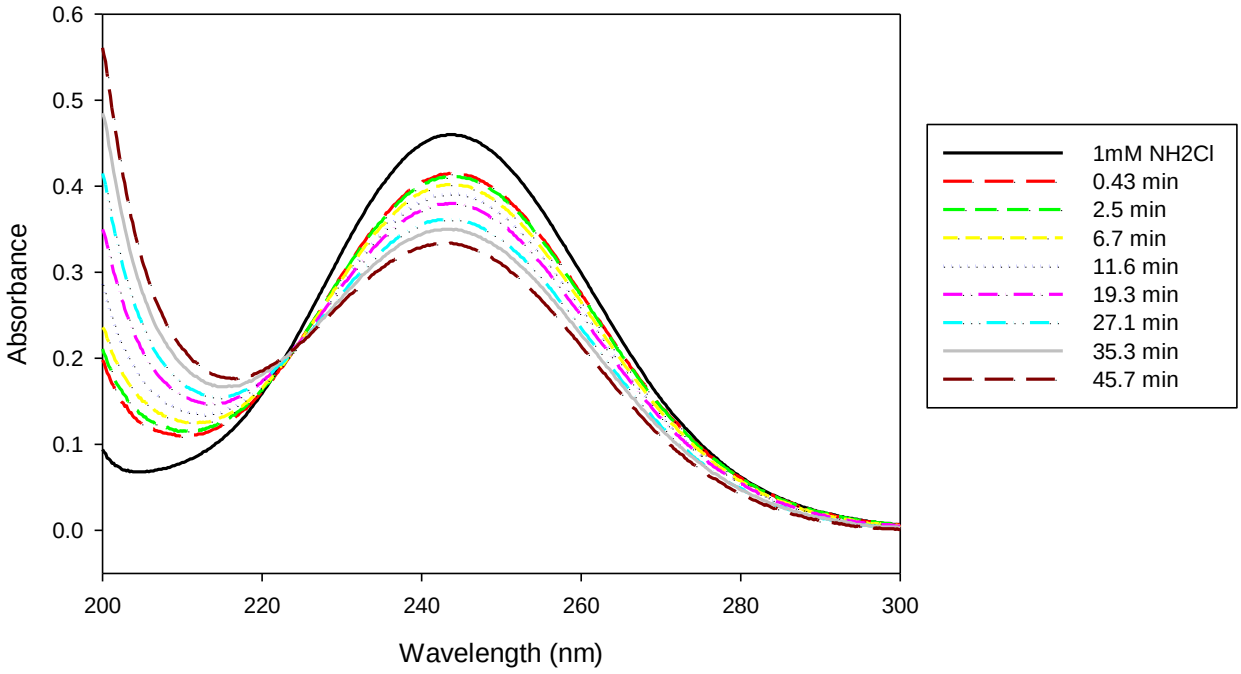

Figure 3.4 Acetaldehyde and monochloramine reaction over time, $[NH_2Cl]_0$ = 1mM, $[CH_3CHO]_{T,0}$ = 10, $[CO_3]_{T,0}$ = 0.02 M, pH 9.01 ± 0.01, μ = 0.1 M, 18 ± 0.1ºC

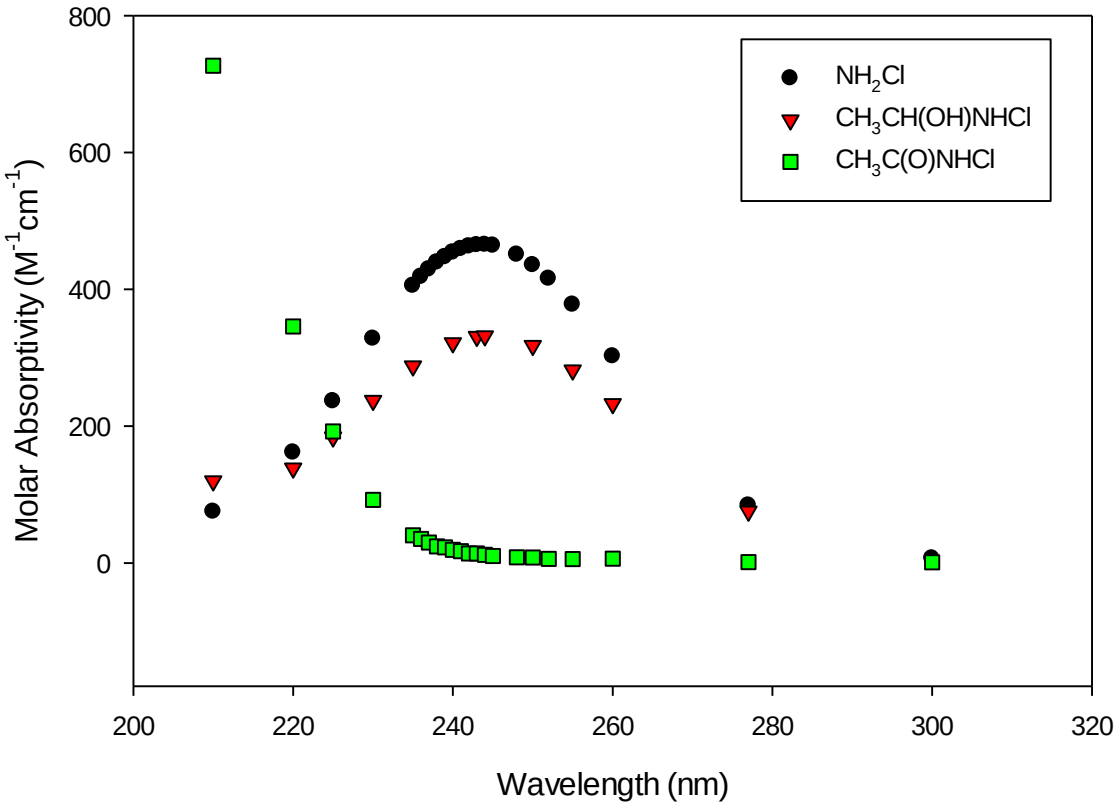

Figure 3.5 Molar absorptivity of monochloramine, 1-(chloroamino)ethanol and *N*-chloroacetamide determined in this study

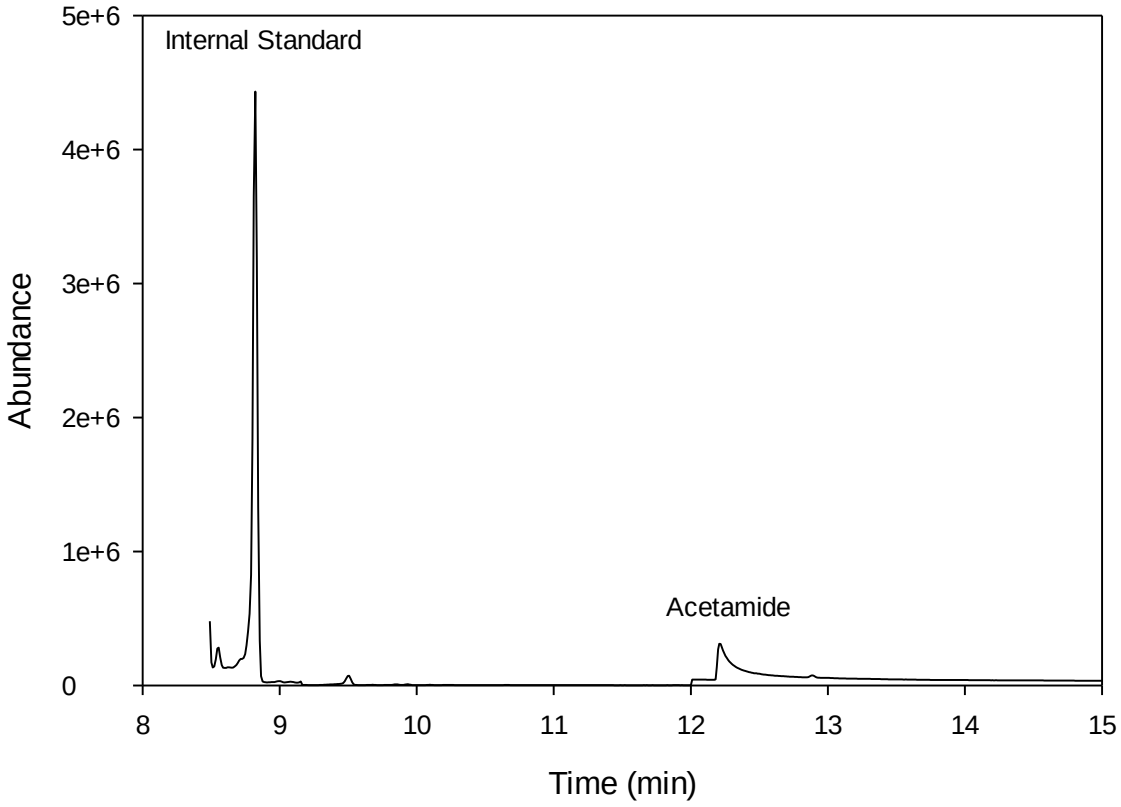

Figure 3.6 Select Ion Monitoring Chromatogram. Sample extraction at 1 hr with LLE $[NH_2Cl]_0$ = 1mM, $[CH_3CHO]_{T,0}$ = 10 mM, $[CO_3]_{T,0}$ = 0.02 M, pH 9.46 ± 0.04, μ = 0.1 M, 18 ± 0.1ºC

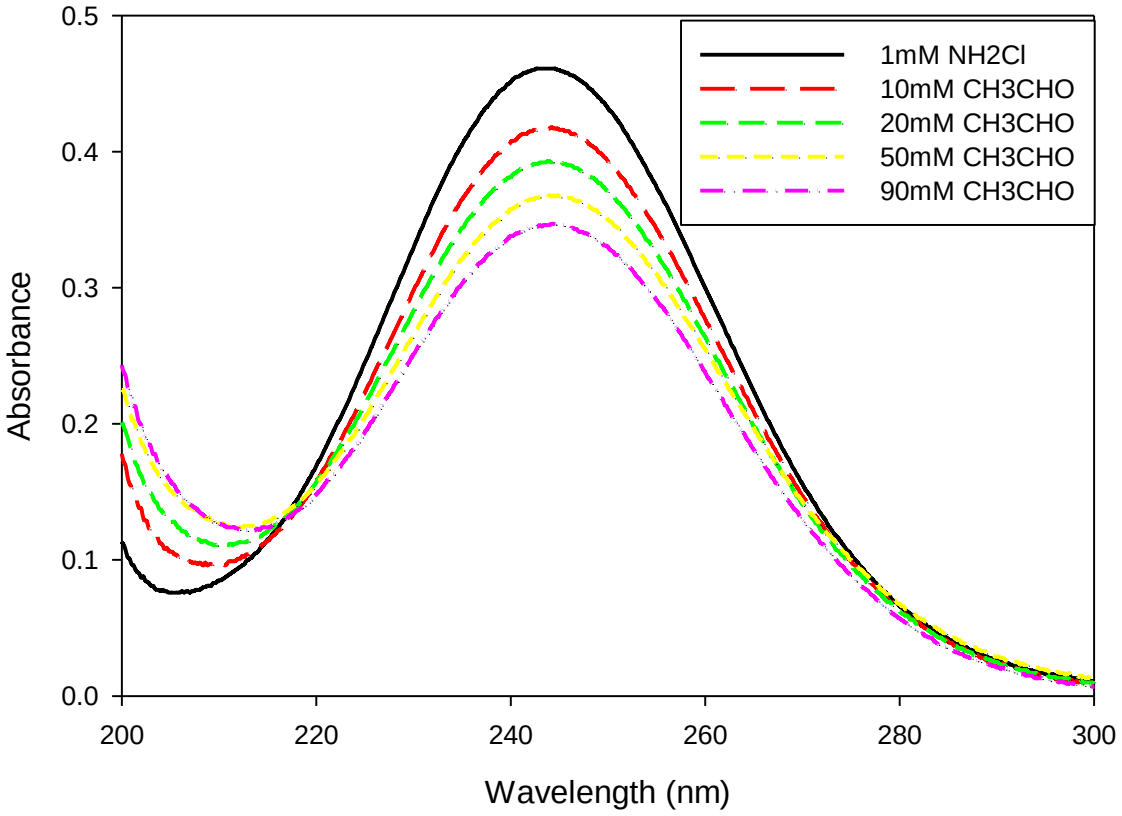

Figure 3.7 Acetaldehyde and monochloramine reaction spectras at 30s – 2.5 min, $[NH_2Cl]_0$ = 1mM, $[CH_3CHO]_{T,0}$ = 10 – 90 mM, $[PO_4^{2-}]_{T,0}$ = 0.02 M, pH 7.46 ± 0.04, μ = 0.1 M, 25 ± 0.1ºC

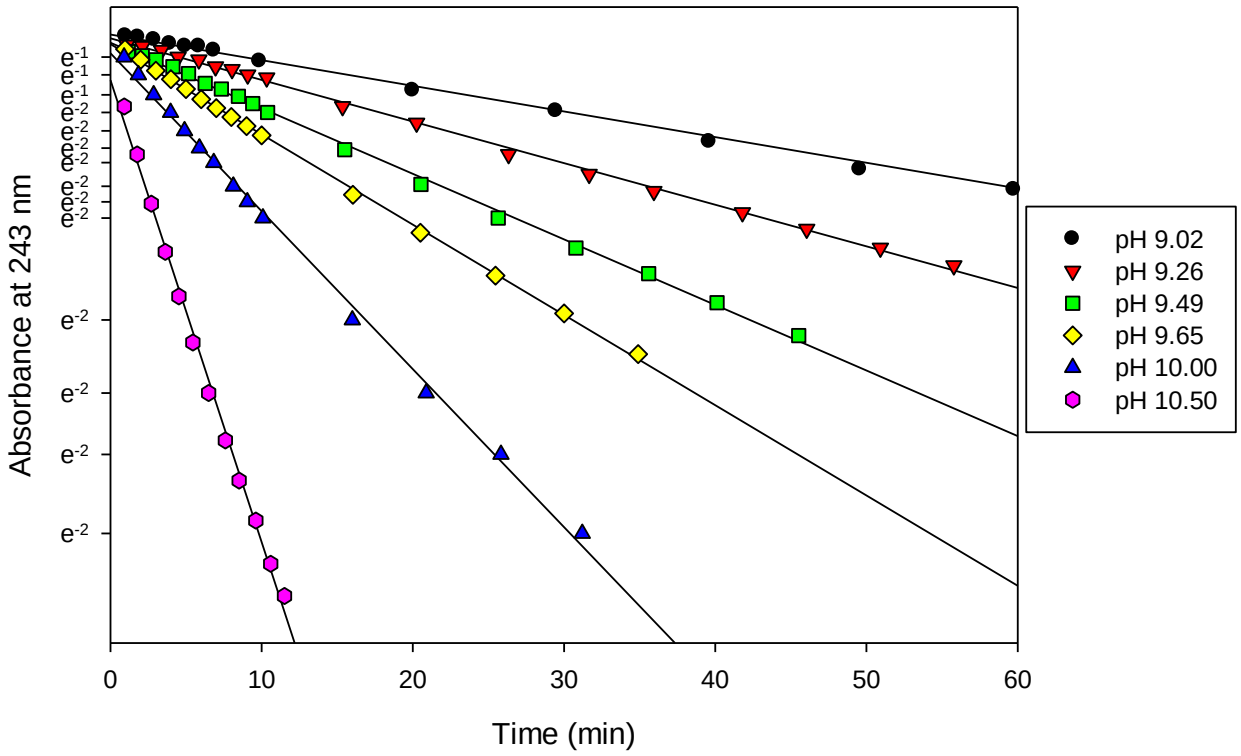

Figure 3.8 Absorbance values of acetaldehyde and monochloramine reaction monitored over time at 243 nm $[NH_2Cl]_0$ = 1mM, $[CH_3CHO]_{T,0}$ = 10 mM, $[CO_3]_{T,0}$ = 0.02 M, pH 9.02- 10.50, μ = 0.1 M, 18 ± 0.1ºC

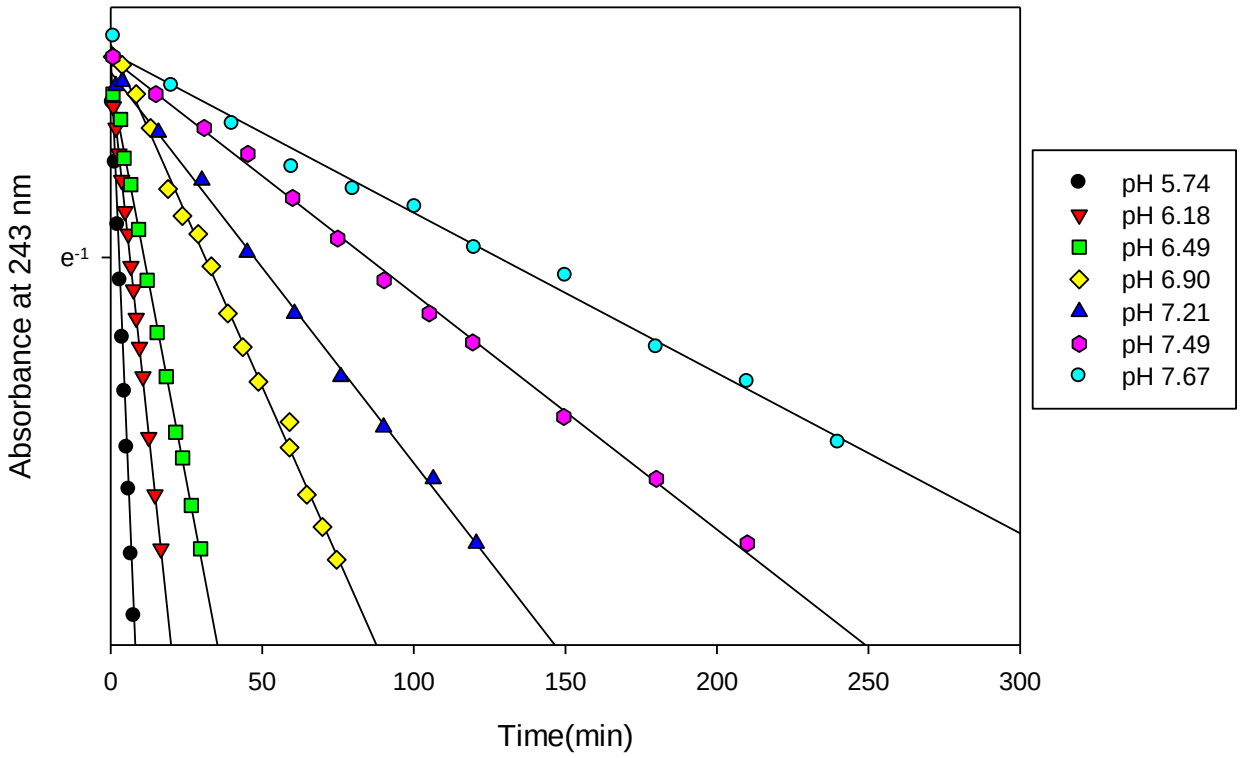

Figure 3.9 Absorbance values of acetaldehyde and monochloramine reaction monitored over time at 243 nm $[NH_2Cl]_0$ = 1mM, $[CH_3CHO]_{T,0}$ = 10 mM, $[PO_4]_{T,0}$ = 0.02 M, pH 5.74-7.67, μ = 0.1 M, 18 ± 0.1ºC

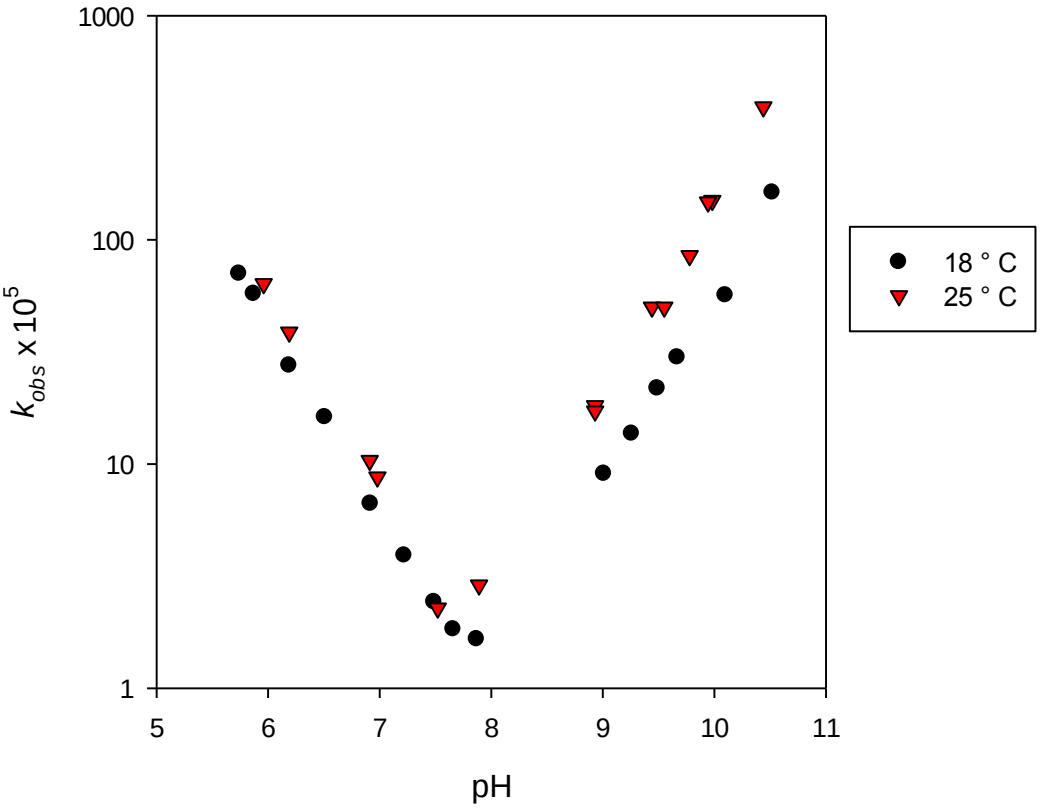

Figure 3.10 Apparent first order observed rate (k_{obs}) at different pH and temperatures

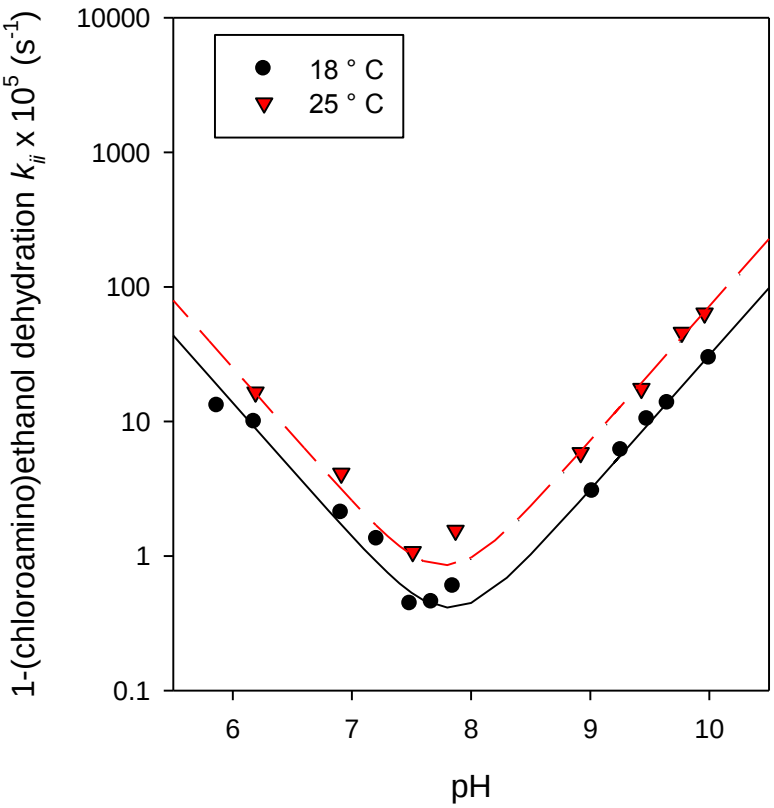

Figure 3.11 1-(chloroamino)ethanol dehydration rates(k_{ii}) as function of pH at 18 and 25°C. Symbols represent experimental rates and lines represent model prediction.

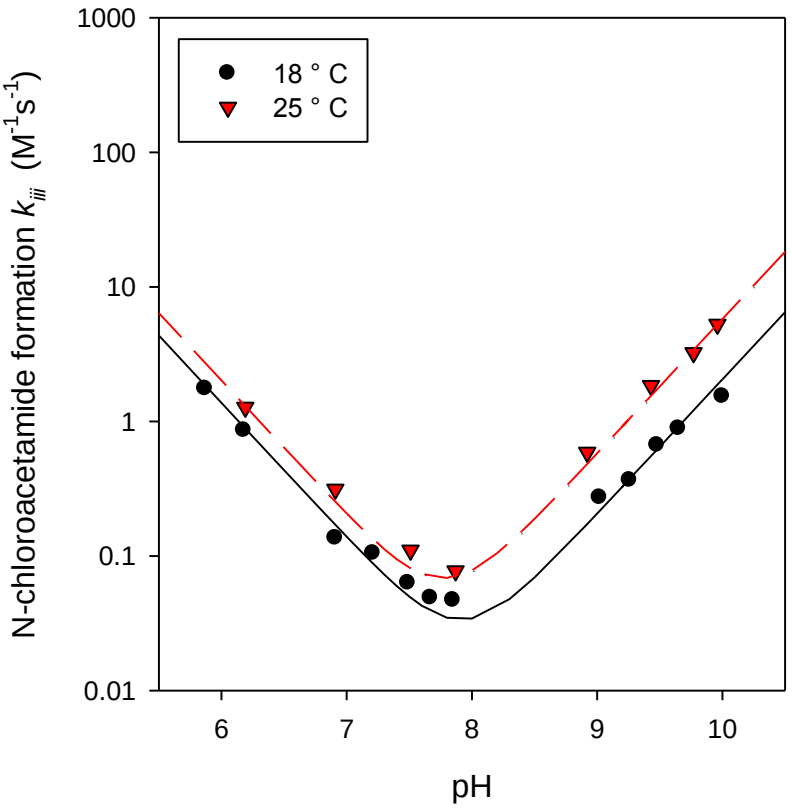

Figure 3.12 *N*-chloroacetamide formation rate k_{iii} in function of pH at 18 and 25°C. Symbols represent experimental rates and lines represent model prediction.

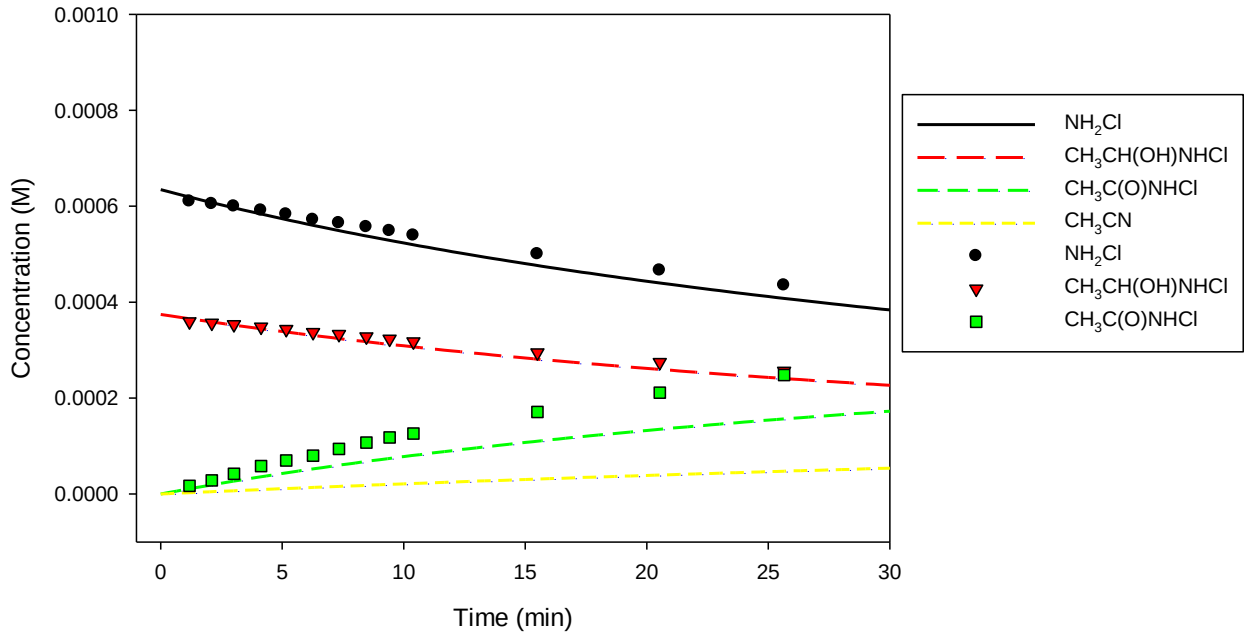

Figure 3.13 Monochloramine, 1-(chloroamino)ethanol, N-chloroacetamide, and acetonitrile over time. Symbols represent experimental rates and lines represent model prediction. $[NH_2Cl]_0$ = 1mM, $[CH_3CHO]_{T,0}$ = 10 mM, $[CO_3]_{T,0}$ = 0.02 M, pH 9.5, μ = 0.1 M, 18 ± 0.1ºC.

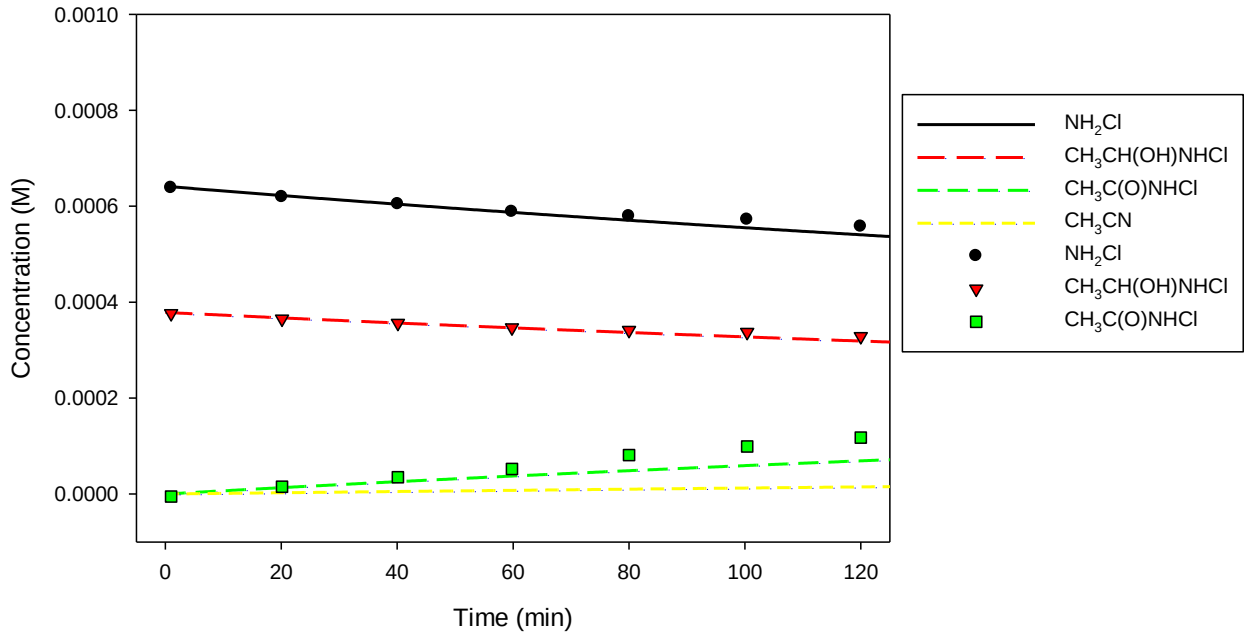

Figure 3.14 Monochloramine, 1-(chloroamino)ethanol, *N*-chloroacetamide, and acetonitrile over time. Symbols represent experimental rates and lines represent model prediction. $[NH_2Cl]_0$ = 1mM, $[CH_3CHO]_{T,0}$ = 10 mM, $[PO_4]_{T,0}$ = 0.02 M, pH 7.87, μ = 0.1 M, 18 ± 0.1ºC.

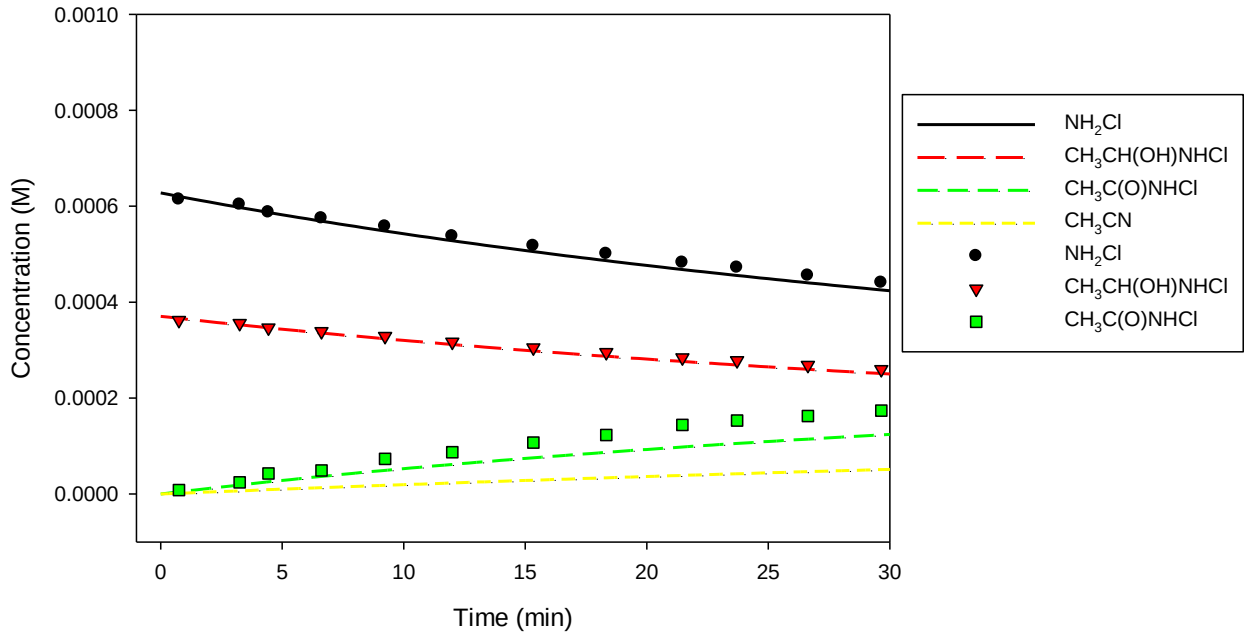

Figure 3.15 Monochloramine, 1-(chloroamino)ethanol, *N*-chloroacetamide, and acetonitrile over time. Symbols represent experimental rates and lines represent model prediction. $[NH_2Cl]_0$ = 1mM, $[CH_3CHO]_{T,0}$ = 10 mM, $[PO_4]_{T,0}$ = 0.02 M, pH 6.5, μ = 0.1 M, 18 ± 0.1ºC.

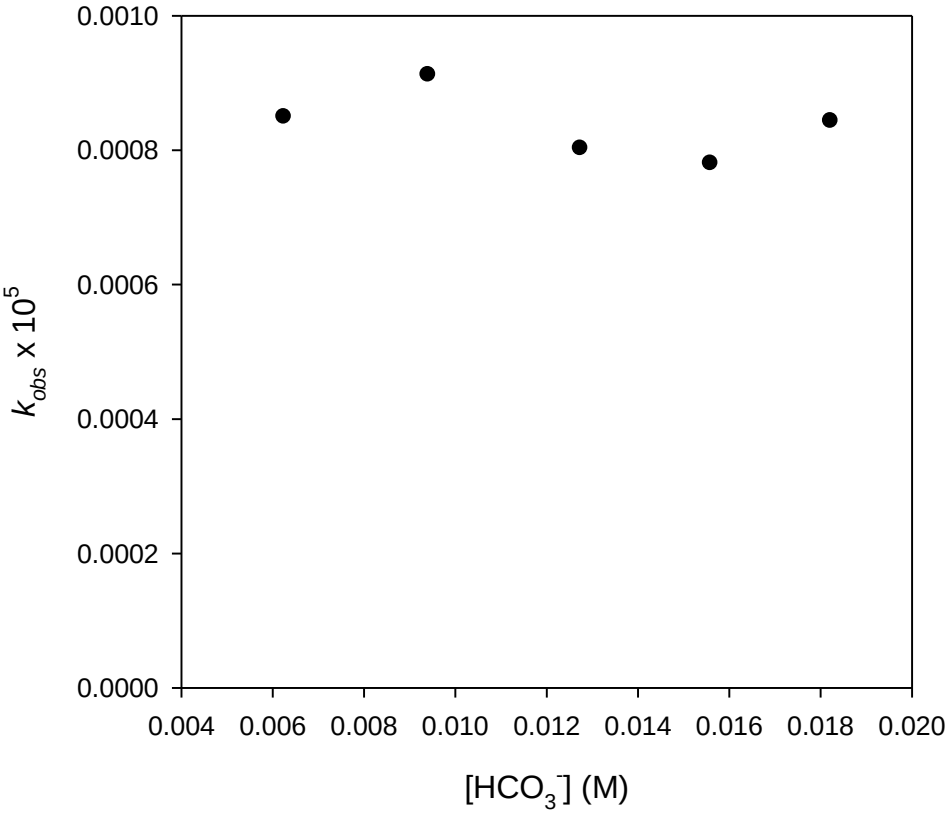

Figure 3.16 Carbonate effect on observed kinetic rates $[NH_2Cl]_0$ = 1mM, $[CH_3CHO]_{T,0}$ = 10 mM, $[CO_3]_{T,0}$ = 0.010-0.035 M, pH 9.7 ± 0.04, μ = 0.1 M, 25 ± 0.1ºC

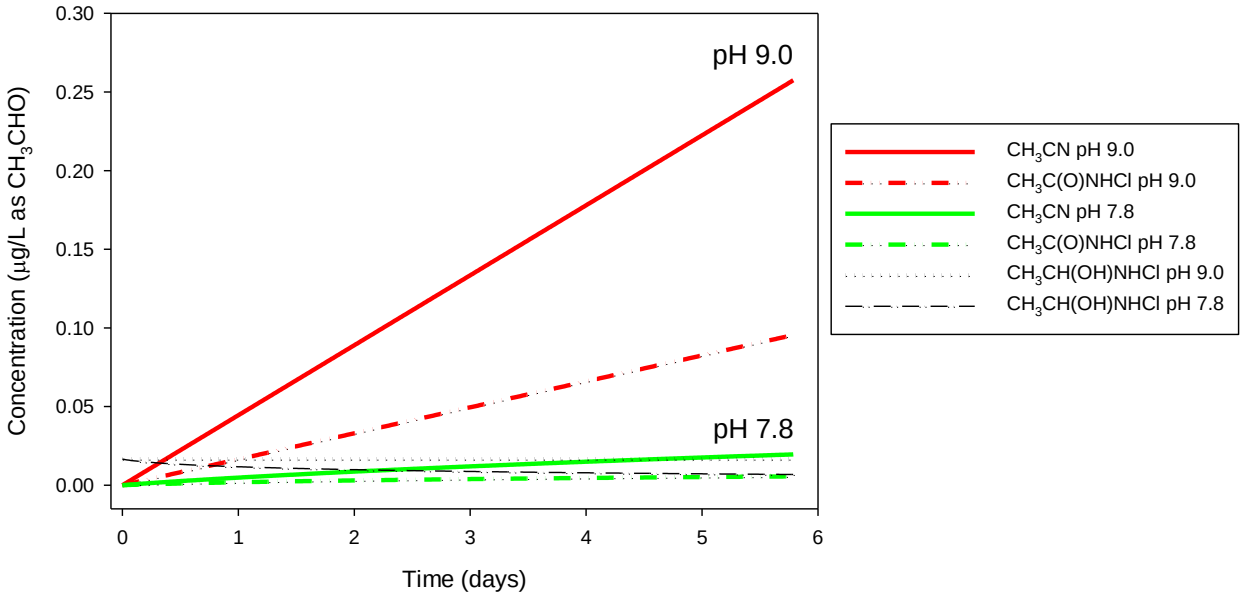

Figure 3.17 pH effect on acetonitrile, *N*-chloroacetamide, and 1-(chloroamino)ethanol formation over time at drinking water conditions. $[NH_2Cl]_0$ = 4 mg/L as Cl_2, $[ClCH_2CHO]_{T,0}$ = 5 µg/L, pH=9.0 & 7.8, 18°C

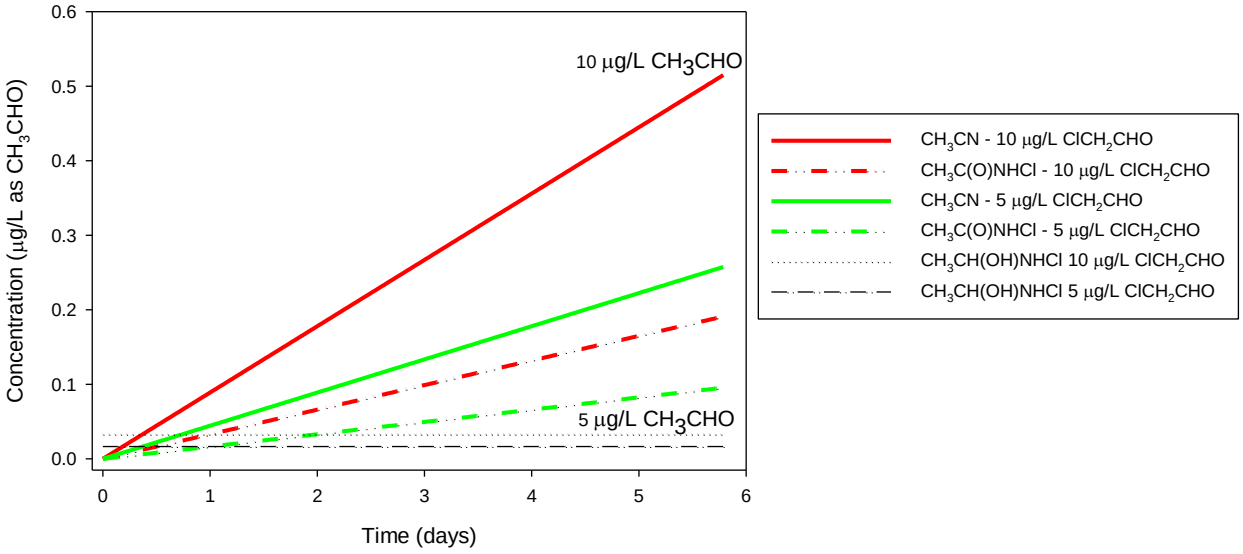

Figure 3.18 Acetaldehyde concentration effect on acetonitrile, *N*-chloroacetamide, and 1-(chloroamino)ethanol formation over time at drinking water conditions. $[NH_2Cl]_0$ = 4 mg/L as Cl_2, $[ClCH_2CHO]_{T,0}$ = 5 & 10 µg/L, pH=9.0, 18°C

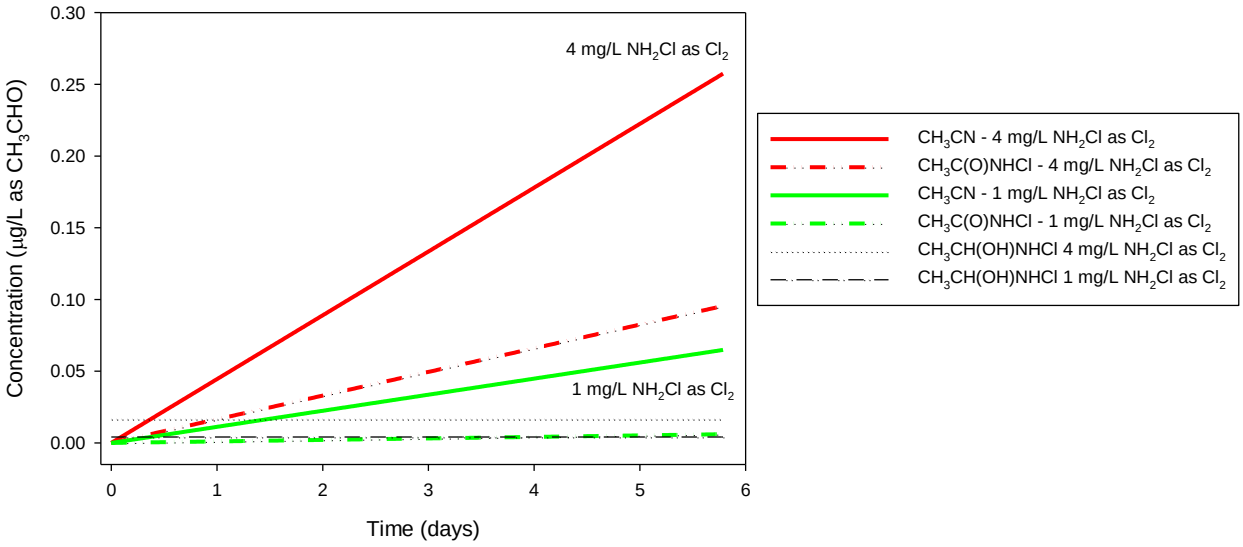

Figure 3.19 Monochloramine concentration effect on acetonitrile, *N*-chloroacetamide, and 1-(chloroamino)ethanol formation over time at drinking water conditions. $[NH_2Cl]_0$ = 1& 4 mg/L as Cl_2, $[ClCH_2CHO]_{T,0}$ = 5 µg/L, pH=9.0, 18°C

CHAPTER 4

BROMOACETONITRILE AND 2-BROMO-*N*-CHLOROACETAMIDE FORMATION FROM THE REACTION OF BROMOACETALDEHYDE AND MONOCHLORAMINE

Abstract

Bromoacetonitrile and bromoacetamide, the later a decomposition product of 2-bromo-*N*-chloroacetamide, have been found to be more cyto- and genotoxic than their chlorinated counterparts posing a health risk even though their detection in treated water are at lower levels. Bromoacetaldehyde reacts with monochloramine to reach equilibrium with 2-bromo-1-(chloroamino)ethanol. The equilibrium constant was determined to be 1900 ± 175 M^{-1}. 2-bromo-1-(chloroamino)ethanol decomposes through concurrent reactions 1) dehydration to 1-bromo-2-(chloroimino)ethane which can further decompose to bromoacetonitrile and 2) oxidation reaction with monochloramine to form 2-bromo-*N*-chloroacetamide. Experiments show that, similar to other aldehydes, the dehydration step is base catalyzed. However, the proposed reaction pathway only occurs at the initial part of the reaction and only 12% of initial monochloramine is incorporated to known products.

4.1. Introduction

Haloacetonitriles and haloacetamides are two classes of unregulated nitrogenous disinfection by-products (N-DBPs) that are significantly more cyto- and genotoxic than regulated disinfection by-products (DBPs). Within each class it has been found that monohalogenated compounds are more toxic than the di- and tri- halogenated species and that the brominated and iodinated compounds are more toxic than the chlorinated homologs [1, 2]. Though brominated acetonitriles and acetamides are found at lower levels than their chlorinated counterparts in finished waters, they might pose a higher health risk due to their higher toxicity [3, 4]. Bromoacetonitrile and bromoacetamide have been identified with maximum concentrations of 0.2 μg/L and 1.1 μg/L in finished waters.

In Chapter 2, it has been shown that monochloramine reacts with chloroacetaldehyde to reach quick equilibrium with the carbinolamine 2-chloro-1-(chloroamino)ethanol. 2-chloro-1-(chloroamino)ethanol is an intermediate that leads to two different products where it dehydrates to an imine that then produce chloroacetonitrile, and is oxidized by monochloramine to produce *N*,2-dichloroacetamide. Bromoacetaldehyde, another monohalogenated aldehyde, might follow a similar reaction pathway to its chlorinated counterpart. Therefore, it is possible that bromoacetaldehyde reacts with monochloramine to produce bromoacetonitrile and 2-bromo-*N*-chloroacetamide as end products.

The objectives of this study are to investigate the formation of bromoacetonitrile and 2-bromo-*N*-chloroacetamide formation from the reaction of monochloramine and bromoacetaldehyde. It is expected that monochloramine reacts with bromoacetaldehyde to form 2-bromo-1-(chloroamino)ethanol intermediate that could undergo parallel reactions 1)

dehydrate to bromoacetonitrile and 2) oxidized by monochloramine to form 2-bromo-*N*-chloroacetamide.

4.2. Experimental Methods

Reagents and Solutions. Bromoacetaldehyde (95%) was custom synthesized from Aldlab Chemicals (West Newton, MA) and was stable for a period of 3-4 months at -20°C. 1-2 M bromoacetaldehyde stock solutions were prepared daily by adding bromoacetaldehyde to a previously weighted flask with anhydrous acetonitrile. Bromoacetonitrile (97%), 2-bromoacetamide (98%), acetonitrile (GC Grade ≥ 99.5%), sodium sulfate (ACS reagent), sodium perchlorate (ACS reagent), and ethyl acetate (LC-MS CHROMASOLV) were purchased from Sigma-Aldrich (St. Louis, MO). Sodium hypochlorite stock solution (5.65-6% Laboratory Grade), sodium thiosulfate (ACS reagent), and ammonium chloride salt (ACS reagent) were purchased from Fisher Scientific (Pittsburgh, PA).

Bromoacetonitrile and 2-bromoacetamide stock solutions used for calibration curves were prepared the same day by diluting bromoacetonitrile in acetonitrile and 2-bromoacetamide in nanopure water. Stock solutions were then diluted to buffered solutions at pH 7.8 that contained similar composition to experimental solutions.

2-bromo-*N*-chloroacetamide was prepared by reacting stoichiometric amounts of 2-bromoacetamide with sodium hypochlorite until completion at pH 7.5. Sodium hypochlorite was standardized before use (λ_{max} = 292 nm, 362 $M^{-1}cm^{-1}$). 2-bromo-*N*-chloroacetamide concentration was calculated from the difference of initial and final hypochlorite concentrations.

Monochloramine and buffer stock solutions were prepared daily as explained in Chapter 2. All solutions were prepared with nanopure water. pH was adjusted to desired pH with Fluka 70% puriss perchloric acid and sodium hydroxide (ACS reagent, Sigma-Aldrich, MO, St. Louis, MO). All solutions were adjusted to ionic strength of 0.1M with sodium perchlorate.

Instrumental Methods. Reaction intermediates and products were identified with a GC/MS model 6850/5975C (Agilent Technologies, Santa Clara, CA). Bromoacetonitrile and 2-bromoacetamide were also quantified with GC/MS. Calibration curve solutions of increasing concentrations of bromoacetonitrile and 2-bromoacetamide were prepared and ran before each experiment. 7 ml aliquots were quenched with 1.5 mM sodium thiosulfate and adjusted to neutral pH (7-7.5) to minimize bromoacetonitrile hydrolysis. Samples were immediately mixed with 1ml ethyl acetate that contained 6 mg/L 1,2-dichloropropane as internal standard and 2 g of sodium sulfate for 2 minutes followed by a 3 minute phase separation. Extracts were then transferred to 200 µL vial inserts with no headspace for immediate analysis. The GC/MS operation program consisted of 2 µL sample splitless injection to a 230 ºC inlet carried by helium gas at 1.0 ml/min thru a DB-624 column (Agilent J&W, Santa Clara, CA). Initial oven temperature was held for 3 minutes, ramped at 10 ºC/min to 90 ºC, held for 1 min and ramped for a second time at 10 ºC/min to 190 ºC. Samples were ionized by electron impact and simultaneously used scan of 35-200 amu and selective ion monitoring specific for bromoacetonitrile, 2-bromoacetamide and internal standard ions.

Equilibrium and reaction experiments were monitored with a UV-Vis Spectrophotometer model 2550 (Shimadzu Scientific Instruments, Columbia, MD). Absorption spectras were scanned in 10 mm quartz cuvettes from 200 to 400 nm. All reactions were maintained at 18ºC with a water bath recirculator model 9501 (PolyScience, Niles, IL).

pH and temperature for all solutions were measured with an Thermo Electron Orion ROSS Ultra pH (Thermo Fisher Scientific, Waltham, MA) and Accumet temperature (Fisher Scientific, Pittsburgh, PA) electrodes connected to an Accumet AB15 Plus pH meter (Fisher Scientific, Pittsburgh, PA). Electrode calibration was performed daily with commercial 4, 7, and 10 pH standards with slope > 97%. Activity coefficients were calculated with the extended DeBye Huckel equation and the Guntelberg approximation and adjusted for actual hydrogen ion concentrations in all experiments.

Equilibrium constant was obtained by fitting experimental data to derived equations with the least squares method available in Micromath Scientist 3.0 (St. Louis, MO).

Experimental Matrix. Experimental sets to determine equilibrium constant (K_I) and reaction rates are shown in Table 4.1. Reactions were conducted at different pH conditions and analyzed by UV-Vis spectrophotometry and GC/MS.

4.3. Results and Discussion

4.3.1. Monochloramine and bromoacetaldehyde reaction products and intermediates

Monochloramine and bromoacetaldehyde can quickly react and reach equilibrium with the carbinolamine 2-bromo-1-(chloroamino)ethanol. 2-bromo-1-(chloroamino)ethanol can dehydrate to 1-bromo-2-(chloroimino)ethane and further decompose to bromoacetonitrile as illustrated in Figure 4.1. In a parallel reaction, 2-bromo-1-(chloroamino)ethanol can be oxidized by monochloramine to form 2-bromo-*N*-chloroacetamide.

Reaction products and intermediates were identified by GC/MS as shown in the total ion chromatogram in Figure 4.2. Bromoacetonitrile and bromoacetamide were also quantified using select ion monitoring for specific ions related to the products (Figure 4.3). As shown in Chapter 2, N,2-dichloroacetamide is an unstable compound and cannot be directly analyzed with GC/MS. For similar reason, 2-bromo-*N*-chloroacetamide was quenched and product bromoacetamide was observed. Intermediate 1-bromo-2-(chloroimino)ethane was also identified (Figure 4.2) confirming the proposed reaction pathway. 1-bromo-2-(chloroimino)ethane was identified by analyzing the mass to charge fractions generated by electron impact from GC/MS at peak 13.095 minutes (Figure 4.4). Although carbinolamine 2-bromo-1-(chloroamino)ethanol was not observed by GC/MS, possibly because it dehydrates in the injection port, the presence of the 1-bromo-2-(chloroimino)ethane confirms that bromoacetonitrile is produced from the proposed reaction pathway.

The total ion chromatogram shown in Figure 4.2 also suggests the presence of other compounds that were not identified. Peaks that are not labeled are impurities associated with the bromoacetaldehyde stock. However, two peaks labeled unknown 1 and 2 participated in the dynamics of the reaction. As the reaction progressed there is a slight increased formation of unknown 1 to eventually disappear towards the end of the reaction. However, unknown 2 steadily increases over time. Therefore, it is possible that unknown 1 is an intermediate and unknown 2 is another end product that forms from the reaction of bromoacetaldehyde and monochloramine. Additional GC/MS experiments that scan a wider m/z range (30-350 amu) are needed to identify the unknown products that are forming from this reaction.

4.3.2. Bromoacetaldehyde and monochloramine equilibrium constant determination

Bromoacetaldehyde hydrates in water and is in equilibrium with bromomethanediol according to

$$K_{h3} = \frac{[\mathrm{BrCH_2CHO}]}{[\mathrm{BrCH_2CH(OH)_2}]} = 0.0157 \quad (1)$$

where, K_{h3} is an estimated value based on the structure of bromoacetaldehyde [5]. Total concentration of bromomethanediol and unhydrated bromoacetaldehyde ($C_{T,\mathrm{BrCH2CHO}}$) is expressed as the sum of both species. Each species is expressed as a fraction of $C_{T,\mathrm{BrCH2CHO}}$

$$\frac{[\mathrm{BrCH_2CHO}]}{C_{T,\mathrm{BrCH2CHO}}} = \frac{K_{h3}}{1+K_{h3}} = \sigma_0 \quad (2)$$

$$\frac{[\mathrm{BrCH_2CH(OH)_2}]}{C_{T,\mathrm{BrCH2CHO}}} = \frac{1}{1+K_{h3}} = \sigma_1 \quad (3)$$

where, σ_0 and σ_0 are equal to 0.0155 and 0.9845.

Bromoacetaldehyde and monochloramine react in a fast and reversible reaction to form 2-bromo-1-(chloroamino)ethanol. The equilibrium expression K_I is defined as

$$K_I = \frac{[\mathrm{BrCH_2CH(OH)NHCl}]_e}{[\mathrm{NH_2Cl}]_e[\mathrm{BrCH_2CHO}]_e} \quad (4)$$

where,

$[\mathrm{NH_2Cl}]_e$ = Monochloramine concentration at equilibrium

$[\mathrm{BrCH_2CH(OH)NHCl}]_e$= 2-bromo-1-(chloroamino)ethanol concentration at equilibrium

$[\mathrm{BrCH_2CHO}]_e$ = Unhydrated bromoacetaldehyde concentration at equilibrium

Equilibrium constant determination method explained in Chapters 2 and 3 was performed to calculate K_I. Equilibrium experiments were performed in excess of bromoacetaldehyde at

conditions specified in UV-1. Therefore, bromoacetaldehyde concentration at equilibrium is approximated to the same as the initial bromoacetaldehyde concentration ($[BrCH_2CHO]_e \approx [BrCH_2CHO]_0$). Bromoacetaldehyde spectra of increasing concentration were subtracted from experimental reaction spectra. Absorption spectra equals to

$$A_{\lambda,e} = \varepsilon_{NH_2Cl_\lambda}[NH_2Cl]_e + \varepsilon_{BrCH_2CH(OH)NHCl_\lambda}[BrCH_2CH(OH)NHCl]_e \quad (5)$$

where, $\varepsilon_{NH_2Cl_\lambda}$ and $\varepsilon_{BrCH_2CH(OH)NHCl_\lambda}$ are the molar absorptivities of monochloramine and 2-bromo-1-(chloroamino)ethanol at wavelength λ respectively.

Monochloramine concentration at equilibrium equals the initial monochloramine minus the product 2-bromo-1-(chloroamino)ethanol.

$$[NH_2Cl]_e = [NH_2Cl]_0 - [BrCH_2CH(OH)NHCl]_e \quad (6)$$

Equation 6 is substituted into equation 4 and 5 and simplified to

$$[BrCH_2CH(OH)NHCl]_e = \frac{[NH_2Cl]_0[BrCH_2CHO]_0}{1/K_1 + [BrCH_2CHO]_0} \quad (7)$$

and

$$A_{\lambda,e} = \varepsilon_{NH_2Cl_\lambda}[NH_2Cl]_0 + (\varepsilon_{BrCH_2CH(OH)NHCl_\lambda} - \varepsilon_{NH_2Cl_\lambda})[BrCH_2CH(OH)NHCl]_e \, . \quad (8)$$

Combining equation 7 and 8 the following expression is obtained

$$A_{\lambda,e} = \varepsilon_{NH_2Cl_\lambda}[NH_2Cl]_0 + (\varepsilon_{BrCH_2CH(OH)NHCl_\lambda} - \varepsilon_{NH_2Cl_\lambda})\frac{[NH_2Cl]_0[BrCH_2CHO]_0}{(1/K_1 + [BrCH_2CHO]_0)} \quad (9)$$

where, K_1 and $\varepsilon_{BrCH_2CH(OH)NHCl_\lambda}$ are two unknowns that are fitted to absorbance values between 235 to 250 of UV-1, conditions at which further reaction of monochloramine and 2-bromo-1-

(chloroamino)ethanol are the slowest. An average K_I value of 1900 ± 175 M^{-1} was calculated. Additionally, a second round fitting of data was performed with K_I =1900 M^{-1} value to obtain molar absorptivity values for 2-bromo-1-(chloroamino)ethanol as shown in Figure 4.5. Monochloramine and 2-bromo-1-(chloroamino)ethanol concentrations were estimated with equations 6 and 7. Absorbance values were then calculated and compared with UV-1 experimental data in Figure 4.6. Results show that predicted values represent a close approximation to the experimental data.

4.3.3. Bromoacetonitrile and 2-bromo-*N*-chloroacetamide formation

Experiments (UV-2 and UV-3) were performed at neutral and high pH to study the reaction kinetics of bromoacetonitrile and 2-bromo-*N*-chloroacetamide formation. Both products, bromoacetonitrile and 2-bromo-*N*-chloroacetamide, absorbed in the lower wavelengths as shown in Figure 4.7. Monochloramine and 2-bromo-1-(chloroamino)ethanol absorption are a bell shaped curve with peak maximum around 243 nm (Figure 4.5). Because products and intermediates absorb in similar regions it was difficult to accurately determine the individual species concentrations over time. Additionally, GC-1 results confirm the formation of unknown compounds that might absorb in the UV region interfering with the species concentration determination. However, general trends were observed and confirmed with GC-1 results.

At pH 9.5 monochloramine and 2-bromo-1-(chloroamino)ethanol absorbance at 243 nm decreases with a steady increase in the low UV region related to bromoacetonitrile and 2-bromo-*N*-chloroacetamide for the first 15 minutes as depicted on Figure 4.9. Both products were quantified with GC-1 experiment as shown in Figure 4.9. GC-1 experiment also confirms that 2-

bromo-*N*-chloroacetamide formed only at the beginning of the experiment and that mostly the bromoacetonitrile formation also occurred initially. Thus, bromoacetonitrile and bromoacetamide represent only ~12% of the initial monochloramine concentration. After 15 minutes, another reaction takes place that consumes monochloramine and forms unknown compounds that also absorb in the low UV region. This is consistent with two unknown peaks observed in the total ion chromatogram results (Figure 4.2).

Monochloramine and bromoacetaldehyde were also reacted at pH 7.8 and monitored over time (Figure 4.10). The reaction suggests that monochloramine and 2-bromo-1-(chloroamino)ethanol decomposition to other products is a slow reaction at neutral pH. The difference between reaction rates at pH 9.5 and 7.8 indicates that there is a base catalysis effect as also observed with other aldehydes in this study.

4.3.4. Implications for Drinking Water

Chloramination of drinking water can minimize the formation of regulated DBPs but can alternately produce more toxic N-DBPs such as HAcAm and HAN. Previous research on chloramination of several natural organic matter models has found that more than 70% of the nitrogen of HAN and HAcAm is incorporated from monochloramine [6, 7]. This indicates the importance of the monochloramine and aldehyde reaction pathway for the formation of HAN and HAcAm. Monochloramine has been shown to react with bromoacetaldehyde to produce bromoacetonitrile and 2-bromo-*N*-chloroacetamide. However, the formation of these two compounds is about ~12% of the initial monochloramine dose which is very low compared to its chlorinated counterparts studied in chapter 2 that can account for all of the initial

monochloramine dose. Therefore, it might be possible that bromoacetonitrile and 2-bromo-*N*-chloroacetamide formation from chloramination will be found a lower concentrations than chloroacetonitrile and *N*,2-dichloroacetamide. An occurrence study that tested several finished waters for several HAN and HAcAm have detected bromoacetonitrile and bromoacetamide however, the concentration and number of samples that detected bromoacetonitrile (75^{th} Percentile = 0.18 μg/L and 2/54) is lower than the ones detected for chloroacetonitrile (75^{th} Percentile = 0.35 μg/L and 16/53) [3, 4].

Literature Cited

1. Muellner, M. G.; Wagner, E. D.; McCalla, K.; Richardson, S. D.; Woo, Y.-T.; Plewa, M. J., Haloacetonitriles vs regulated haloacetic acids are nitrogen-containing DBPs more toxic. *Environmental Science & Rechnology* **2007,** *41*, 645-51.

2. Plewa, M. J.; Muellner, M. G.; Richardson, S. D.; Fasano, F.; Buettner, K. M.; Yin-Tak, W.; McKague, A. B.; Wagner, E. D., Occurrence, Synthesis, and Mammalian Cell Cytotoxicity and Genotoxicity of Haloacetamides: An Emerging Class of Nitrogenous Drinking Water Disinfection Byproducts. *Environmental Science & Technology* **2008,** *42*, (3), 955-961.

3. Weinberg, H. S.; Krasner, S. W.; Richardson, S. D.; Thruston, A. D. J., 2002. *The Occurrence of Disinfection By-Products (DBPs) of Health Concern in Drinking Water : Results of a Nationwide DBP Occurrence Study*. Environmental Protection Agency, National Exposure Research Laboratory, Athens, GA. EPA/600/R-02/068.

4. Krasner, S. W.; Weinberg, H. S.; Richardson, S. D.; Pastor, S. J.; Chinn, R.; Sclimenti, M. J.; Onstad, G. D.; Thruston Jr, A. D., Occurrence of a New Generation of Disinfection Byproducts. *Environmental Science & Technology* **2006,** *40*, (23), 7175-7185.

5. Greenzaid, P.; Luz, Z.; Samuel, D., A Nuclear Magnetic Resonance Study of the Reversible Hydration of Aliphatic Aldehydes and Ketones. I. Oxygen-17 and Proton Spectra and equilibrium constants. *Journal of the American Chemical Society* **1966,** *89*, 749-756.

6. Huang, H.; Wu, Q. Y.; Hu, H. Y.; Mitch, W. A., Dichloroacetonitrile and dichloroacetamide can form independently during chlorination and chloramination of drinking waters, model organic matters, and wastewater effluents. *Environmental Science & Technology* **2012,** *46*, (19), 10624-10631.

7. Yang, X.; Fan, C.; Shang, C.; Zhao, Q., Nitrogenous disinfection byproducts formation and nitrogen origin exploration during chloramination of nitrogenous organic compounds. *Water Research* **2010,** *44*, (9), 2691-2702.

Table and Figures

Table 4.1 Bromoacetaldehyde and monochloramine experimental conditions and instrumentation used to monitor the reaction

Exp Set	$p[H^+]$	$[NH_2Cl]_0$ (M)	$C_{T,ALDEHYDE}$ (M)	Buffer	$C_{T,\ Buffer}$ (M)	Instrument
UV-1	7.8	0.001	0.010 – 0.026	Phosphate	0.020	UV-Vis
UV-2	9.5	0.001	0.010	Carbonate	0.020	UV-Vis
UV-3	6.0-7.88	0.001	0.010	Phosphate	0.020	UV-Vis
GC-1	9.5	0.001	0.010	Carbonate	0.020	GC/MS

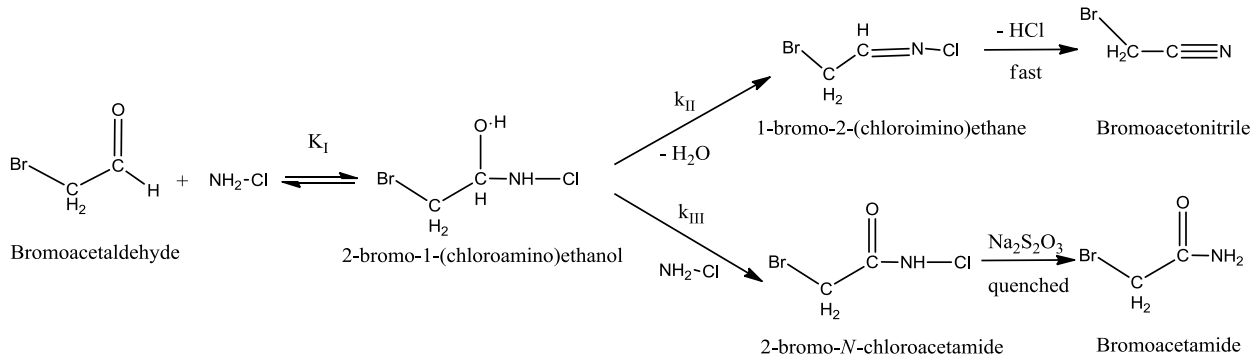

Figure 4.1 2-bromo-*N*-chloroacetamide and bromoacetonitrile proposed reaction pathway

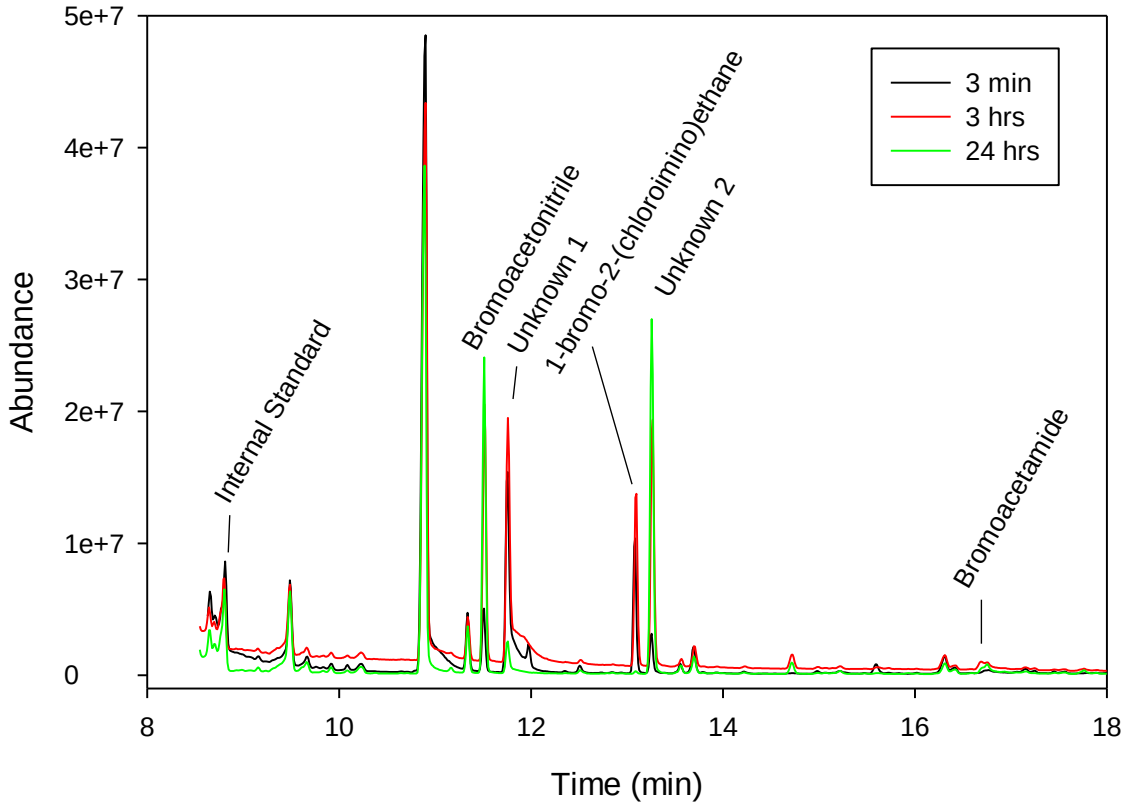

Figure 4.2. GC/MS Total Ion Chromatogram. Reaction samples at 3 min, 3 hrs, and 24 hrs of reaction $[NH_2Cl]_0$ = 1 mM, $[BrCH_2CHO]_{T,0}$ = 10 mM, $[CO_3]_{T,0}$ = 0.02 M, pH 9.5 ± 0.1, μ = 0.1 M, 18 ± 0.1^{0}C

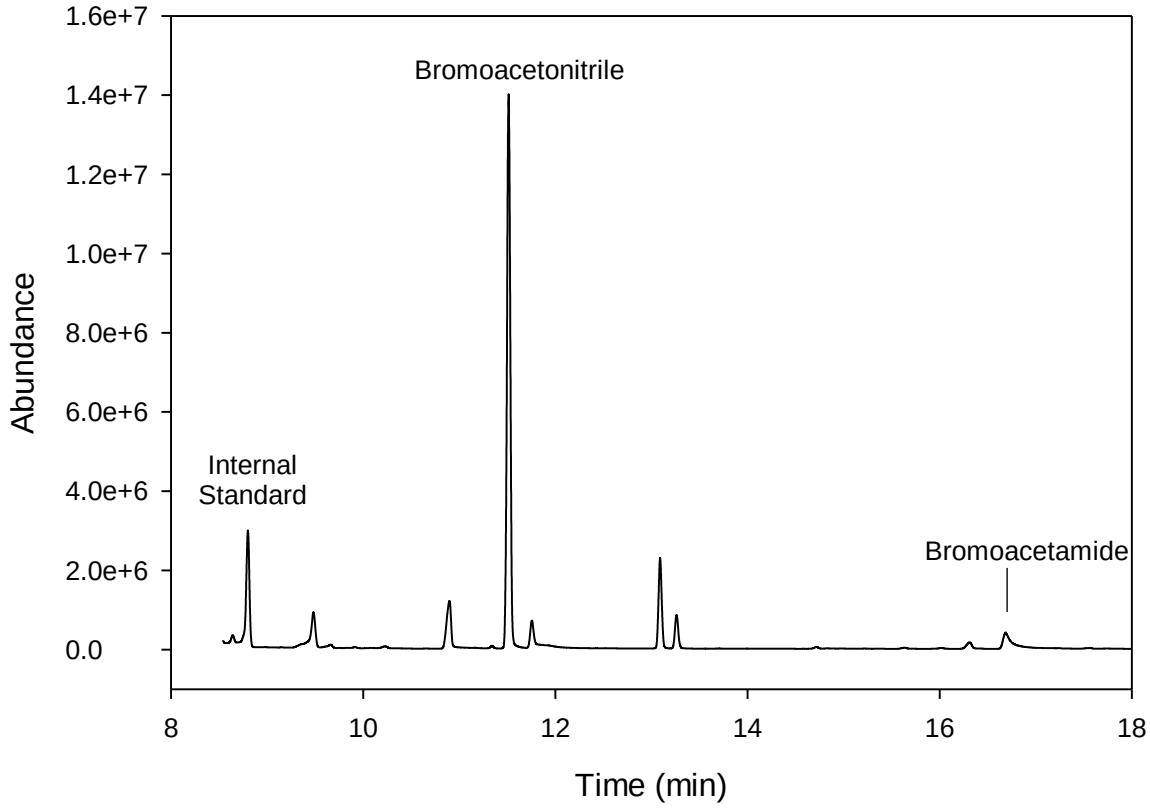

Figure 4.3 GC/MS Select Ion Monitoring. Extraction after 3 hrs of reaction, $[NH_2Cl]_0$ = 1 mM, $[BrCH_2CHO]_{T,0}$ = 10 mM, $[CO_3]_{T,0}$ = 0.02 M, pH 9.5 ± 0.1, μ = 0.1 M, 18 ± 0.1^{0}C

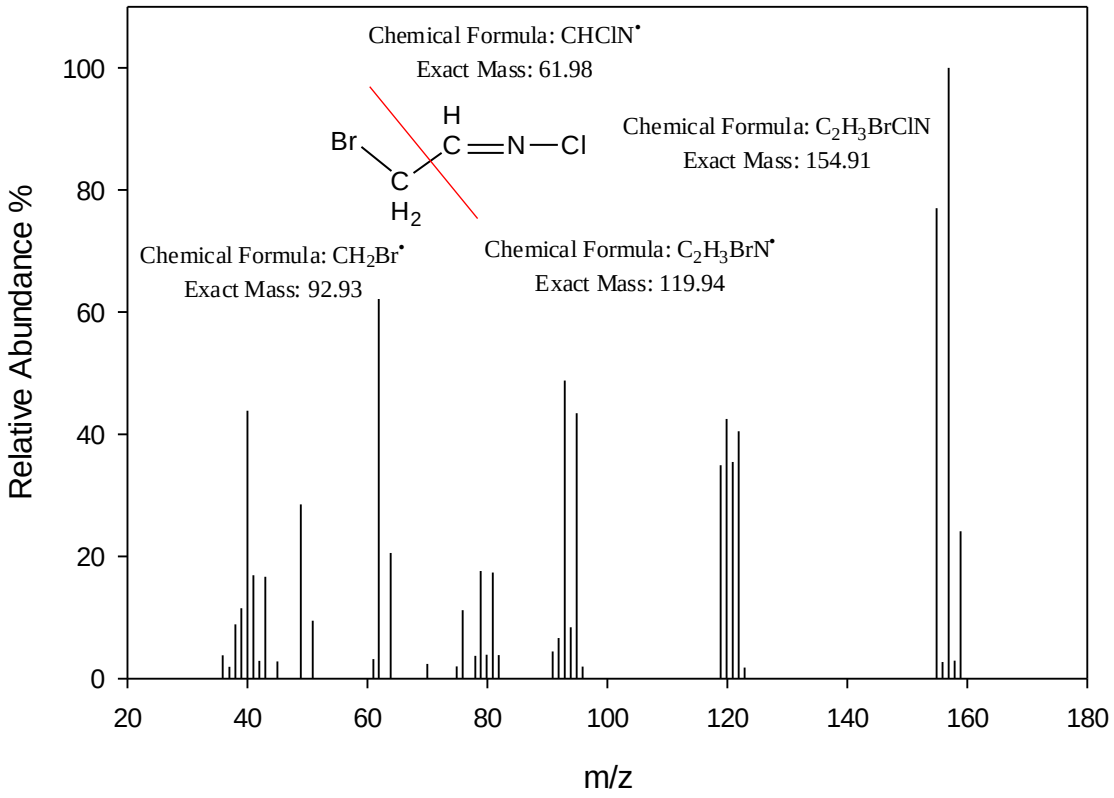

Figure 4.4 1-bromo-2-(chloroimino)ethane mass spectra m/z: 155(77%), 157(100%), 159 (25%), 119(35%), 120(43%), 121(35%), 122(40%), 93 (49%), 95(43%), 62 (62%), 64(21%)

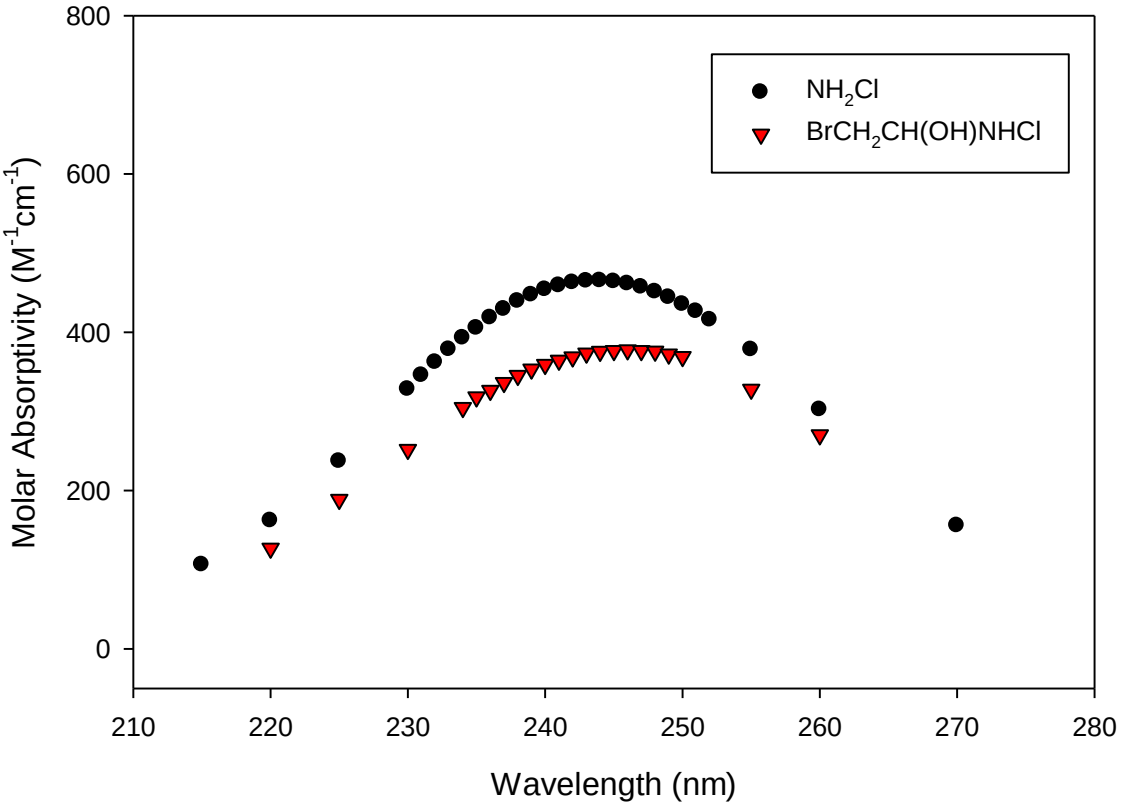

Figure 4.5 Monochloramine and 2-bromo-1-(chloroamino)ethanol molar absorptivity coefficients determined in this study

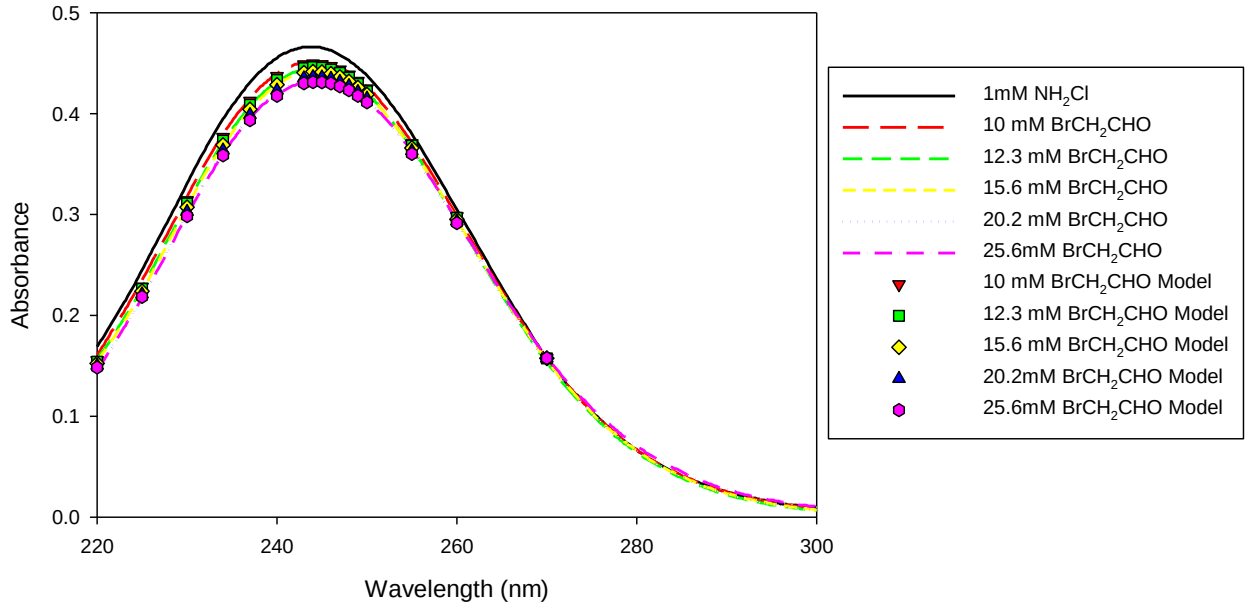

Figure 4.6 Bromoacetaldehyde and monochloramine reaction taken between 1-3 min (UV-1) with increasing bromoacetaldehyde concentrations and absorbance predictions calculated with K_I and 2-bromo-1-(chloroamino)ethanol molar absorptivities

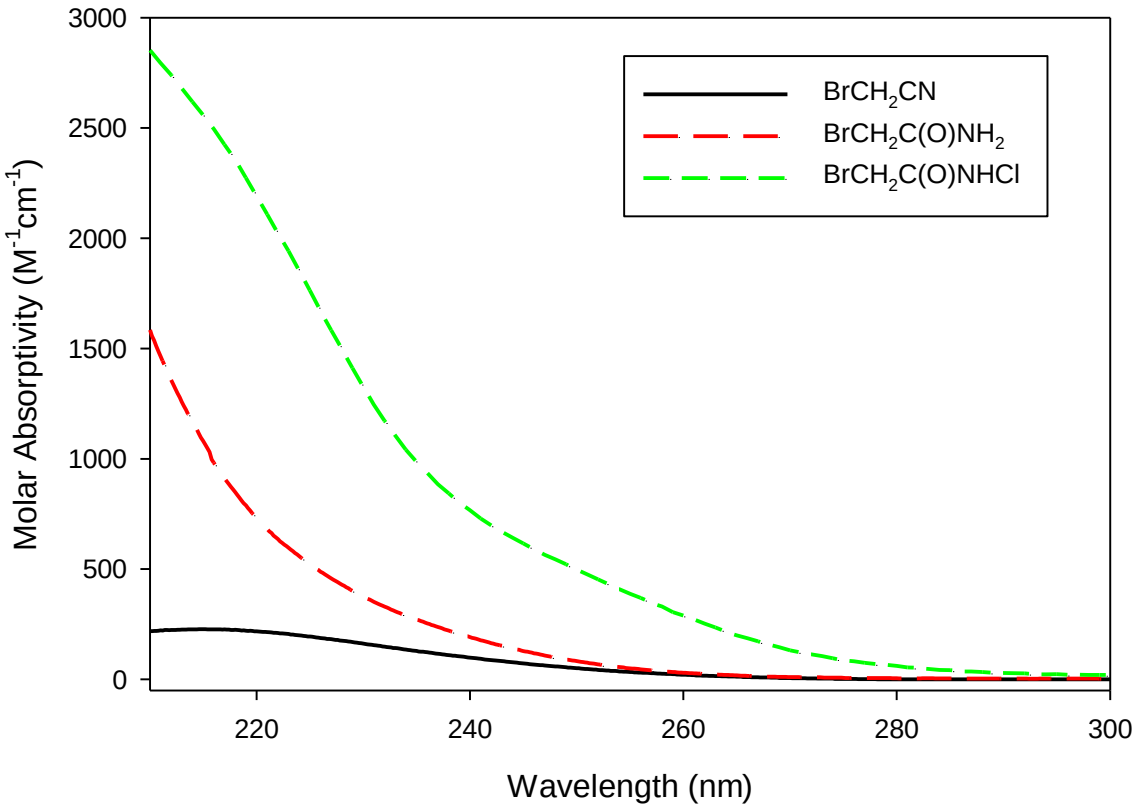

Figure 4.7 Bromoacetonitrile, bromoacetamide, and 2-bromo-*N*-chloroacetamide molar absorptivities determined in this study

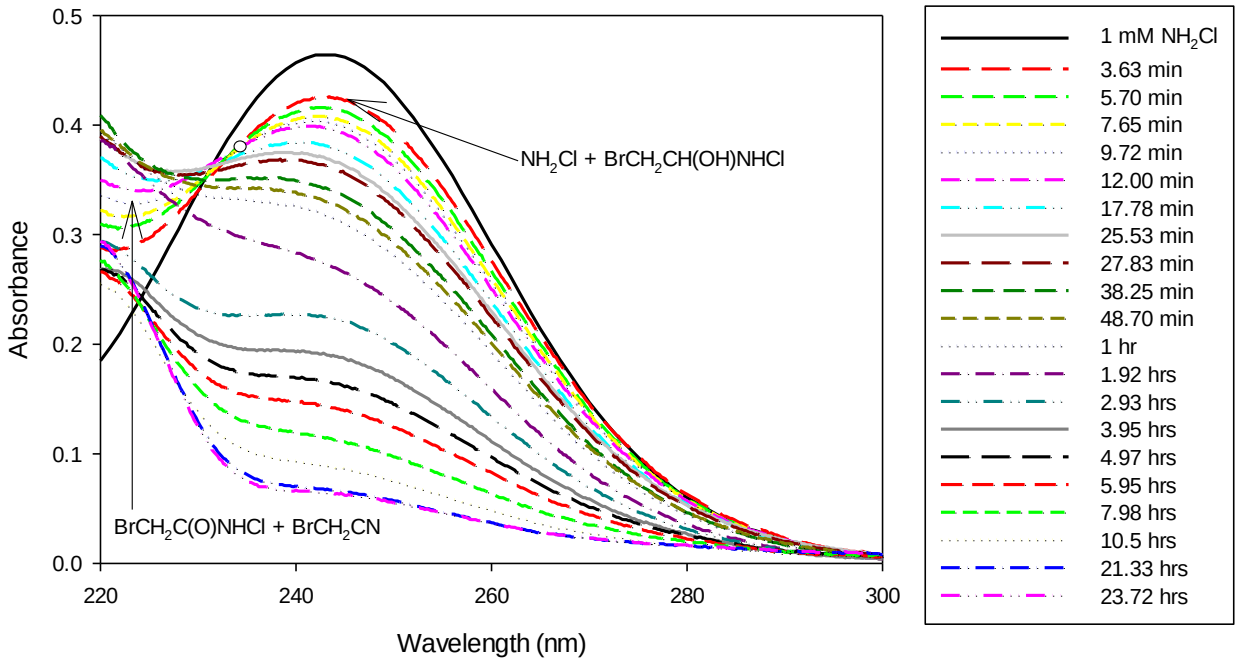

Figure 4.8 Bromoacetaldehyde and monochloramine reaction spectras over time $[NH_2Cl]_0$ = 1 mM, $[BrCH_2CHO]_{T,0}$ = 10 mM, $[CO_3]_{T,0}$ = 0.02 M, pH 9.5 ± 0.1, μ = 0.1 M, 18 ± 0.1^0C

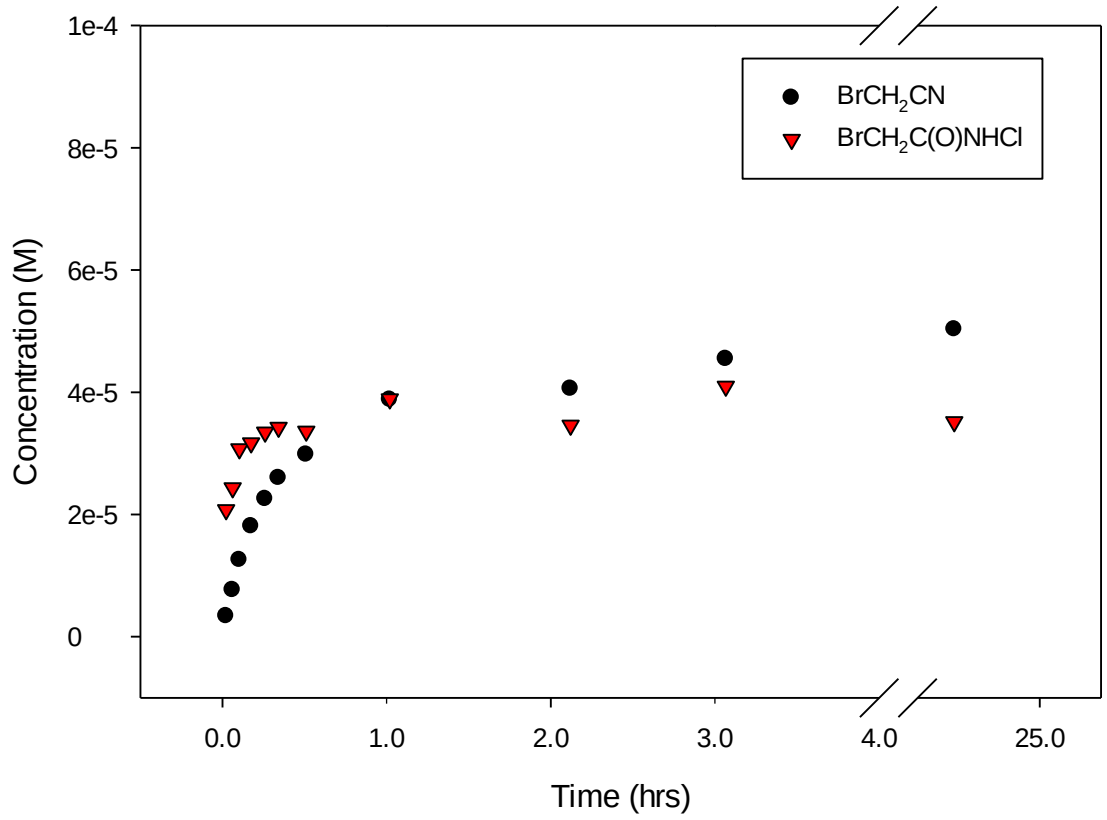

Figure 4.9 Bromoacetonitrile and 2-bromo-*N*-chloroacetamide concentrations over time, $[NH_2Cl]_0$ = 1 mM, $[BrCH_2CHO]_{T,0}$ = 10 mM, $[CO_3]_{T,0}$ = 0.02 M, pH 9.5 ± 0.1, μ = 0.1 M, 18 ± 0.1^{0}C

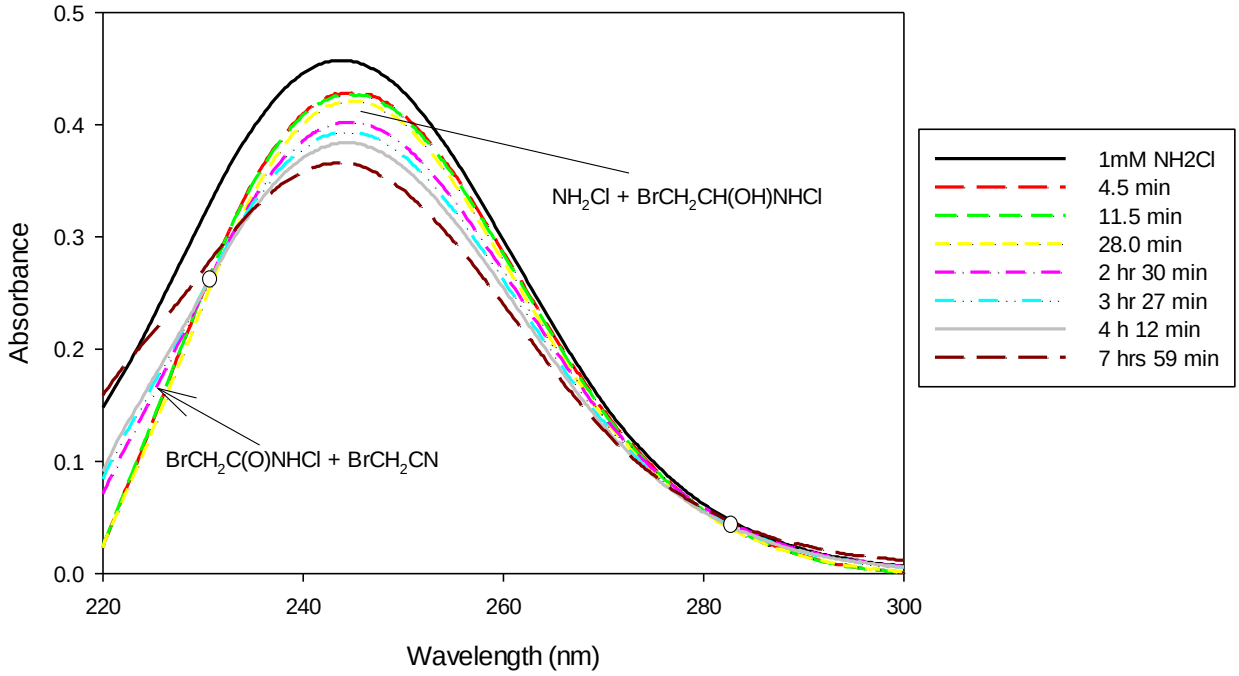

Figure 4.10 Bromoacetaldehyde and monochloramine reaction spectras over time, $[NH_2Cl]_0$ = 1 mM, $[BrCH_2CHO]_{T,0}$ = 10 mM, $[PO_4]_{T,0}$ = 0.02 M, pH 7.8 ± 0.1, μ = 0.1 M, 18 ± 0.1 ^{0}C

CHAPTER 5

CONCLUSIONS

(Halo)acetaldehydes (chloroacetaldehyde, bromoacetaldehyde, and acetaldehyde) react with monochloramine to form carbinolamines (2-chloro-1-(chloroamino)ethanol, 2-bromo-1-(chloroamino)ethanol and 1-(chloroamino)ethanol). Carbinolamines are relatively stable intermediates that will be present in equilibrium with initial reactants. While the formation of end products of such reactions are important, exposure to intermediate compounds is also relevant. However, measurement of such compounds presents a challenge because they convert back to initial reactants when samples are quenched for preservation prior to analysis.

Carbinolamines undergo parallel reactions: 1) dehydration to its corresponding imine that further decomposes to (halo)acetonitriles (chloroacetonitrile, bromoacetonitrile, and acetonitrile), and 2) oxidation by monochloramine to form *N*-haloacetamides (*N*,2-dichloroacetamide, 2-bromo-*N*-chloroacetamide, and *N*-chloroacetamide). The dehydration reaction to chloroacetonitrile formation was found to be acid and base catalyzed. However, the oxidation reaction to *N*,2-dichloroacetamide was found to be only base catalyzed. It is possible that at low pH conditions the oxidation reaction is slow and was not detectable with the analytical instruments. Both reactions were found to be slow in the neutral pH region. Acetonitrile and *N*-chloroacetamide formation were both found to be acid and base catalyzed. Their formation was also the slowest at neutral pH. Bromoacetonitrile and 2-bromo-*N*-chloroacetamide had similar reaction pathway as the other two (halo)acetonitriles and (halo)acetamides however, it was observed that it would only occur at the beginning of the reaction between bromoacetaldehyde and monochloramine. The product formation of brominated compounds was low and accounted

for only 12% of the initial monochloramine concentration. Other reactions and products formed that were not identified in this study. This is consistent with low detection of bromoacetonitrile compared to chloroacetonitrile in an occurrence study summarized in Table 1.1.

Acetonitrile and *N*-chloroacetamide formation rates were influenced by temperature. 1-(chloroamino)ethanol disappearance and product formation were tested at 18 and 25 ° C. Reaction rates were higher at 25 ° C.

(Halo)acetamides are among the most cyto- and genotoxic chemical class found in treated waters. However, *N*-chloroacetamides have not been previously tested for their cytotoxicity. In this study *N*,2-dichloroacetamide was tested for cytotoxicity and found to be slightly lower potent than the monochloroacetamide but more toxic than the di- and trichloroacetamide. Therefore, monitoring N,2-dichloroacetamide is of importance for treated waters.

Understanding the chemistry of the formation of (halo)acetonitriles and (halo)acetamides is important to devise appropriate sampling techniques for their detection in treated waters and for DBP control strategies. In this study, it was found that the reaction of ascorbic acid and monochloramine was slow and thus DBP formation would continue after quenching. Additionally, it is common practice to adjust to low pH after quenching which will accelerate the formation of (halo)acetonitriles and (halo)acetamides. Results with such sampling techniques will provide different concentrations found in finished water that the public would be exposed to. Alternately, it was found that the addition of sodium thiosulfate as a quencher and adjustment to neutral pH before immediate analysis would not significantly affect (halo)acetonitrile and (halo)acetamide concentrations. Additionally, to minimize the formation of these products in treated waters a high pH should be avoided.

CHAPTER 6

FUTURE RESEARCH

This research investigated the chemical formation of (halo)acetonitriles and (halo)acetamides from the reaction of aldehydes and monochloramine. However, several findings were not answered and need further exploration. 1) The reaction of bromoacetaldehyde and monochloramine produced other intermediates and products that were not identified in this study. Identification of such products would provide insight to other reactions that are relevant in water treatment. 2) Temperature had a significant impact on kinetic rates therefore, further temperatures should be tested to obtain activation energies to extrapolate the kinetic rates for real water modeling predictions. 3) Relevance of (monohalo)acetonitriles and (monohalo)acetamides formation from the reaction of (monohalo)acetaldehydes and monochloramine in real waters should be tested. 4) Investigate if iodoacetonitrile and 2-iodo-N-chloroacetamide are formed from the reactions of iodoacetaldehyde and monochloramine.

This study focused mainly on monohalogenated acetamides and acetonitriles. Based on the chemistry of these compounds it is recommended to extend the relevance of monochloramine and haloacetaldehyde reaction in the formation of di- and tri- halogenated acetonitriles and acetamides. Water conditions such as pH and temperature should also be explored. Understanding the chemistry of the mono-, di-, and tri- halogenated acetonitriles and acetamides should explain the formation of such compounds in treated waters and provide strategies to minimize their formation.

APPENDIX A

EXPERIMENTAL DATA FOR CHAPTER 2

Experimental conditions and raw data used for Chapter 2 are described in the following. Interpretations of the data sets are included in Chapter 2.

Table A.1. Summary of experimental conditions for chloroacetaldehyde and monochloramine reaction at 18°C and ionic strength of 0.1 M studied in chapter 2

Exp Set	$p[H^+]$	$[NH_2Cl]_0$ (M)	$C_{T,ClCH2CHO}$ (M)	Buffer	$C_{T,\ Buffer}$ (M)	Instrument
UV-1.1	7.6	0.001	0.010	Phosphate	0.020	UV-Vis
UV-1.2	7.6	0.001	0.015	Phosphate	0.020	UV-Vis
UV-1.3	7.6	0.001	0.020	Phosphate	0.020	UV-Vis
UV-1.4	7.6	0.001	0.030	Phosphate	0.020	UV-Vis
UV-1.5	7.6	0.001	0.040	Phosphate	0.020	UV-Vis
UV-2.1	9.39	0.001	0.010	Carbonate	0.020	UV-Vis
UV-2.2	9.61	0.001	0.010	Carbonate	0.020	UV-Vis
UV-2.3	9.67	0.001	0.010	Carbonate	0.020	UV-Vis
UV-2.4	9.83	0.001	0.010	Carbonate	0.020	UV-Vis
UV-2.5	9.90	0.001	0.010	Carbonate	0.020	UV-Vis
UV-2.6	9.99	0.001	0.010	Carbonate	0.020	UV-Vis
UV-3.1	3.64	0.001	0.010	Phosphate	0.020	UV-Vis
UV-3.2	4.00	0.001	0.010	Phosphate	0.020	UV-Vis
GC-1.1	7.49	0.002	0.005	Phosphate	0.020	GCMS
GC-1.2	7.50	0.002	0.005	Phosphate	0.020	GCMS
GC-2.1	9.39	0.001	0.010	Carbonate	0.020	GCMS
GC-2.2	9.87	0.001	0.010	Carbonate	0.020	GCMS
GC-3.1	4.22	0.001	0.010	Phosphate	0.020	GCMS
GC-3.2	5.19	0.001	0.010	Phosphate	0.020	GCMS
GC-3.3	5.27	0.001	0.010	Phosphate	0.020	GCMS
GC-3.4	5.46	0.001	0.010	Phosphate	0.020	GCMS
GC-3.5	5.99	0.001	0.010	Phosphate	0.020	GCMS

Figure A.1. Data sets UV-1.1 to UV-1.5

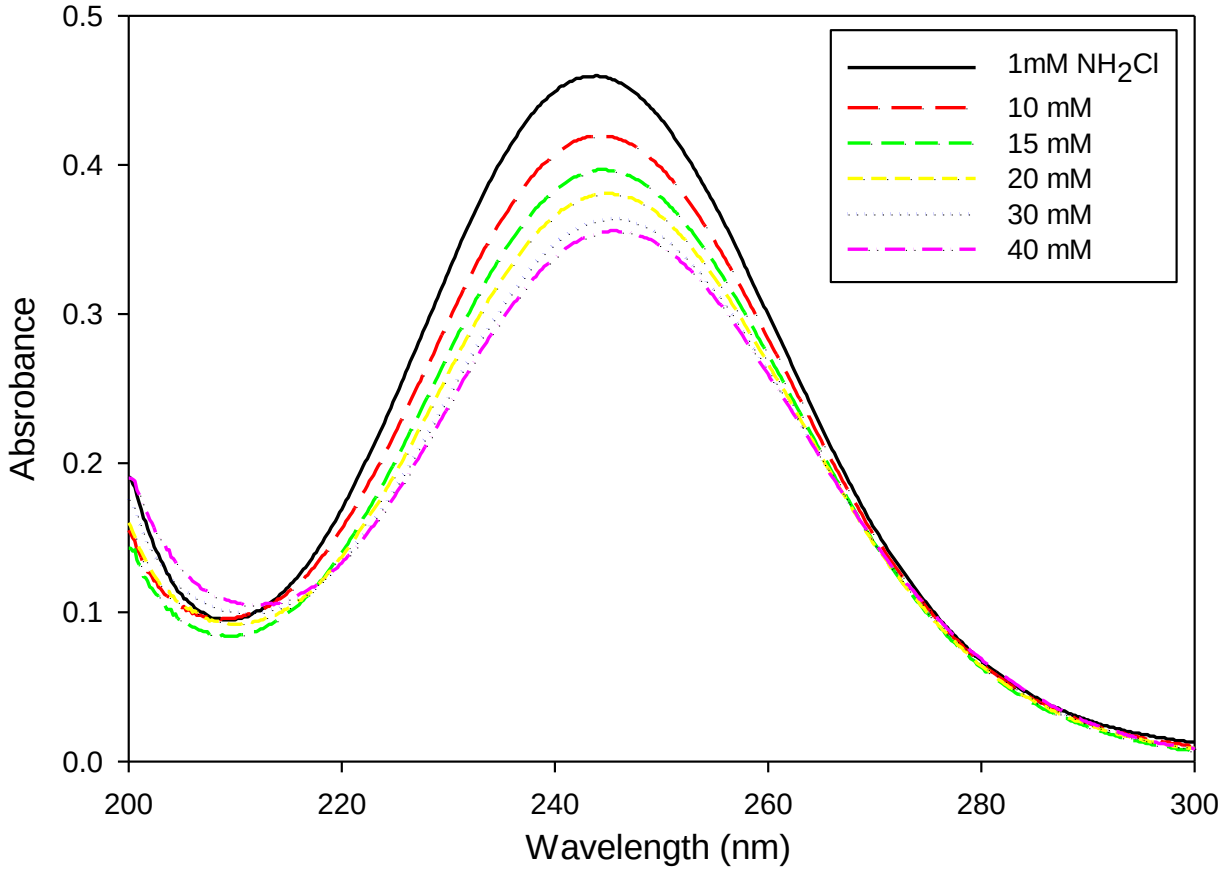

Table A.2. Data set UV-2.1

Time min	210 nm	231 nm	243 nm
0.5	0.135	0.319	0.428
1.7	0.181	0.314	0.414
4.0	0.255	0.306	0.394
7.3	0.341	0.292	0.367
10.3	0.406	0.279	0.346
13.5	0.481	0.274	0.326
16.2	0.524	0.261	0.309
20.4	0.572	0.247	0.288
25.3	0.616	0.222	0.262
30.3	0.644	0.21	0.243
35.3	0.658	0.188	0.223
40.5	0.681	0.181	0.208
45.2	0.668	0.145	0.19

Table A.3. Data set UV-2.2

Time	210 nm	231 nm	243 nm
0.4	0.092	0.315	0.424
1.3	0.123	0.308	0.41
2.4	0.177	0.3	0.395
4.9	0.27	0.289	0.366
6.8	0.333	0.28	0.347
8.9	0.388	0.275	0.331
10.8	0.432	0.266	0.316
12.8	0.474	0.255	0.301
16.5	0.532	0.236	0.277
19.1	0.558	0.209	0.263
23.7	0.598	0.19	0.235
27.2	0.612	0.198	0.223

Table A.4. Data set UV-2.3

Time min	210 nm	231 nm	243 nm
0.4	0.151	0.314	0.423
1.3	0.201	0.305	0.406
2.1	0.25	0.298	0.388
2.9	0.291	0.291	0.374
3.7	0.322	0.287	0.363
6.6	0.446	0.277	0.329
8.3	0.502	0.265	0.31
10.6	0.551	0.252	0.288
12.7	0.586	0.247	0.273
15.4	0.621	0.235	0.252
18.6	0.649	0.229	0.233

Table A.5. Data set UV-2.4

Time min	210 nm	231 nm	243 nm
0.4	0.153	0.308	0.415
1.1	0.204	0.3	0.398
2.1	0.255	0.293	0.379
3.0	0.304	0.285	0.364
4.0	0.354	0.279	0.349
5.5	0.415	0.267	0.325
7.1	0.473	0.261	0.307
9.1	0.542	0.252	0.285
11.3	0.589	0.239	0.263
13.3	0.624	0.236	0.25
15.9	0.661	0.223	0.228
18.5	0.69	0.213	0.211

Table A.6. Data set UV-2.5

Time min	210 nm	231 nm	243 nm
0.4	0.16	0.312	0.418
1.2	0.222	0.297	0.391
2.0	0.279	0.288	0.372
2.7	0.324	0.283	0.356
3.4	0.364	0.275	0.339
4.2	0.409	0.272	0.327
4.9	0.439	0.269	0.316
5.7	0.471	0.265	0.303
6.6	0.503	0.263	0.293
7.3	0.546	0.253	0.278
8.4	0.575	0.251	0.266
10.4	0.617	0.237	0.242
12.8	0.647	0.234	0.225

Table A.7. Data set UV-2.6

Time min	210 nm	231 nm	243 nm
0.4	0.156	0.313	0.417
1.2	0.237	0.298	0.385
2.1	0.301	0.291	0.363
3.6	0.423	0.282	0.325
4.9	0.486	0.282	0.311
5.7	0.53	0.275	0.296
6.8	0.571	0.272	0.28
7.8	0.587	0.268	0.267
8.8	0.624	0.258	0.252
9.9	0.645	0.258	0.242
11.1	0.66	0.245	0.225

Table A.8. Data set UV-3.1

Time min	210 nm	231 nm	243 nm
0.3	0.146	0.308	0.41
1.0	0.196	0.309	0.395
1.8	0.259	0.309	0.376
2.5	0.321	0.309	0.357
3.1	0.374	0.309	0.341
3.9	0.436	0.309	0.322
4.6	0.486	0.308	0.308
5.3	0.527	0.308	0.294
6.1	0.564	0.306	0.281

Table A.9. Data set UV-3.2

Time min	210 nm	231 nm	243 nm
0.5	0.256	0.313	0.374
1.3	0.284	0.314	0.366
1.9	0.312	0.316	0.361
2.5	0.33	0.314	0.352
3.1	0.353	0.313	0.346
3.7	0.372	0.316	0.342
4.3	0.367	0.306	0.331
4.9	0.383	0.306	0.326
5.6	0.419	0.312	0.324
6.2	0.439	0.315	0.321
6.9	0.454	0.315	0.317

Table A.10. Data set GC-1.1

Time min	Chloroacetonitrile uM	Chloroacetamide uM
3.5	N/A	17.2
20.0	13.7	26.6
40.0	N/A	29.0
60.0	N/A	30.6
120.0	15.8	57.5
180.0	13.7	64.9
240.0	20.0	103.0
565.0	17.2	131.3
893.0	30.6	198.5
1185.0	35.3	219.0
1567.0	30.7	216.8
2325.0	57.2	264.6
2882.0	38.1	224.1
3790.0	57.3	245.4

Table A.11. Data set GC-1.2

Time min	Chloroacetonitrile uM	Chloroacetamide uM
3.3	3.5	0.0
20.8	4.1	20.6
41.6	6.2	21.6
60.0	6.6	27.7
120.1	10.3	47.1
185.0	13.5	59.8
244.0	16.8	72.3
462.0	25.3	118.5
692.0	43.5	206.0
945.0	44.1	233.1

Table A.12. Data set GC-2.1

Time min	Chloroacetonitrile uM	Chloroacetamide uM
1.4	11.8	31.3
3.5	19.8	82.7
5.4	39.3	107.1
7.5	35.3	142.6
10.3	60.5	180.1
15.2	69.6	205.8
20.2	49.0	200.3
30.5	65.6	249.3

Table A.13. Data set GC-2.2

Time min	Chloroacetonitrile uM	Chloroacetamide uM
1.3	35.2	39.2
3.5	60.9	113.9
5.4	66.8	183.3
7.3	74.0	229.4
10.3	77.9	282.5
15.3	158.3	306.8
20.0	165.2	376.0
25.2	175.8	420.7
30.0	191.4	335.3

Table A.14. Data set GC-3.1

Time min	Chloroacetonitrile uM
1.4	6.3
5.2	11.6
9.5	17.8
14.7	27.9
19.9	24.7
25.6	30.0
29.5	32.7
45.1	39.5
60.2	46.7
90.2	51.2

Table A.15. Data set GC-3.2

Time min	Chloroacetonitrile uM
1.4	4.2
5.2	3.1
10.3	5.8
15.3	5.5
20.3	9.3
30.2	9.4
45.6	13.1
60.6	15.3
90.7	20.8
165.0	38.8

Table A.16. Data set GC-3.3

Time min	Chloroacetonitrile uM
1.3	0.0
3.4	0.0
5.3	1.7
10.3	4.4
15.3	2.8
20.1	5.8
30.4	6.4
45.7	8.6
60.3	10.4
90.8	13.9

Table A.17. Data set GC-3.4

Time min	Chloroacetonitrile uM
1.3	5.9
5.3	5.9
10.2	6.7
15.3	8.0
20.3	8.4
30.5	9.8
46.0	12.7
60.8	12.3
90.6	14.1

Table A.18. Data set GC-3.5

Time min	Chloroacetonitrile uM
1.3	0
5.0	0
10.2	2.11
15.2	2.71
20.2	3.85
30.7	0.31
45.4	3.44
61.2	3.8
90.8	4.7
168.0	4.74

APPENDIX B

EXPERIMENTAL DATA FOR CHAPTER 3

Experimental conditions and raw data used for Chapter 3 are described in the following. Interpretations of the data sets are included in Chapter 3.

Table B.1. Summary of experimental conditions for acetaldehyde and monochloramine reactions with ionic strength of 0.1 M studied in chapter 3

Exp Set	$p[H^+]$	$[NH_2Cl]_0$ (M)	$C_{T,CH3CHO}$ (M)	Buffer	$C_{T, Buffer}$ (M)	Temperature (°C)
UV-1.1	7.78	0.00099	0.010	Phosphate	0.020	18
UV-1.2	7.78	0.00099	0.015	Phosphate	0.020	18
UV-1.3	7.81	0.00099	0.020	Phosphate	0.020	18
UV-1.4	7.76	0.00098	0.040	Phosphate	0.020	18
UV-1.5	7.83	0.00099	0.050	Phosphate	0.020	18
UV-1.6	7.82	0.00099	0.060	Phosphate	0.020	18
UV-1.7	7.85	0.00099	0.070	Phosphate	0.020	18
UV-1.8	7.84	0.00098	0.080	Phosphate	0.020	18
UV-1.9	7.82	0.00098	0.090	Phosphate	0.020	18
UV-2.1	7.59	0.001	0.010	Phosphate	0.020	25
UV-2.2	7.59	0.001	0.015	Phosphate	0.020	25
UV-2.3	7.59	0.001	0.020	Phosphate	0.020	25
UV-2.4	7.58	0.001	0.025	Phosphate	0.020	25
UV-2.5	7.59	0.001	0.030	Phosphate	0.020	25
UV-2.6	7.56	0.001	0.035	Phosphate	0.020	25
UV-2.7	7.55	0.001	0.040	Phosphate	0.020	25
UV-2.8	7.56	0.001	0.045	Phosphate	0.020	25
UV-2.9	7.55	0.001	0.050	Phosphate	0.020	25
UV-2.10	7.55	0.001	0.060	Phosphate	0.020	25
UV-2.11	7.53	0.001	0.070	Phosphate	0.020	25
UV-3.1	5.87	0.001	0.010	Phosphate	0.020	18
UV-3.2	6.18	0.001	0.010	Phosphate	0.020	18
UV-3.3	6.92	0.001	0.010	Phosphate	0.020	18
UV-3.4	7.21	0.001	0.010	Phosphate	0.020	18
UV-3.5	7.49	0.001	0.010	Phosphate	0.020	18

Table B.1. (Cont)

Exp Set	$p[H^+]$	$[NH_2Cl]_0$ (M)	$C_{T,CH3CHO}$ (M)	Buffer	$C_{T,\ Buffer}$ (M)	Temperature (°C)
UV-3.6	7.67	0.001	0.010	Phosphate	0.020	18
UV-3.7	7.90	0.001	0.010	Phosphate	0.020	18
UV-4.1	6.18	0.001	0.010	Phosphate	0.020	25
UV-4.2	6.91	0.001	0.010	Phosphate	0.020	25
UV-4.5	7.51	0.001	0.010	Phosphate	0.020	25
UV-4.6	7.86	0.001	0.010	Phosphate	0.020	25
UV-5.1	9.02	0.001	0.010	Carbonate	0.020	18
UV-5.2	9.26	0.001	0.010	Carbonate	0.020	18
UV-5.3	9.49	0.001	0.010	Carbonate	0.020	18
UV-5.4	9.65	0.001	0.010	Carbonate	0.020	18
UV-5.5	10	0.001	0.010	Carbonate	0.020	18
UV-6.1	8.92	0.001	0.010	Carbonate	0.020	25
UV-6.2	9.43	0.001	0.010	Carbonate	0.020	25
UV-6.3	9.96	0.001	0.010	Carbonate	0.020	25
UV-7.1	9.77	0.001	0.010	Carbonate	0.010	25
UV-7.2	9.76	0.001	0.010	Carbonate	0.015	25
UV-7.3	9.76	0.001	0.010	Carbonate	0.020	25
UV-7.4	9.77	0.001	0.010	Carbonate	0.025	25
UV-7.5	9.80	0.001	0.010	Carbonate	0.030	25

Figure B.1. Data sets UV-1.1 to UV-1.9

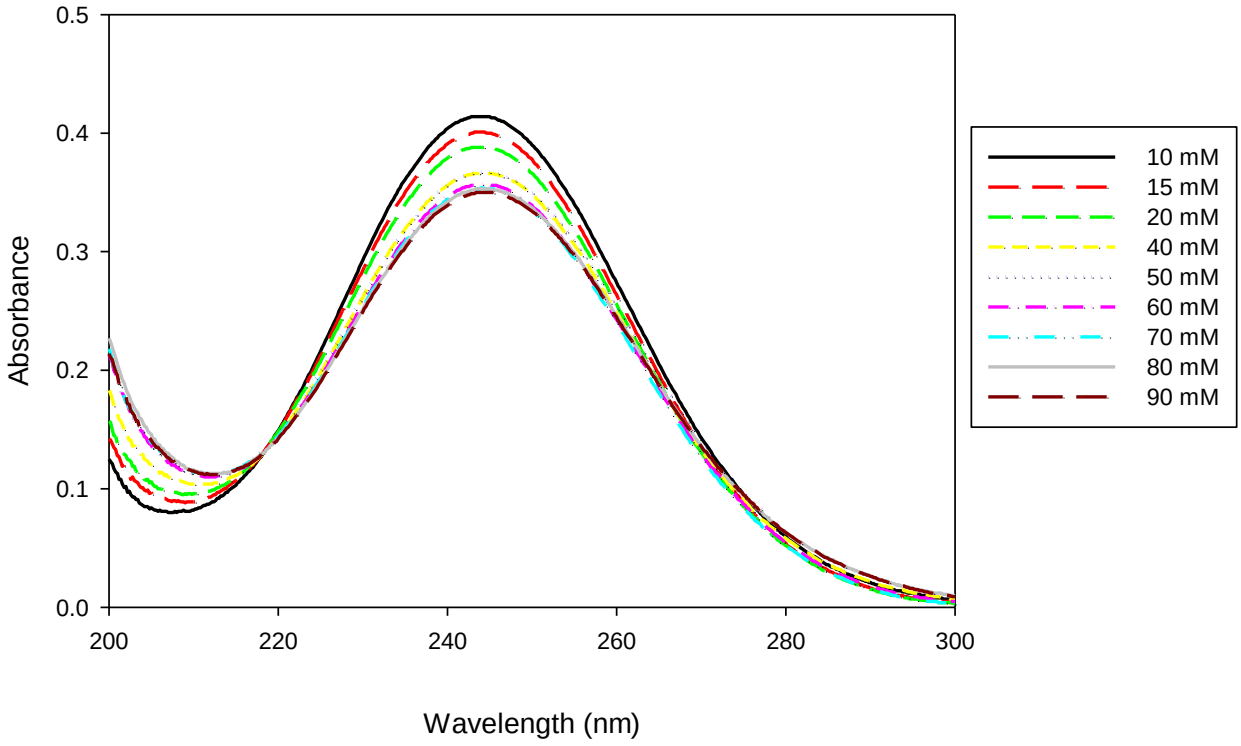

Figure B.2. Data sets UV-2.1 to UV-2.11

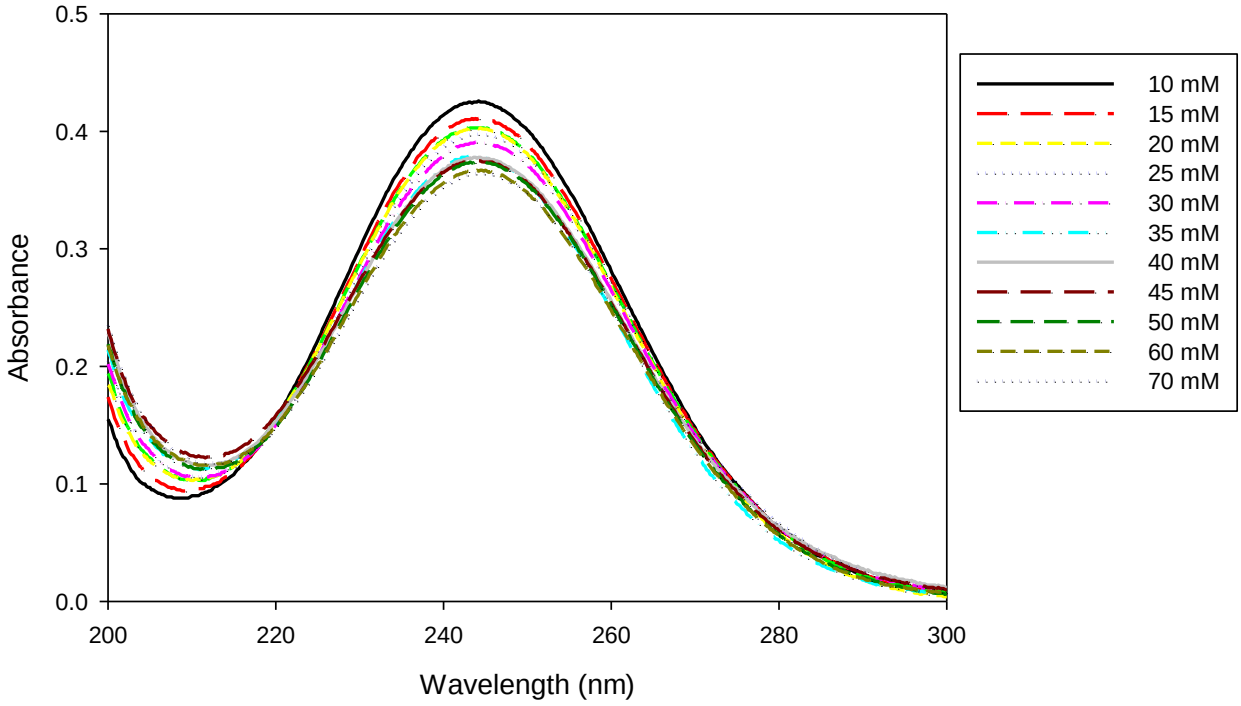

Table B.2. Data set UV-3.1

Time min	210 nm	220 nm	243 nm
0.7	0.148	0.181	0.405
1.9	0.194	0.201	0.391
3.0	0.23	0.217	0.376
4.3	0.269	0.232	0.359
5.2	0.295	0.243	0.348
6.3	0.326	0.255	0.335
7.0	0.347	0.264	0.326
7.9	0.37	0.273	0.317
8.7	0.388	0.28	0.308
9.5	0.407	0.287	0.299

Table B.3. Data set UV-3.2

Time min	210 nm	220 nm	243 nm
0.9	0.126	0.167	0.402
1.8	0.14	0.174	0.397
2.7	0.155	0.18	0.391
3.7	0.17	0.186	0.385
4.7	0.186	0.193	0.378
5.8	0.201	0.199	0.373
6.7	0.216	0.204	0.366
7.6	0.228	0.21	0.361
8.4	0.239	0.214	0.355
9.5	0.253	0.219	0.349
10.6	0.267	0.225	0.343
12.6	0.288	0.233	0.331
14.6	0.309	0.241	0.32
16.6	0.33	0.249	0.31

Table B.4. Data set UV-3.3

Time min	210 nm	220 nm	243 nm
0.7	0.092	0.154	0.414
3.8	0.104	0.158	0.412
8.4	0.122	0.166	0.405
13.2	0.137	0.172	0.397
18.9	0.151	0.175	0.383
23.7	0.165	0.181	0.377
28.9	0.182	0.188	0.373
33.2	0.199	0.196	0.366
38.7	0.202	0.195	0.356
43.6	0.216	0.2	0.349
48.8	0.221	0.201	0.342
59.0	0.235	0.206	0.334
59.0	0.241	0.209	0.329
64.7	0.25	0.21	0.32
69.9	0.257	0.213	0.314
74.6	0.261	0.213	0.308

Table B.5. Data set UV-3.4

Time min	210 nm	220 nm	243 nm
1.7	0.098	0.153	0.407
3.8	0.103	0.156	0.408
15.8	0.125	0.164	0.396
30.1	0.152	0.175	0.385
45.0	0.172	0.18	0.369
60.6	0.2	0.192	0.356
76.0	0.213	0.196	0.343
90.0	0.234	0.203	0.333
106.4	0.261	0.215	0.323
120.6	0.263	0.214	0.311

Table B.6. Data set UV-3.5

Time min	210 nm	220 nm	243 nm
0.8	0.087	0.149	0.414
14.9	0.105	0.156	0.405
30.9	0.122	0.16	0.397
45.3	0.138	0.166	0.391
60.0	0.152	0.17	0.381
74.9	0.166	0.174	0.372
90.2	0.18	0.179	0.363
105.1	0.19	0.181	0.356
119.5	0.202	0.186	0.35
149.5	0.226	0.193	0.335
180.0	0.248	0.2	0.323
210.0	0.27	0.208	0.311

Table B.7. Data set UV-3.6

Time min	210 nm	220 nm	243 nm
0.9	0.087	0.149	0.429
14.8	0.099	0.154	0.422
29.8	0.113	0.158	0.416
44.9	0.123	0.162	0.407
59.8	0.137	0.167	0.402
75.0	0.15	0.172	0.395
90.0	0.159	0.174	0.387
120.6	0.182	0.183	0.375
150.0	0.204	0.19	0.365
180.7	0.221	0.197	0.352
211.9	0.237	0.201	0.341
238.2	0.255	0.206	0.333

Table B.8. Data set UV-3.7

Time min	210 nm	220 nm	243 nm
1.0	0.089	0.15	0.419
20.1	0.102	0.153	0.407
40.1	0.115	0.156	0.398
59.8	0.126	0.158	0.388
80.0	0.147	0.166	0.383
100.4	0.16	0.17	0.379
120.0	0.172	0.171	0.37
150.0	0.197	0.181	0.364
180.0	0.204	0.18	0.349
210.0	0.22	0.186	0.342
240.0	0.233	0.186	0.33

Table B.9. Data set UV-4.1

Time min	210 nm	220 nm	243 nm
0.5	0.129	0.171	0.415
1.4	0.145	0.178	0.409
2.1	0.159	0.183	0.403
2.8	0.174	0.188	0.396
3.5	0.188	0.194	0.389
4.2	0.202	0.2	0.383
4.9	0.216	0.205	0.377
5.6	0.228	0.21	0.371
6.7	0.249	0.218	0.362
7.8	0.267	0.225	0.351
8.6	0.29	0.239	0.345
9.9	0.309	0.247	0.337
11.4	0.319	0.246	0.325
12.2	0.331	0.249	0.318
13.5	0.347	0.256	0.31
14.5	0.359	0.26	0.304

Table B.10. Data set UV-4.2

Time min	210 nm	220 nm	243 nm
0.5	0.089	0.149	0.413
1.3	0.09	0.149	0.412
2.9	0.097	0.151	0.408
4.2	0.103	0.154	0.405
5.5	0.11	0.157	0.403
6.8	0.115	0.158	0.399
8.2	0.122	0.161	0.396
9.9	0.129	0.164	0.392
11.2	0.134	0.165	0.388
12.6	0.14	0.168	0.385
14.4	0.147	0.17	0.381
15.8	0.153	0.172	0.378

Table B.11. Data set UV-4.3

Time min	210 nm	220 nm	243 nm
0.6	0.099	0.162	0.414
1.3	0.097	0.159	0.414
5.5	0.101	0.16	0.409
11.5	0.126	0.173	0.415
15.8	0.131	0.172	0.413
20.6	0.142	0.178	0.407
25.8	0.145	0.178	0.402
31.2	0.161	0.183	0.4
35.7	0.161	0.182	0.395
40.8	0.172	0.187	0.393
45.7	0.177	0.187	0.39
51.3	0.176	0.185	0.381
56.0	0.182	0.186	0.38

Table B.12. Data set UV-4.4

Time min	210 nm	220 nm	243 nm
0.5	0.083	0.15	0.428
1.3	0.084	0.149	0.428
4.8	0.087	0.15	0.424
9.6	0.096	0.154	0.419
15.2	0.099	0.153	0.414
19.8	0.113	0.159	0.416
26.1	0.115	0.161	0.409
30.9	0.122	0.164	0.408
36.1	0.126	0.166	0.403
41.4	0.132	0.168	0.401
45.8	0.132	0.16	0.393
50.8	0.133	0.159	0.388
55.2	0.141	0.166	0.388
61.1	0.14	0.163	0.383

Table B.13. Data set UV-5.1

Time min	210 nm	220 nm	243 nm
1.0	0.105	0.157	0.414
1.8	0.109	0.159	0.413
2.9	0.112	0.16	0.411
3.9	0.115	0.16	0.408
4.9	0.118	0.161	0.406
5.9	0.122	0.163	0.406
6.9	0.124	0.164	0.403
9.9	0.133	0.166	0.395
20.0	0.162	0.174	0.374
29.5	0.189	0.185	0.36
39.6	0.209	0.188	0.34
49.6	0.224	0.191	0.323
59.8	0.249	0.2	0.311
69.8	0.274	0.209	0.3
79.7	0.284	0.211	0.287

Table B.14. Data set UV-5.2

Time min	210 nm	220 nm	243 nm
1.1	0.096	0.151	0.407
2.1	0.103	0.154	0.406
3.4	0.111	0.159	0.403
4.5	0.116	0.16	0.398
5.9	0.123	0.164	0.396
7.0	0.128	0.164	0.391
8.1	0.135	0.167	0.389
9.1	0.137	0.168	0.385
10.3	0.147	0.171	0.383
15.4	0.162	0.172	0.363
20.3	0.183	0.181	0.352
26.3	0.198	0.181	0.332
31.7	0.217	0.187	0.32
36.0	0.227	0.189	0.31
41.8	0.244	0.194	0.298
46.1	0.256	0.197	0.289
50.9	0.263	0.198	0.279
55.8	0.27	0.199	0.27

Table B.15. Data set UV-5.3

Time min	210 nm	220 nm	243 nm
1.2	0.102	0.153	0.402
2.1	0.11	0.158	0.399
3.0	0.12	0.163	0.396
4.1	0.131	0.168	0.391
5.2	0.139	0.17	0.386
6.3	0.145	0.17	0.379
7.3	0.155	0.175	0.375
8.5	0.164	0.178	0.37
9.4	0.171	0.18	0.365
10.4	0.176	0.181	0.359
15.5	0.205	0.187	0.335
20.5	0.231	0.194	0.314
25.7	0.255	0.2	0.295
30.8	0.282	0.208	0.279
35.6	0.306	0.218	0.266
40.1	0.319	0.22	0.252
45.5	0.332	0.222	0.237

Table B.16. Data set UV-5.4

Time min	210 nm	220 nm	243 nm
1.0	0.113	0.16	0.404
2.0	0.127	0.166	0.396
3.0	0.136	0.17	0.388
4.0	0.147	0.174	0.382
5.0	0.158	0.177	0.375
6.0	0.168	0.18	0.368
7.0	0.179	0.184	0.362
8.0	0.191	0.188	0.356
9.0	0.199	0.19	0.35
10.0	0.21	0.193	0.344
16.0	0.252	0.205	0.308
20.5	0.286	0.218	0.287
25.5	0.313	0.225	0.265
30.0	0.335	0.232	0.247
34.9	0.349	0.233	0.229

Table B.17. Data set UV-5.5

Time min	210 nm	220 nm	243 nm
0.9	0.095	0.136	0.398
1.9	0.119	0.148	0.385
2.9	0.141	0.156	0.371
4.0	0.167	0.168	0.359
4.9	0.179	0.17	0.347
5.9	0.194	0.173	0.336
6.8	0.214	0.18	0.327
8.1	0.232	0.188	0.313
9.1	0.242	0.187	0.304
10.1	0.259	0.196	0.295
16.0	0.305	0.198	0.244
20.9	0.346	0.211	0.213
25.8	0.399	0.24	0.19
31.2	0.431	0.253	0.164

Table B.18. Data set UV-6.1

Time min	210 nm	220 nm	243 nm
0.5	0.115	0.167	0.426
1.2	0.12	0.167	0.422
1.9	0.124	0.168	0.418
2.6	0.128	0.169	0.415
3.3	0.132	0.169	0.413
4.1	0.135	0.17	0.409
4.7	0.138	0.171	0.405
5.5	0.143	0.171	0.403
6.4	0.149	0.173	0.399
7.9	0.157	0.175	0.393
9.6	0.169	0.179	0.386
13.3	0.182	0.178	0.368
16.9	0.201	0.182	0.355
20.7	0.214	0.18	0.341
25.7	0.229	0.183	0.324
30.2	0.241	0.18	0.31

Table B.19. Data set UV-6.2

Time min	210 nm	220 nm	243 nm
0.5	0.125	0.165	0.415
1.2	0.134	0.169	0.408
2.0	0.15	0.173	0.398
2.8	0.161	0.175	0.389
3.6	0.175	0.179	0.381
4.3	0.184	0.18	0.37
5.1	0.195	0.182	0.362
5.9	0.208	0.188	0.354
6.9	0.221	0.191	0.345
7.7	0.231	0.193	0.336
8.7	0.241	0.194	0.328
9.5	0.253	0.198	0.321
10.3	0.261	0.199	0.314
12.4	0.279	0.201	0.296
14.3	0.291	0.203	0.281
16.0	0.309	0.209	0.27

Table B.20. Data set UV-6.3

Time min	210 nm	220 nm	243 nm
0.5	0.14	0.171	0.403
1.1	0.17	0.178	0.381
1.7	0.196	0.183	0.361
2.3	0.227	0.192	0.342
3.0	0.253	0.2	0.321
3.6	0.272	0.207	0.305
4.2	0.291	0.211	0.289
4.8	0.304	0.212	0.275
5.5	0.32	0.216	0.261
6.1	0.337	0.22	0.247
7.1	0.359	0.228	0.228

Table B.21. Data set UV-7.1

Time min	210 nm	220 nm	243 nm
0.6	0.121	0.159	0.405
1.3	0.141	0.166	0.391
2.0	0.162	0.171	0.377
2.7	0.18	0.178	0.363
3.4	0.199	0.182	0.351
4.1	0.215	0.186	0.338
4.8	0.23	0.19	0.326
5.6	0.247	0.193	0.315
6.3	0.261	0.197	0.304
7.0	0.277	0.201	0.293
7.8	0.287	0.204	0.283
8.5	0.302	0.208	0.274
9.3	0.313	0.211	0.264

Table B.22. Data set UV-7.2

Time min	210 nm	220 nm	243 nm
0.5	0.087	0.141	0.401
1.3	0.112	0.148	0.386
2.0	0.13	0.152	0.369
2.7	0.151	0.159	0.356
3.4	0.17	0.165	0.342
4.1	0.179	0.165	0.328
4.8	0.203	0.172	0.318
5.5	0.218	0.176	0.306
6.2	0.235	0.182	0.295
7.0	0.25	0.185	0.283
7.7	0.263	0.187	0.273
8.4	0.281	0.193	0.263
9.2	0.291	0.196	0.253
10.0	0.303	0.2	0.243

Table B.23. Data set UV-7.3

Time min	210 nm	220 nm	243 nm
0.5	0.085	0.143	0.406
1.3	0.111	0.157	0.392
2.0	0.127	0.16	0.379
2.8	0.151	0.169	0.365
3.6	0.169	0.173	0.351
4.4	0.186	0.178	0.338
5.1	0.204	0.183	0.328
5.7	0.218	0.189	0.316
6.5	0.235	0.193	0.305
7.2	0.246	0.196	0.295
7.9	0.257	0.198	0.287
8.6	0.266	0.198	0.277
9.4	0.281	0.203	0.267
10.1	0.29	0.204	0.258

Table B.24. Data set UV-7.4

Time min	210 nm	220 nm	243 nm
0.6	0.142	0.171	0.407
1.4	0.168	0.182	0.394
2.1	0.177	0.187	0.381
2.7	0.188	0.19	0.37
3.5	0.223	0.197	0.356
4.1	0.228	0.198	0.346
4.8	0.246	0.204	0.335
5.5	0.253	0.208	0.325
6.2	0.267	0.21	0.315
7.0	0.282	0.217	0.303
7.7	0.296	0.219	0.296
8.5	0.295	0.221	0.285
9.2	0.327	0.222	0.276
10.0	0.314	0.22	0.266

Table B.25. Data set UV-7.5

Time min	210 nm	220 nm	243 nm
0.6	0.121	0.171	0.402
1.4	0.159	0.181	0.389
2.1	0.177	0.186	0.373
2.8	0.197	0.193	0.36
3.5	0.211	0.197	0.348
4.2	0.228	0.201	0.335
4.9	0.245	0.206	0.324
5.6	0.262	0.209	0.313
6.3	0.277	0.215	0.307
6.9	0.277	0.214	0.294
7.6	0.288	0.215	0.285
8.3	0.298	0.216	0.275
9.1	0.314	0.226	0.284
9.8	0.324	0.229	0.275